The Non-canonical Growth Activating Functions of Highly Expressed Human Mdm2-C

by

Danielle Okoro

A dissertation submitted to the Graduate Faculty in Biology in partial fulfillment of the requirements for the degree of Doctor of Philosophy, The City University of New York
2013

This manuscript has been read and accepted for the
Graduate Faculty in Biology in satisfaction of the
dissertation requirement for the degree of Doctor of Philosophy

Date	Dr. Jill Bargonetti, Hunter College Chair of Examining Committee
Date	Dr. Laurel Eckhardt, The Graduate Center Executive Officer

Supervision Committee

Dr. Karen Hubbard, City College of New York, CUNY

Dr. Frida E. Kleiman, Hunter College, CUNY

Dr. Diego Loayza, Hunter College, CUNY

Dr. Carol Prives, Columbia University

The City University of New York

ABSTRACT

The Non-canonical Growth Activating Functions of Highly Expressed Human Mdm2-C

By

Danielle Okoro

Adviser: Professor Jill Bargonetti

Mdm2 is an oncoprotein that regulates the tumor suppressor protein, p53 via the Mdm2 canonical pathway. The pathway involves p53 protein degradation and transcriptional repression. Mdm2 is often found over-expressed in cancers. In the presence of Mdm2 over-expression, the activity of p53 is frequently attenuated and the protein levels remain paradoxically high. Cancers with Mdm2 over-expression also over-express *mdm2* splice variant transcripts. There are over forty identified spliced variants of *mdm2*. Therefore, we hypothesized that in the presence of Mdm2 over-expression, a different form of Mdm2 protein exists that does not function in the Mdm2 canonical pathway. In this study, the functions of an Mdm2 isoform, Mdm2-C, were investigated. We observed that Mdm2 over-expressing cells have high basal levels of *mdm2-C* transcript. We have cloned and expressed *mdm2-C in vitro.* We created an Mdm2-C specific antibody, Mdm2 C410, to the splice junction of exons four and ten (Mdm2 C410) and validated the C410 antibody using *in vitro* translated full-length Mdm2 compared to Mdm2-C. The Mdm2 C410 antibody did not detect Mdm2-FL. We saw that different human cancer cell lines, liposarcoma and breast cancer tissues, over-expressed endogenous Mdm2-C protein. We also observed that there was an estrogen-dependent increase in endogenous Mdm2-C protein in ER+ *mdm2* SNP309 breast

cancer cells that was p53-independent. In addition, the exogenous expression of Mdm2-C in human *p53*-null cancer cells showed that Mdm2-C does not function in the Mdm2 canonical pathway. Immunofluorescence utilizing the Mdm2 C410 antibody displayed that Mdm2-C was localized to the cytoplasm and nucleolus in a speckled pattern that might be integral to its cellular functions. We observed that the over-expression of Mdm2-C in the presence or absence of p53 in human and mouse cell lines promoted cell growth. Furthermore, the partial down regulation of *mdm2-C* via siRNA in mutant p53 G/G *mdm2*SNP309 breast cancer cells, T47D resulted in increased cell death. Thus suggesting that unlike other Mdm2 isoforms and full-length Mdm2, Mdm2-C has distinct roles in cell survival and p53-independent Mdm2 molecular pathways. Here we report the first identification of an endogenous tumor-associated splice variant Mdm2 protein, and document that Mdm2-C functions through a non-canonical growth activation pathway that is p53-independent.

Acknowledgements

I would like to thank God for His favor, strength and grace throughout the years.

I would like to thank my family, especially my mother and grandmother. Even though they were oblivious to what getting a doctorate really meant, their enthusiasm, support and pride has helped brought me to where I am today.

I would like to thank Dr. Jill Bargonetti who took in a young naïve undergraduate girl into her laboratory and turned her into a scientist. I came into her laboratory as a medical school oriented girl but now I am leaving with a doctorate in cancer biology; to say she has shaped me into a different person is an understatement. My experience in Dr. Bargonetti's lab for the past eight years has been great. She has been like a mother to me and I will always treasure the time I spent in her laboratory.

I would like to thank my lab members, both past and present, who have made the experience in Dr. Bargonetti's laboratory a pleasant and rewarding one.

I would like to thank my friends and sisters who have kept me sane during my years in graduate school, with their support, prayers and laughs. I would also like to thank my church family. They have also been a great support system towards the completion of my graduate degree.

Table of Contents

List of Tables

List of Figures

CHAPTER 1:

Introduction

1.1 **Mdm2: Background and Significance**

Murine Double Minute 2 (Mdm2) was discovered in 1987 by the laboratory of Donna L. George (Cahilly-Snyder et al., 1987) and found in the immortalized murine cell line, BALB/c 3T3, to be associated with spontaneous transformation. The cell line had 25-30 copies of chromatic bodies that were called double minutes. The protein was classified as an oncogene in 1991 in the same laboratory (Fakharzadeh et al., 1991). Mdm2 is over-expressed in several types of tumors such as acute myeloid leukemia (Bueso-Ramos et al., 1993) and breast carcinomas (Freedman et al., 1999). Mdm2 over-expression occurs as a result of different mechanisms: gene amplification (Meddeb et al., 1996; Oliner et al., 1992), increased transcription (Bueso-Ramos et al., 1993; Watanabe et al., 1994) and enhanced translation (Haines et al., 1994; Landers et al., 1997). Interestingly, cells that over-express Mdm2 form tumors when injected into immuno-compromised mice (Cahilly-Snyder et al., 1987; Fakharzadeh et al., 1991)

Mdm2 is a negative regulator of the tumor suppressor protein, p53 and is required for development. In mice with both *mdm2* gene copies deleted, embryos die in utero before implantation (Jones et al., 1995; Montes de Oca Luna et al., 1995). However with the simultaneous deletion of both copies of the *p53* gene, this lethality is rescued. Interestingly, the deletion of the p53 target gene, *p21* in *mdm2* knockout mice does not rescue the lethality; thus indicating that the cause of death is due multiple p53 downstream activities (Montes de Oca Luna et al., 1997). The deletion of *p53* results in increased tumorigenesis, (Armstrong et al., 1995; Donehower et al., 1992; Jacks et al., 1994) and these mice are not physically different from the wild-type mice (Jones et al., 1996).

1.2 *p53* Gene and Protein

The p53 protein was discovered in 1979 (Linzer and Levine, 1979) and was originally classified as an oncogene because it is highly expressed in simian virus 40 (SV40) and adenovirus driven cancers (Parada et al., 1984). In 1989, the protein was identified as a tumor suppressor (Baker et al., 1989). It is called p53 because the protein isolated was a 53 kilodalton protein (kDa). The p53 protein is a transcription factor involved in the transcription of genes responsible for various cellular activities such as growth arrest, DNA repair and apoptosis (Brown et al., 2009; Vogelstein et al., 2000; Vousden and Lu, 2002) (Fig. 1). Under conditions without stress, p53 has a short half life and is kept at low levels by the negative regulator, Mdm2. p53 regulation by Mdm2 occurs in three ways: the repression of p53 transcriptional activity, p53 protein degradation and *p53* mRNA translation. In the presence of cellular stress, p53 is activated and phosphorylated at Serine 15 by Ataxia Telengiectasia-Mutated (Gilkes et al.) (Gilkes et al.) protein kinase, which acts upstream of the p53 signal transduction pathway (Canman et al., 1998; Giaccia and Kastan, 1998). Subsequently, transcription effectors such as p300 further stabilize p53 through acetylation (Sakaguchi et al., 1998) and promote p53 transcriptional activities (Avantaggiati et al., 1997; Gu et al., 1997; Lill et al., 1997). p53 is found conserved in a number of organisms such as *C. elegans*, flies, mice, fish, arachnids, frogs etc. (Lane et al., 2010a; Lane et al., 2010b).

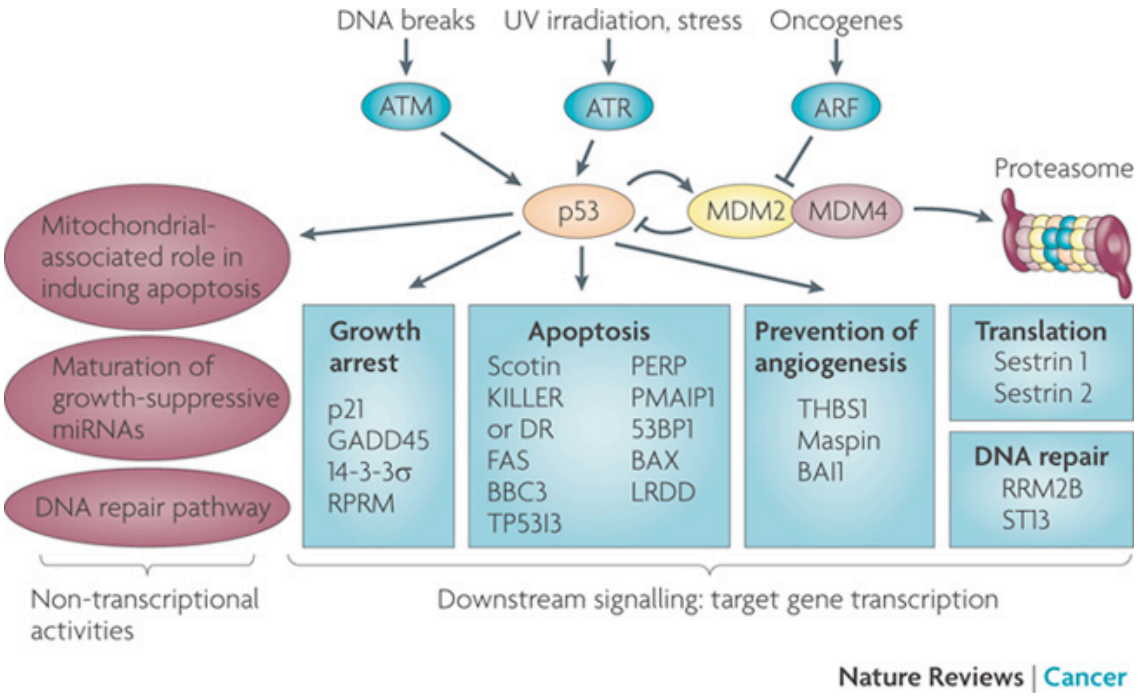

(Brown et al., 2009)

Figure 1: **The p53 activation pathway-** *The p53 protein is important for keeping the integrity of the cell. p53 can be activated by Ataxia Telengiectasia Mutated (Gilkes et al.) after DNA breaks. Phosphorylation of p53 by ATM can promote growth arrest, apoptosis or DNA repair. There is a negative feedback loop that exists between Mdm2 and p53. The* mdm2 *gene is a transcriptional target for p53 and the Mdm2 protein targets p53 for ubiquitin-mediated proteasomal degradation.*

Mdm2 binds to p53 and regulates p53 in three ways- ubiquitin-mediated proteasomal degradation, transcription repression and RNA translation (Fig. 2). The two proteins, Mdm2 and p53, exist in a negative feedback loop. The p53 protein induces the transcription of the *mdm2* gene and in turn the Mdm2 protein helps keep p53 levels low in the absence of cellular stress by acting as an E3 ubiquitin ligase. This leads to the degradation of p53 mediated by the ubiquitin proteasome pathway (Momand et al., 1992; Oliner et al., 1993; Thut et al., 1997; Wu et al., 1993). Mdm2 functions as an E3 ubiquitin ligase for p53 by attaching ubiquitin residues onto the protein, thus leading to

its cytoplasmic transport (Freedman and Levine, 1998) and proteasomal degradation (Haupt et al., 1997; Kubbutat et al., 1997). Mdm2 promotes p53 degradation by binding to p53 using three domains (Chen et al., 1993; Poyurovsky et al., 2010): the amino terminus (N-), (Poyurovsky et al., 2010), which is the p53 binding domain, the central acidic domain (Meulmeester et al., 2003) and the carboxyl terminus (C-) RING Finger domain, which is responsible for the E3 ligase function of the protein (Poyurovsky et al., 2007).

The regulation of p53 levels is important because high levels of p53 lead to apoptosis (Jones et al., 1995; Montes de Oca Luna et al., 1995). This Mdm2-p53 feedback results in an oscillation between Mdm2 and p53 that involves p53 stability after cellular stress (Hu et al., 2007). There is also a p53-dependent increase in Mdm2 observed after cellular stress (Ciliberto et al., 2005).

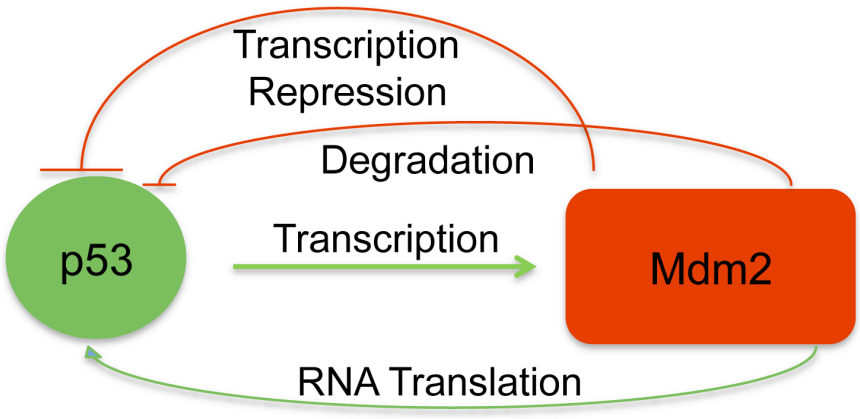

Figure 2: **Regulation of p53 by Mdm2**. *The regulation of p53 by Mdm2 occurs in three ways: the repression of p53 transcriptional activity, p53 protein ubiquitin-mediated proteasomal degradation and* p53 *mRNA translation. Red lines indicate repression and green lines indicate activation.*

1.3 **The *mdm2* Gene and Protein**

The *mdm2* gene is a 33 kilobases (33 kb) nucleotide sequence, which is found on chromosome 12 (q14.3-q15). The gene has twelve exons, eleven introns and encodes for an open reading frame mRNA of approximately 1.4 kb (Iwakuma and Lozano, 2003). Transcription of the *mdm2* gene is initiated at two promoters: P1 and P2, which are p53-independent and p53-dependent respectively (Barak et al., 1993; Juven et al., 1993) (Fig. 3A). Transcription from P1 represents the basal transcription of the *mdm2* gene in the cell. The P2 promoter is considered inactive except when induced under stressful cellular conditions such as DNA damage (Barak et al., 1993; Perry et al., 1993). The *mdm2* gene contains p53 responsive elements within intron one adjacent to P2 (Juven et al., 1993; Zauberman et al., 1995). Within this region, there are binding sites for Sp1 (Bond et al., 2004) and a composite AP1-ETS motif involved in transcription from P2 independent of p53 (Phelps et al., 2003). The P2 derived transcript has an enhanced translation potential compared to the transcript from the P1 promoter (Brown et al., 1999; Haines et al., 1994; Landers et al., 1997). This is due to the nature of the P2 transcript 5' leader sequence, while the P1 5' leader sequence has translational inhibitory abilities (Landers et al., 1997).

The *mdm2* transcript is translated into a protein of 491 amino acids (Fig. 3B). The full-length protein has been shown to migrate at multiple sizes ranging from 50-110 KDa (Olson et al., 1993). Cleavage protein products of 76 kDa and 60 kDa have also been reported (Olson et al., 1993; Perry et al., 1993; Saucedo et al., 1999). Mdm2 regulation occurs at different levels including gene expression (Barak et al., 1993), protein-protein

interactions (Honda and Yasuda, 1999; Zhang et al., 1998) and sub-cellular localization (Weber et al., 1999).

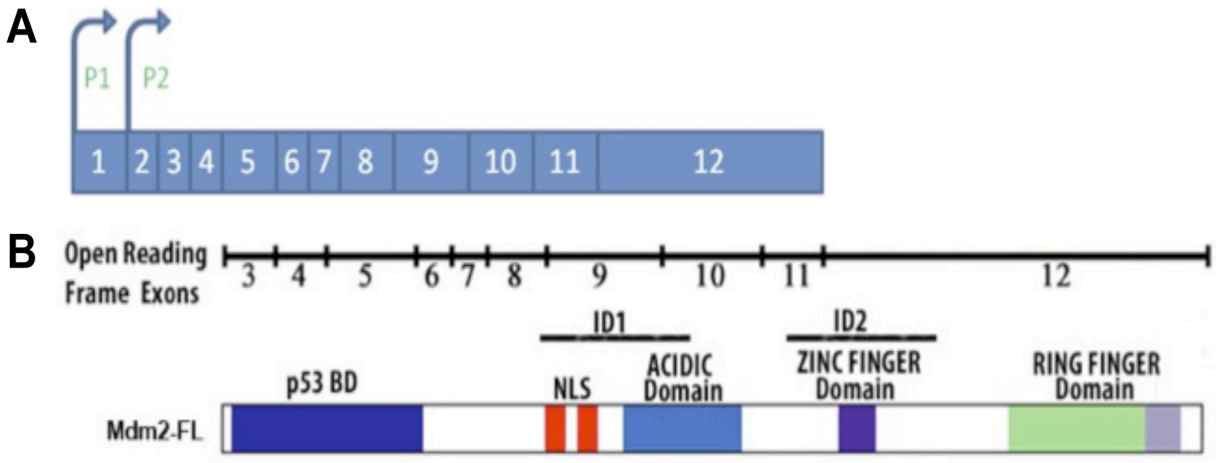

Adapted from (Bartel et al., 2002; Ganguli and Wasylyk, 2003)

Figure 3**: The *mdm2* gene and its protein domains. A.** *The* mdm2 *gene has twelve exons and two promoters, P1 and P2, p53-independent and p53-dependent respectively.* **B.** *The Mdm2 protein has four major domains: p53 binding domain, Acidic domain, ZINC finger domain and the RING finger domain. It possesses two growth Inhibitory domains- ID1 and ID2, involved in growth inhibition in the cell.*

1.4 **Mdm2 Post-Translational Modifications**

Post-translational modifications of amino acid residues are important in the modulation of several cellular processes. Lack of, or aberrant amino acid modifications are implicated in a number of diseases such as cancer, diabetes, liver diseases and neurodegenerative disorders (Karve and Cheema, 2011). Like many key regulatory proteins, Mdm2 undergoes post-translational modifications that influence its cellular activities (Hay and Meek, 2000; Meek and Knippschild, 2003) (Fig. 4A). Mdm2 contains several serine and threonine residues that are phosphorylated by several proteins in the

cell. Post-translational modifications of Mdm2 result in different outcomes in which Mdm2 substrate degradation is enhanced or inhibited.

Mdm2 phosphorylation can result in the stability or degradation of its substrate proteins. For example, ATM phosphorylates Mdm2 and this inhibits the interaction with p53 and increases p53 protein stability (de Toledo et al., 2000; Khosravi et al., 1999; Maya et al., 2001). Similarly, the protein-tyrosine kinase, c-Abl (Goldberg et al., 2002; Sionov et al., 1999) and Caesin kinase 1 delta (CK1δ) (Winter et al., 2004) phosphorylate Mdm2 and promote p53 stability. These modifications inhibit Mdm2-dependent degradation of p53 through reduced Mdm2 phosphorylation (Blattner et al., 2002; Cheng et al., 2011). Alternatively, increased phosphorylation of Mdm2 can lead to enhanced substrate degradation. For example, PI3/AKT phosphorylates Mdm2 and promotes p53 degradation (Mayo and Donner, 2001; Milne et al., 2004; Ogawara et al., 2002). Also, protein Caesin kinase 2 (CK2) phosphorylates Mdm2 to enhance p53 degradation (Allende-Vega et al., 2005; Gotz et al., 1999; Hjerrild et al., 2001).

Mdm2 is can be modified by ubiquitylation and sumoylation. Mdm2 undergoes auto-ubiquitylation and targets itself for degradation (Fang et al., 2000; Honda and Yasuda, 2000; Wallace et al., 2006). Mdm2 is also sumoylated and this reduces Mdm2 auto-ubiquitylation and increases Mdm2 substrate ubiquitylation (Buschmann et al., 2001). In addition, Mdm2 has residues that could be myristoylated and glycosylated, both of which are large modifications that may play important roles in membrane targeting and cell-cell adhesion, respectively (Varki et al., 2009; Zha et al., 2000).

The Mdm2 polypeptide has a large number of cysteine residues and can therefore be considered a high cysteine containing polypeptide (Fig. 4B). As a result of its high cysteine content, Mdm2 can easily form disulfide bridges between amino acids, which could influence the proteins' tertiary structure. The Mdm2 protein has a calculated mass of 55 kDa. However, numerous studies show the protein migrates on an SDS-PAGE with an apparent molecular weight above 90 kDa. The reason for this might lie in the post-translational modifications that occur on Mdm2 as well as the number of cysteine residues present in the polypeptide. We have observed in the Bargonetti lab that the reduction of protein samples with iodoacetamide (a reducing agent that prevents the re-ligation of disulfide bonds) considerably reduces the mobility of Mdm2 protein forms observed by antibody protein detection in western blot. This suggests that the cysteine residues present in Mdm2 contribute to the observed higher molecular mass.

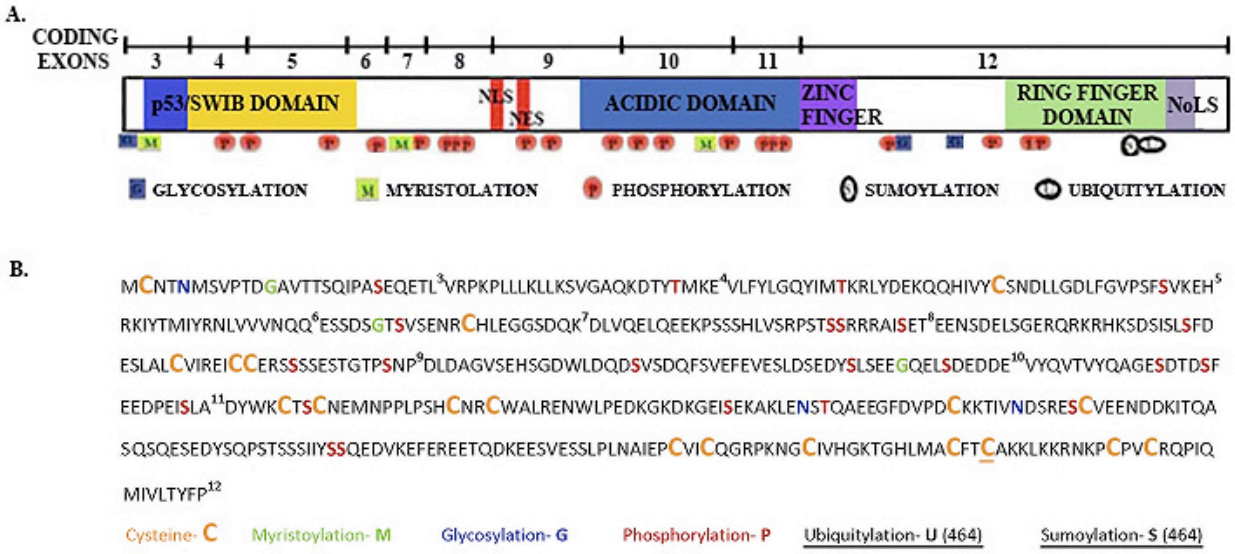

Okoro D, Rosso M and Bargonetti J 2012

Figure 4: **The Mdm2 polypeptide can be post-translationally modified at various amino acid residues**. **A**. *The post-translational modifications that occur in the domains of Mdm2 include: Glycosylation, Myristoylation, Phosphorylation, Sumoylation and Ubiquitylation.* **B.** *Represents the Mdm2 polypeptide sequence. Each residue that is modified is highlighted in color. Blue- Glycosylation; Green- Myristolylation; Red- Phosphorylation; Black- Sumoylation and Ubiquitylation. The underlined cysteine residue represents the site of sumoylation and ubiquitylation. The Cysteine residues are colored in orange and represent amino acids that can form disulfide bonds with each other.*

1.5 **Mdm2 Protein Domains and Interacting Proteins**

Mdm2 binds to a wide range of proteins. Some of the proteins that interact with Mdm2 are shown in Figure 5. A few will be described here as delineated by the Mdm2 interacting domains. The N-terminus encompasses exons 3 - 6. It is a hydrophobic domain, which binds to p53 and regulates p53 transcriptional activity and protein levels. This region also has a similar fold to the SWIB family proteins, which are chromatin-remodeling proteins (Bennett-Lovsey et al., 2002).

The central region of Mdm2 consists of the nuclear localization and exports signals and the acidic domain. It encompasses exons 7 - 11. The nuclear localization and export signals are required for protein entry and exit out of the nucleus and are important for Mdm2-dependent cytoplasmic p53 degradation (Freedman and Levine, 1998; Roth et al., 1998). The acidic domain is required for Mdm2-dependent p53 degradation (Argentini et al., 2001; Kawai et al., 2003; Ma et al., 2006; Meulmeester et al., 2003). The acidic domain of Mdm2 binds regulatory protein, p300 (Grossman et al., 1998), which is a co-activator protein that acts as an E4 ubiquitin ligase to aid in the degradation of p53 via the ubiquitin proteasome pathway (Grossman et al., 2003; Zeng et al., 2003). In addition, p300 binds to Mdm2 and promotes Mdm2 protein stability and this occurs in the absence of Mdm2 acetylation by p300 (Zeng et al., 2003). It has been shown that mutations in the acidic domain of Mdm2 disrupt the binding of p300 and result in inefficient p53 degradation, although, the protein can still be monoubiquitylated (Zhu et al., 2001). The Mdm2 and p300 interaction also abrogates p53 acetylation and thus inhibits transcription (Jin et al., 2002). Mdm2 also interacts with Nbs1, a component of the MRN complex involved in DNA repair (Alt et al., 2005). The acidic domain of Mdm2 binds the ubiquitous transcription factor, Sp1 (Ganguli and Wasylyk, 2003) that has been shown to promote *mdm2* transcription in G/G *mdm2* SNP309 homozygous cells (Bond et al., 2004). Mdm2 also inhibits the transcriptional activity of Sp1 through a protein:protein interaction (Johnson-Pais et al., 2001).

The C-terminus of Mdm2 consists of the RING and Zinc finger domains. The carboxyl terminus spans exon 12 and is the largest portion of the Mdm2 protein, with 190 amino acid residues (Fig. 5). The Zinc finger domain of Mdm2 contains sequences

similar to those found in proteins involved in transcription and translation (Yu et al., 2006). However, it has not been shown to bind nucleic acids *in vivo*. The RING finger domain possesses the ubiquitin ligase activity of Mdm2 (Fang et al., 2000; Honda and Yasuda, 2000). The RING finger of Mdm2 also binds RNA (Elenbaas et al., 1996). Using its RING finger domain, Mdm2 binds to the TAFII250 protein, which is a component of the basal transcription machinery (Ganguli and Wasylyk, 2003). The RING finger domain is also implicated in histone ubiquitylation and transcriptional repression via monoubiquitylation of H2B (Minsky and Oren, 2004). In addition, Mdm2 forms a homodimer and it also interacts with MdmX, the Mdm2 homologous protein using the RING finger domain (Sharp et al., 1999; Tanimura et al., 1999).

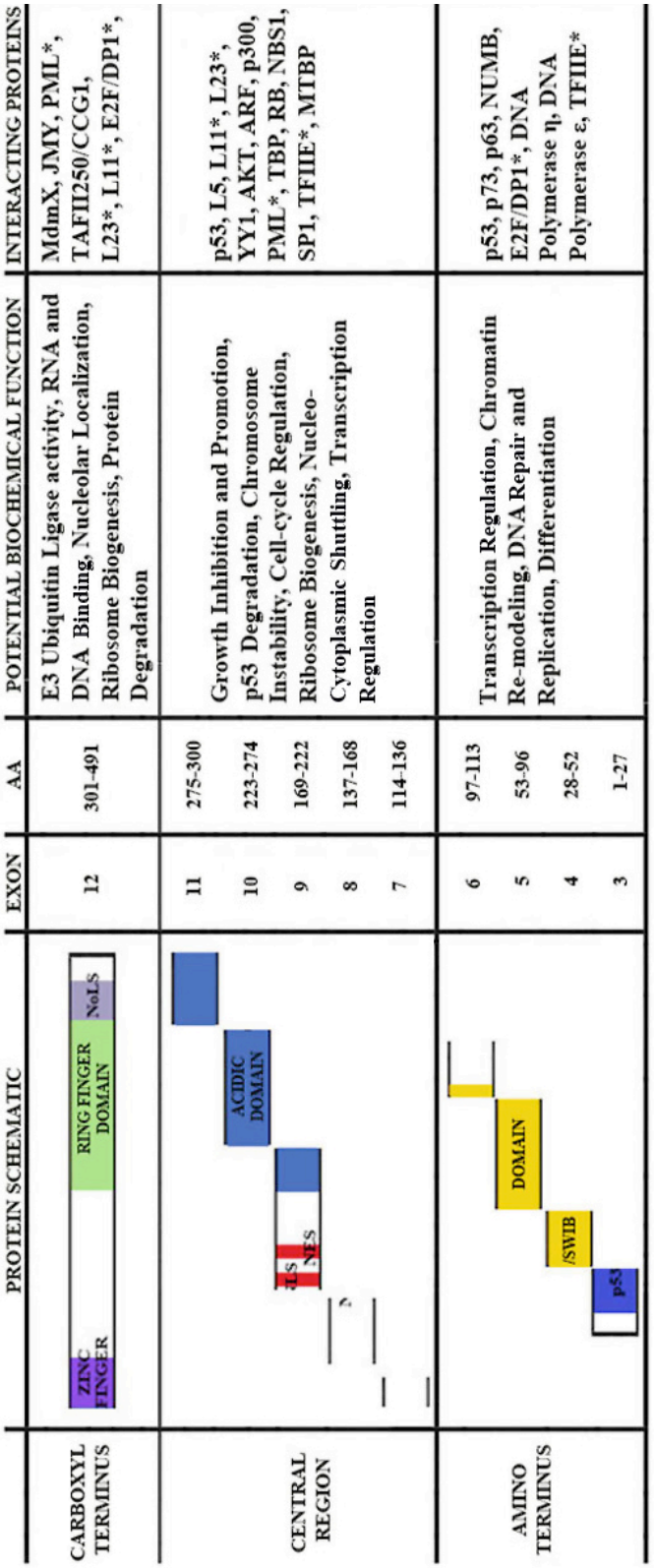

Adapted from (Okoro et al., 2012)

Figure 5: **Mdm2 interacting proteins**. *Mdm2 interacts with various proteins with diverse functions. As a result of its promiscuity, it can be implicated in a number of cellular processes. The organization of the figure is as follows from top to bottom: The carboxyl (C-) terminus spans exon 12. The C-terminus contains the Zinc finger, the RING finger and the nucleolar localization signal domains. The central region spans exons 7 – 11. The central region contains the nuclear localization and export signals and the acidic domain. The Amino (N-) terminus spans exons 3 – 6. The N-terminus contains the p53 binding and the SWIB domains.*

1.6 **Mdm2 Canonical Pathway**

1.6.1 **Mdm2 as an E3 Ubiquitin Ligase**

Mdm2 is an E3 ubiquitin ligase characterized by its RING finger domain in the C-terminal region. The E3 ligase activity of Mdm2 targets p53 (Haupt et al., 1997; Honda et al., 1997; Kubbutat et al., 1997) (Fig. 6), p21 (Enge et al., 2009; Zhang et al., 2004), RB (Uchida et al., 2006), MdmX (Pan and Chen, 2003) as well as itself for degradation (Fang et al., 2000; Honda and Yasuda, 2000; Wallace et al., 2006). The decision by Mdm2 to mono vs. poly-ubiquitylate substrates is dependent on the levels of Mdm2 and MdmX. At low levels of Mdm2, p53 is mono-ubiquitylated at the C-terminus and this targets the protein for cytoplasmic transport, where p53 is poly-ubiquitylated by p300 and then targeted for degradation via the ubiquitin proteasome pathway (Grossman et al., 2003; Grossman et al., 1998). In the presence of high Mdm2 levels, p53 is poly-ubiquitylated and targeted for nuclear degradation (Li et al., 2003). Interestingly, at high levels of the Mdm2 protein, the protein undergoes auto-ubiquitylation and promotes its degradation; thus creating a level of self-regulation. Mdm2 also binds to its family member protein, MdmX and leads to MdmX degradation (Pan and Chen, 2003). Mdm2 and MdmX can exist in heterodimers, and depending on the ratio of Mdm2:MdmX, you can have primarily Mdm2, MdmX or p53 degradation (Linke et al., 2008). Mdm2 targets p21 for degradation (Zhang et al., 2004) in a non-ubiquitylation-dependent manner, which is not abrogated with the removal of the Mdm2 RING finger domain (Jin et al., 2003; Xu et al., 2010).

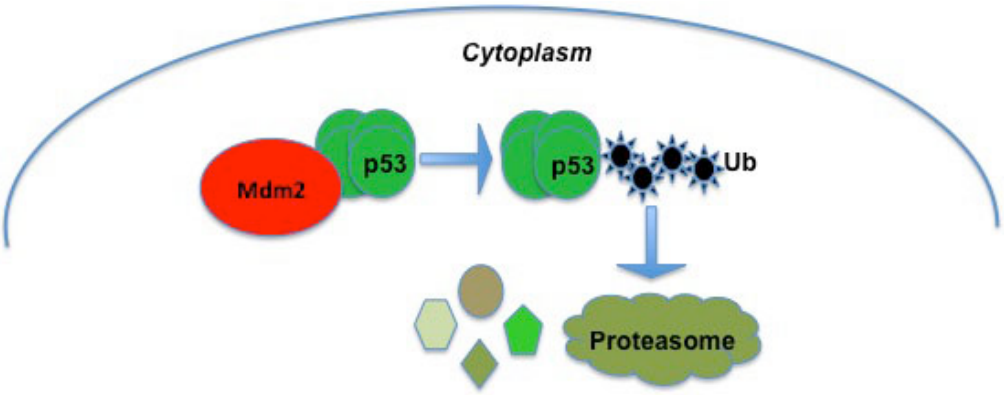

Figure 6: **Ubiquitin proteasome pathway-mediated degradation of p53**. *Mdm2 is an E3 ubiquitin ligase that attaches ubiquitin subunits to the p53 protein and targets it for degradation via the ubiquitin proteasome pathway.*

1.6.2 **Mdm2 as a Transcription Regulator**

The Mdm2 protein has been found to regulate the functions of a few transcription factors. Two important standouts are: p53 and E2F.

p53

Mdm2 represses the transactivation activity of p53 (Arva et al., 2005; Arva et al., 2008; Bond et al., 2004; Chen et al., 1995; Momand et al., 1992; Oliner et al., 1993; White et al., 2006) (Fig. 7). In the absence of cellular stress, chromatin bound p53 is transcriptionally repressed by Mdm2 thus preventing the transcription of genes involved in cell cycle arrest, apoptosis or DNA repair (Arva et al., 2005; White et al., 2006). In the absence of p53 on the chromatin, Mdm2 is absent at p53 target genes (White et al., 2006). Reports have shown that in cells with Mdm2 over-expression, p53 inhibition is caused by excess Mdm2 bound to p53 on the chromatin. The knockdown of *mdm2* led to the activation of p53 transcriptional activity (Arva et al., 2005; Arva et al., 2008).

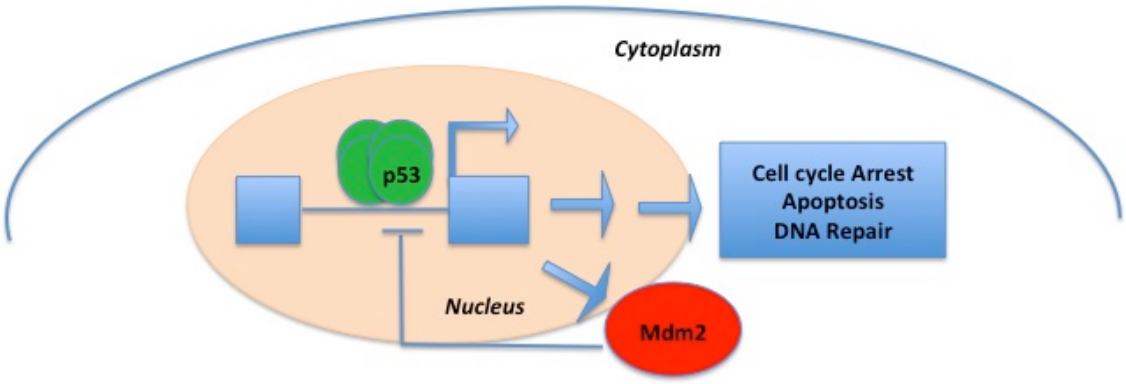

Figure 7: **Trans-repression of p53 by Mdm2**. *Mdm2 and p53 exist in a feedback loop. The* mdm2 *gene is a transcription target for p53 and the resulting Mdm2 protein represses p53 transcriptional activity by binding to the p53 protein on the chromatin at its target genes to prevent cell cycle arrest, apoptosis and or DNA repair.*

E2F1

Mdm2 regulates the transcription activity of the transcription factor and cycle regulatory protein, E2F1. In the presence of increased Mdm2 protein, there is an increase in E2F1 activity and the transcription of E2F1 target genes required for cell cycle progression (Martin et al., 1995). Mdm2 also enhances E2F1 activity by stabilizing the co-activator protein, DP1 (Loughran and La Thangue, 2000). Similar to p53, Mdm2 regulates E2F1 at the protein level. Unlike its down-regulation of p53, Mdm2 stabilizes E2F1 protein by preventing the protein's ubiquitylation (Zhang et al., 2005). Interestingly, the down-regulation of *mdm2* transcript and protein results in E2F-dependent apoptosis (Udayakumar et al., 2008). This suggests that the presence of Mdm2 shifts the activity of E2F to cell proliferation instead of cell death.

1.7 **Mdm2 Non-Canonical Pathway**

1.7.1 **Mdm2 RNA/ Nucleotide Binding**

In addition to interacting with cellular proteins, Mdm2 also interacts with RNA (Elenbaas et al., 1996). Some of the RNAs Mdm2 binds to are: *p53* (Fig. 8) (Naski et al., 2009), X-linked Inhibitor-of-Apoptosis (*XIAP*) (Gu et al., 2009), *MYCN* (Gu et al., 2012) and Vascular endothelial growth factor (*VEGF*) (Zhou et al., 2011). Mdm2 can directly bind to the *p53* mRNA through its RING finger domain, which is the same region that possesses its ubiquitin ligase function (Candeias et al., 2008). On the other hand, the Mdm2-*p53* mRNA interaction also occurs through interaction with ribosomal proteins (Takagi et al., 2005). The Mdm2-*p53* mRNA interaction can result in two alternate outcomes of translation enhancement or translation repression. The ability to enhance or repress translation is dependent on whether the cell is in a stressed or non-stressed condition (Ofir-Rosenfeld et al., 2008).

Mdm2 can bind the *p53* mRNA and repress translation (Candeias et al., 2008; Ofir-Rosenfeld et al., 2008). In non-stressed conditions, Mdm2 can bind to ribosomal protein, L26 (RPL26). RPL26 is a protein that enhances the translation of *p53* mRNA by binding to the 5' un-translated region of the *p53* mRNA (Takagi et al., 2005). The Mdm2-RPL26 interaction results in the proteasome-mediated degradation of RPL26 (Ofir-Rosenfeld et al., 2008). Therefore by targeting RPL26 for degradation, Mdm2 reduces the translation of p53. This maintains low p53 levels in the cell. Alternatively, Mdm2 can directly bind to the *p53* mRNA and promote translation (Candeias et al., 2008; Naski et al., 2009; Takagi et al., 2005). In addition, in the presence of stress, the Mdm2-RPL26 interaction is disrupted and this allows for efficient translation of the *p53*

mRNA by RPL26. Thus the disruption of the Mdm2-RPL26 interaction increases p53 protein levels (Ofir-Rosenfeld et al., 2008). Interestingly, in an *in vitro* system, Mdm2 was also shown to bind DNA through its Zinc finger domain in a non-sequence specific manner (Challen et al., 2011). Therefore Mdm2 could be implicated in the regulation of chromatin-based functions.

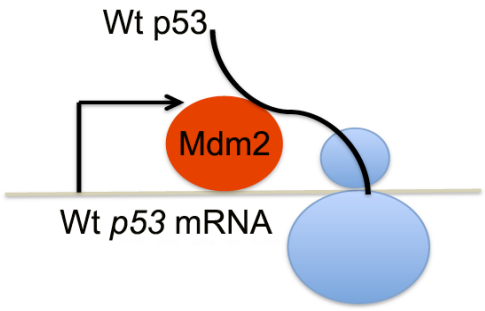

Adapted from (Naski et al., 2009)

Figure 8: **Translational control of p53 by Mdm2**. *Mdm2 has been shown to bind to* p53 *mRNA and this interaction enhances translation. Interestingly, the enhancement of translation occurs when the cell is stressed and needs to increase p53 protein levels. In non-stressed conditions, Mdm2 binds to Ribosomal protein L23 to prevent the enhancement of* p53 *mRNA translation.*

1.7.2 **DNA Repair and Synthesis**

Mdm2 binds to and regulates the function of proteins involved in DNA repair. Mdm2 has been shown to bind to the catalytic subunit of DNA polymerase epsilon (DNA Pol ε), a protein involved in DNA synthesis (Asahara et al., 2003; Vlatkovic et al., 2000). DNA Pol ε also participates in sensing DNA lesions during cell cycle progression and its proof reading properties help abate spontaneous cancer formation (Albertson et al., 2009). In addition, Mdm2 binds DNA polymerase eta (DNA Pol η), a protein involved in

translesion DNA synthesis. In response to Ultra Violet irradiation, Mdm2 leads to the ubiquitin proteasome-mediated degradation of DNA pol η (Jung et al., 2011). Mdm2 also binds to Nbs1, a component of the MRN (Mre11/Rad50/Nbs1) complex involved in sensing double strand breaks (Paull and Lee, 2005). The Mdm2-Nbs1 interaction disrupts double strand break repair (Alt et al., 2005). Additionally, the over-expression of Mdm2 increases chromosomal instability in B- cells (Bouska et al., 2008) independent of p53 and also provides these cells with a growth advantage (Wang et al., 2008).

1.7.3 **Cell Cycle Control**

The involvement of Mdm2 in cell cycle control is associated with its interaction with cell cycle-related proteins (Fig. 9). Mdm2 has been shown to bind and regulate E2F1 as well as its negative regulator, RB (Sdek et al., 2004; Xiao et al., 1995). Recently, Mdm2 was shown to be required for E2F1-mediated oncogenesis in melanoma-derived cells (Verhaegen et al., 2012). Mdm2 also binds to retinoblastoma protein (RB) and this inhibits the ability of RB to repress the function of E2F1 (Sdek et al., 2004). Therefore, the Mdm2-RB interaction prevents G1 cell cycle arrest. In addition, Mdm2 targets RB for proteasomal degradation (Sdek et al., 2005). Mdm2 also negatively regulates p21 by facilitating its binding with the proteasomal C8 subunit thus promoting the proteins' degradation (Zhang et al., 2004).

Mdm2 also binds to Cyclin G1 (CCNG1). Mdm2 results in the degradation of CCNG1 via the proteasome pathway (Zhao et al., 2003). In addition, there is a correlation between increased expression of cyclin D1 and Mdm2 in various cancers (Coupland et al., 2000; Lai et al., 1998; Morgan et al., 1999; Pignataro et al., 1998).

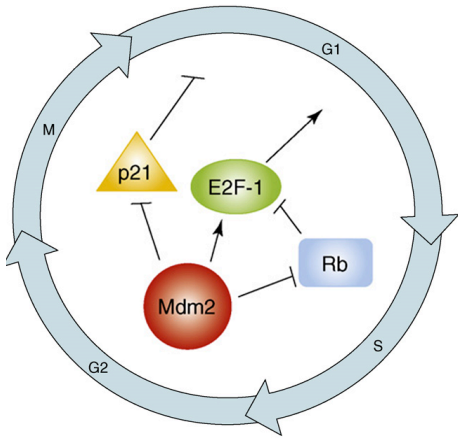

(Bouska et al., 2008)

Figure 9: **Mdm2 Modulates Cell Cycle Control**. *Mdm2 has been shown to interact with E2F1, RB and p21. These interactions lead to G1 arrest or cell cycle progression depending on whether the cell is stressed or healthy.*

1.7.4 **Ribosome Biosynthesis**

Mdm2 binds to ribosomal proteins L5 (Dai and Lu, 2004; Marechal et al., 1994), L11 (Lohrum et al., 2003; Zhang et al., 2011; Zhang et al., 2003), L23 (Dai et al., 2004; Jin et al., 2004) and L26 (Ofir-Rosenfeld et al., 2008). Binding of Mdm2 to ribosomal proteins, L5, L11 and L23 results in p53 activation in response to ribosomal stress. Mdm2 binds to L5, L11 and L23 and promotes p53 activation by the reduction of Mdm2-mediated degradation (Dai et al., 2004; Zhang et al., 2010; Zhang et al., 2003). Interestingly, although L11 binds to Mdm2 and activates p53 activity, this binding results in the accumulation of ubiquitylated Mdm2 through the inhibition of the 26S subunit of the proteasome (Dai et al., 2006).

1.8 **Alternative Splicing**

Alternative splicing is a process through which the cell creates a variety of protein species are created from a single gene, thereby enriching the cellular proteomic diversity (Graveley, 2001). There are five distinct alternative splicing patterns that have been identified. They include: the skipping or inclusion of an exon, the use of an alternative 5' splice site, the use of an alternative 3' splice site, the inclusion of one or two mutually exclusive exons and the inclusion of an intron (Black, 2003). In individual cases, altered splice site recognition and usage in alternative splicing may result from inherited somatic mutations in *cis*-regulatory elements, oncogenic signaling and variations in *trans*-acting regulatory factors (Goldstrohm et al., 2001; Kalnina et al., 2005). Alternative splicing can be influenced by stress, where the regulation of splice site recognition is due to changes in the composition or activity of splicing factors and via transcription regulation (Stamm, 2002).

Evidence has shown a direct interaction between the carboxyl-terminal domain (CTD) of RNA polymerase II (RNA pol II) and the splicing machinery, (Goldstrohm et al., 2001). This suggests that there is coupling between transcription and splicing that is mediated by the phosphorylated CTD tail. The transcription of genes involves the assembly of the pre-initiation complex, promoter clearance and elongation. RNA pol II and the basal transcription machinery, which begin transcription upon promoter clearance, are part of the pre-initiation complexes. Transcription elongation is accomplished by hyper-phosphorylation of the CTD linked to the channel of RNA pol II. Upon emergence of the 5' end of the transcript from the RNA pol II channel, the splicing machinery attaches to the emerging transcript.

The process of splicing involves several factors that make up the spliceosome and consist of a family of small nuclear RiboNucleoProteins (snRNP). They include: U1, U2, U4, U5 and U6. The snRNPs are recycled after intron excision. The same process occurs during alternative splicing. This is with the exception of the retention of some exons during splicing and sometimes, the preserving of introns (Goldstrohm et al., 2001).

1.8.1 *mdm2* Splicing

The *mdm2* gene transcript undergoes alternative splicing that results in over seventy identified transcripts (Fig. 10) (Bartel et al., 2002), with additional transcripts discovered recently (Sam et al., 2012). The pattern of alternative splicing and transcripts differ between normal and cancerous tissues and are also possibly functionally different. The functions of the splice variants have been shown to differ in various tissues. It has been shown that *mdm2* alternative splicing is induced during stress (Chandler et al., 2006; Dias et al., 2006; Singh et al., 2009). Evans et al. demonstrated that a particular human *mdm2* splice variant, HDM2ALT-1 (Mdm2-B), missing exons 4 through 11, binds to full-length Mdm2 and sequesters it to the cytoplasm thus enhancing p53 activation (Evans et al., 2001; Harris, 2005). Dang et al. also showed that Mdm2 splice variants with retention of the RING finger domain interact with full-length Mdm2 to result in the inhibition of cell proliferation (Dang et al., 2002).

Additionally, the Harris laboratory has shown that Mdm2-A, an *mdm2* splice variant missing exons 4 through 9, has opposing functions depending on the presence

or absence of p53. They show that in the presence of wild-type and functional p53, Mdm2-A expressing mouse embryonic fibroblasts (MEFs) have reduced growth, increased p21 protein expression and enhanced senescence. Interestingly, homozygous *mdm2-A* transgenic mice exhibit a lethal phenotype that is rescued by a reduction in p53 expression thus showing that this effect is p53-dependent (Volk et al., 2009b). On the other hand, in the presence of compromised p53 or the complete absence of p53, Mdm2-A has tumorigenic properties. They also show that mice with no p53 or reduced p53 expression and the over-expression of Mdm2-A have an altered tumor spectrum and derived MEFs have increased transformation *in vivo*. Also, *p53* heterozygous (*p53 +/-)* mice expressing Mdm2-A develop aggressive mammary tumors compared to the non-Mdm2-A expressing mice (Volk et al., 2009a).

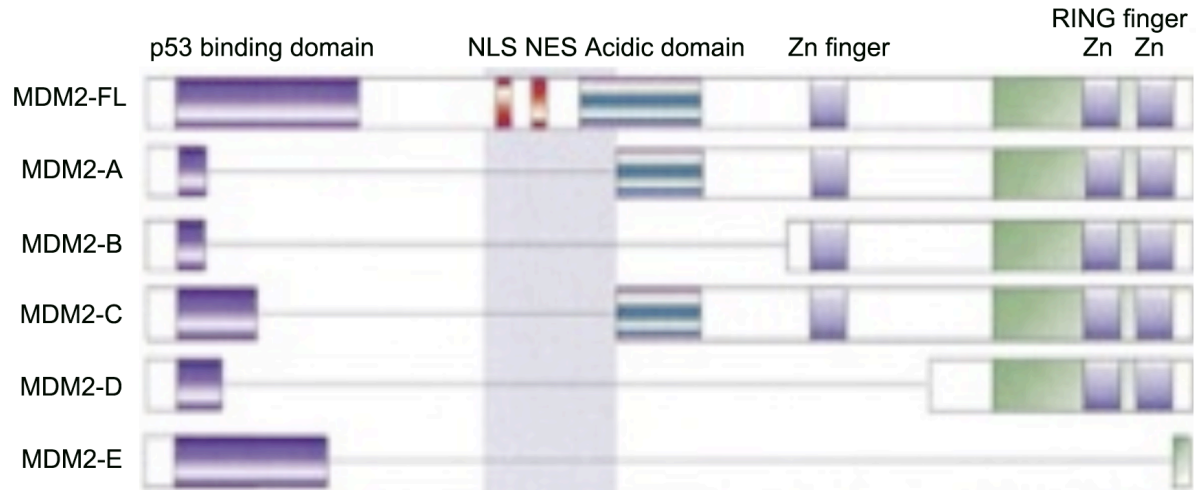

Adapted from(Bartel et al., 2004)

Figure 10: ***mdm2* splice variants and their putative protein domains**. *There are over seventy* mdm2 *splice variants known. This depicts a representation of five of them and their putative protein domains. These five have been* in vitro *translated in rabbit reticulocyte lysates and shown to form protein. Most* mdm2 *splice variants have lost the nuclear localization and most of the p53 binding domain regions.*

There are three well-characterized *mdm2* splice variant transcripts. They are *mdm2-A, mdm2-B* and *mdm2-C,* ALT2, ALT1 and ALT 3 respectively (Fig. 10) (Jeyaraj et al., 2009). These variant transcripts are expressed by numerous cancer types including soft tissue sarcoma, Hodgkin's' lymphoma, liposarcomas and breast cancers (Bartel et al., 2002; Bartel et al., 2001b; Sanchez-Aguilera et al., 2006; Sigalas et al., 1996; Tamborini et al., 2001). Interestingly, some *mdm2* splice transcripts are not expressed in normal tissues (Bartel et al., 2002; Chandler et al., 2006; Harris, 2005; Lukas et al., 2001; Momand et al., 1998; Sigalas et al., 1996). The presence of *mdm2* splice variant transcripts in tumors is associated with poor prognosis for patient survival (Bartel et al., 2001a; Matsumoto et al., 1998). Therefore, characterizing the functions of *mdm2* alternative splice variants could help categorize them as prognostic markers in certain cancers.

1.9 **Mdm2 Over-Expression**

Mdm2 is over-expressed in cancers and is often associated with increased aggressiveness of the disease. Mdm2 is over-expressed usually in three ways: genomic amplification (Meddeb et al., 1996; Oliner et al., 1992; Reifenberger et al., 1993), enhanced translation (He et al., 1994; Landers et al., 1997; Landers et al., 1994) and enhanced transcription (Bueso-Ramos et al., 1993; Sheikh et al., 1993; Watanabe et al., 1994). A naturally occurring example of enhanced transcription of the *mdm2* gene is a G/G single nucleotide polymorphism at position 309 (SNP309). This single nucleotide change lies in the first intron of the *mdm2* gene, adjacent to the p53 responsive elements of the stress-dependent *mdm2* P2 promoter (Bond et al., 2004).

1.9.1 **Single Nucleotide Polymorphism at Position 309 (SNP309) in the *mdm2* Gene**

In 2004, Bond et al. discovered the SNP 309 in the *mdm2* gene. This SNP is a nucleotide change from a Thymine to a Guanine (T to G), and leads to increased transcription from the *mdm2* P2 promoter (Fig. 11). The extra G in the DNA sequence increases the binding affinity of the *mdm2* gene for the transcription factor, Sp1. The increased Sp1 binding allows for increased transcription from the *mdm2* P2 promoter (Bond et al., 2004). Therefore due to the increased transcription and translation potential of the P2-derived mRNA transcripts (Brown et al., 1999; Landers et al., 1997), Mdm2 is over-expressed. In addition, there is a simultaneous attenuation of p53 activity observed in cells with Mdm2 over-expression through the G/G *mdm2* SNP309 (Arva et al., 2005; Bond et al., 2004).

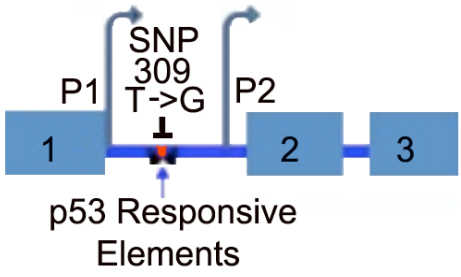

Figure 11**: *mdm2* Single Nucleotide Polymorphism at position 309-** *The single nucleotide change from a Thymine to a Guanine (T -> G) in the* mdm2 *gene increases the affinity of the promoter region for the ubiquitous transcription factor, Sp1. This increased affinity for Sp1 increases transcription from the* mdm2 *P2 promoter.*

1.10 **Mdm2 and Cancer**

Christine Eischens' laboratory showed that in mice, increased levels of Mdm2 result in B-cell lymphomagenesis. This is due to increased proliferation and reduced susceptibility to p53-dependent apoptosis, which leads to an increase in chromosomal breaks (Alt et al., 2005). The B-cells consequently acquire a growth advantage (Wang et al., 2008) and become transformed (Bouska et al., 2008). Unlike cancers with wild-type p53, cancers with mutant p53 and Mdm2 over-expression are more aggressive (Cordon-Cardo et al., 1994). Interestingly, work by Lundgren et al. has shown that targeted over-expression of Mdm2 in the mammary gland of mice inhibits normal development, increases aneuploidy and promotes tumorigenesis in the mice epithelial cells (Lundgren et al., 1997). Similarly, in melanoma, Mdm2 over-expression sustains oncogenesis via E2F-1 (Verhaegen et al., 2012). Additional experiments have shown that mice lacking *p53* but having two copies of the *mdm2* gene develop tumors faster (140.2 days) compared to their *mdm2* -/+ heterozygous (156.5 days) counterparts (McDonnell et al., 1999).

Another connection between cancer and Mdm2 can be found in SNP309 homozygous cancers. There are correlations between the G/G SNP309, cancer susceptibility, aggressiveness and patient survival (Bond et al., 2006a; Bond et al., 2005; Bond et al., 2006b; Gryshchenko et al., 2008; Walsh et al., 2007). Bond et al. showed that the G/G SNP309 status accelerates tumor formation in a gender and hormone-dependent manner (Bond et al., 2006a; Bond et al., 2004; Bond et al., 2006b). Boersma et al. also showed a positive correlation between G/G *mdm2* SNP309 status and breast cancer (Boersma et al., 2006).

The Lozano laboratory has made a humanized mouse with the G/G *mdm2* SNP309 gene region from the human gene loci inserted into the mouse *mdm2* gene loci. They observed that the humanized mouse has more *mdm2* transcript and protein made compared to the T/T SNP309 mouse. In addition, these G/G *mdm2* SNP309 mice exhibit a different tumor spectrum compared to their T/T *mdm2* SNP309 counterparts and develop tumors a year earlier (Post et al., 2010). This strongly suggests that the G/G *mdm2* genotype potentiates the incidence of tumors and that its presence denotes a vital biomarker in cancer detection. In our laboratory, we have observed that cells with the G/G *mdm2* genotype exhibit a wide range of *mdm2* splice variants (missing exons- 5 - 9; 5 - 9, 11; 6 - 8; 7 - 8) compared to their T/T counterparts (missing exons- 5; 10) (Arva et al., 2008). This suggests that in cells with the G/G *mdm2* genotype, the generation of various *mdm2* splice variants and potential variable Mdm2 polypeptides may be the means through which the G allele contributes to cancer incidence.

In Estrogen Receptor positive (ER+) women, increased hormone levels lead to increased proliferation of cells and tumorigenesis. Estrogen has been shown to increase Mdm2 protein and transcript levels in ER+ breast cancer cells in a p53-independent manner (Brekman et al., 2011). The increase in Mdm2 also increases cell proliferation. The influence of the SNP309 in cancer outcome and prognosis is still under investigation as the interacting pathways and methods of action are not well understood.

CHAPTER 2:

Materials And Methods

2.1 ***Plasmids-*** pCR II-TOPO (Invitrogen); Human Mdm2 expression plasmid, pcDNA3.1-F-hdm2 was a generous gift from Dr. Carol Prives; PGL2-Basic; *p21*-Luciferase (*p21* p53 responsive elements adjacent to the luciferase gene) (Datto et al., 1995); Sn3 (p53) (Baker et al., 1990), PNY and pAAV-LAZ were generous gifts from Dr. Diego Loayza; PRK53 (p53), pBabe-puro/cherry was a generous gift from Dr. Xuejun Jiang.

2.1.1 ***Plasmid DNA cloning-*** pcDNA3-F-hdm2 was used as a swap backbone to generate the clone containing exons- 2, 3, 4, 10, 11 and 12 for pcDNA3.1-P2mdm2-C plasmid. Restriction enzymes- BamHI and EcoRI (New England Labs) were used for this swap to sub-clone exon 2-12 for mdm2-C into the pcDNA3-F plasmid retaining just the end of exon 12. DNA sequences for *mdm2-FL* and *mdm2-C* from the pcDNA3.1 vector were sub-cloned with enzymes- BamHI and EcoRI (New England Labs), into the pBABE-PURO/CHERRY vector. The *mdm2* knock out construct consists of sequences of the left arm (exon 1 and part of intron 1), the deleted region (part of intron 1, exon2 and 3 and intron 2) and the right arm (exon2 part of intron 3). These regions were amplified via PCR and sub-cloned into the pNY vector and then transferred into the pAAV-LAZ vector (eliminating the LACZ gene). The pcDNA3 vector is a mammalian expression vector that contains a eukaryotic pCMV promoter and a bacteria T7 promoter. The pBabe-puro vector is a mammalian expression vector created in the Robert Weinberg's laboratory (Morgenstern and Land, 1990). It contains an SV40 promoter for insert expression. The pBabe-puro/cherry vector was created in the Jiang lab at Memorial Sloan Kettering Cancer Center (MSKCC).

2.1.2 ***cDNA cloning for* mdm2 *splice variant analysis-*** Cells were pelleted at 1,100 rpm for 6 minutes at 4^{o}C, washed twice with ice-cold phosphate buffered saline (1XPBS), and cells were frozen at -80^{o}C overnight. The RNA was isolated using QIAshredder columns and the RNeasy Mini Kit (Qiagen) following manufacturer's protocol and the resulting RNA was stored at -80^{o}C. 5µg of RNA was used for cDNA synthesis using the High Capacity cDNA Archive Kit reagents and protocol (Applied Biosystems), where the Reverse Transcription (RT) master mix (containing RT buffer, dNTPs, random primers and MultiScribe reverse transcriptase) along with the RNA was incubated at room temperature for 10 minutes and then at 37^{o}C for 2 hours. 3µl cDNA was combined with 5.25ul nuclease-free water, 12.5µl Taqman Universal Master Mix and 0.50µM primer mix containing primers flanking *mdm2* exons 2 and 12 (forward: TGTGTTCAGTGGCGATTGGAG, reverse: GGGGGATTCATTTCATTGCATG) for amplification via polymerase chain reaction (PCR) in a GeneAmp 5400 (Perkin Elmer, Waltham, Mass). The amplification steps were as follows: one cycle, 10 minutes, 95^{o}C; 35 cycles, 30 seconds, 95^{o}C, 30 seconds, 59^{o}C, and 2 minutes 72^{o}C; and 10 minutes, 72^{o}C. The PCR products were cloned into the pCR II-TOPO plasmid using the TOPO TA Cloning Kit (Invitrogen). Plasmids were isolated with the FastPlasmid Mini Kit (Eppendorf) and 500ng was digested with EcoRI (New England Biolabs). Digested plasmids were resolved by agarose gel electrophoresis. 500ng of plasmids that contained inserts were sent for sequencing using the M13 forward (TGTAAAACGACGGCCAGT) and reverse (CAGGAAACAGCTATGAC) primers. The plasmids were sequenced using an Applied Biosystems Prism 3730 DNA Analyzer.

2.2 ***Identification of mdm2 splice variants-*** After sequencing, the cDNA sequences obtained were compared with the full-length *mdm2* sequence (GenBank AF527840.1) using the BL2SEQ program. A PERL script based on Bio:Graphics, a BioPerl (bioperl.org) module, was written (Dr. Weigang Qiu) to graphically render BL2SEQ results using bidirectional-sequencing output. Genomic sequences were translated to amino acid by using the Expasy amino acid to protein translation tool (www. Expasy.org/tools/DNA).

2.3 ***Cell culture –*** The tissue culture cells used in this study were: A875, K562, ML-1, MANCA, SJSA-1, H1299, -/- MEFs (*p53/mdm2*), T47D and MCF-7. A875 cells were a generous gift from Arnold Levine; K562, SJSA-1, H1299, MCF-7 and T47D cells were purchased from American Type Culture Collection (ATCC); ML-1 cells were a generous gift from Michael Kastan; MANCA cells were a generous gif from Andrew Koff; *mdm2/p53* double knockout Mouse embryonic fibroblasts (-/- MEFs) were a generous gift from Guillermina Lozano. Tissue culture cells were grown in RPMI 1640 media (Mediatech) or DMEM media (CellGro), containing 10% fetal bovine serum (FBS, Gemini) and 50 U/ml of penicillin and 50µg/ml of streptomycin (Mediatech). All cells were incubated with 5% CO_2 at 37^{o}C. Estrogen (E2) treatments were performed using phenol red-free DMEM or RPMI with 10% charcoal stripped FBS and 50U/ml of penicillin and 50µg/ml of streptomycin.

2.3.1 **Radioactive labeling of endogenous proteins**- $2x10^7$ MANCA cells were washed in 2X labeling medium- RPMI minus L Methionine (Mediatech). The cells were

re-suspended in 25ml labeling medium plus 0.02μci/μl ^{35}S methionine (> 1000mCi). Cells were incubated at 37^{o}C with CO_2 for 16 hours. Activated charcoal was placed in the incubator during incubation to capture sulfuric gases emitted during ^{35}S methionine incorporation. Cells were collected after 16 hours, washed in cold 1XPBS and lysed for protein concentration. The ^{35}S methionine incorporated was measured via a scintillation counter (Perkin Elmer).

2.3.2 ***Drug treatments –*** Drugs used in this study include: DMSO, etoposide, estrogen (17β Estradiol, E2). All drugs were purchased from Sigma. Cells were treated for 3 or 24 hours at the concentration of 8μM of etoposide and three or five days at 10nM E2.

2.3.3 ***Cellular protein extracts***

– Whole cell extracts- Cells were pelleted at 1,100 rpm for 6 minutes at 4^{o}C, washed twice with ice-cold PBS and re-suspended in 1.5-2X packed cell volumes of 1X lysis buffer (0.1% TritonX-100, 50mM Tris.Cl PH-7.5, 15mM EGTA, 100mM NaCl, 1mM PMSF, 8.5 μg/ml Aprotinin and 2 μg/ml Leupeptin). The cell suspension was incubated on ice for 30 minutes and vortexed at 6 minutes intervals to lyse the cells. The suspension was centrifuged at 13,000 rpm for 20 minutes at 4^{o}C. The supernatant was stored at -80^{o}C.

- ***Nuclear extraction-*** Cells were pelleted at 1,100 rpm for 6 minutes at 4^{o}C, washed twice with ice-cold PBS and re-suspended in 5 X packed cell volumes of 1X Buffer A (1M Hepes, 1M $MgCl_2$, 2M KCl, 1mM PMSF, 8.5 μg/ml Aprotinin and 2 μg/ml Leupeptin,

0.1mM DTT, 1:100 protease inhibitor cocktail). Cells were spun down at 2,000 rpm for 5 minutes at 4^{o}C and the supernatant was discarded. The pellet was re-suspended in 2X Buffer A and passed through a 20 G1/2 needle five times. The mixture was placed on ice for 10 minutes. The cell suspension was pun down for 10 minutes at 12,000 rpm at 4^{o}C and the supernatant was transferred to a new microtube. This is the cytoplasmic extract and it was stored at - 80^{o}C.

- ***Cytoplasmic extraction-*** The pellet from the cytoplasmic extraction was resuspended in 2X the packed cell volume of 1X Buffer C (1M Hepes, 1M $MgCl_2$, 5M NaCl, 0.5M EDTA, 25% Glycerol, 1mM PMSF, 8.5 µg/ml Aprotinin and 2 µg/ml Leupeptin, 0.1mM DTT, 1:100 protease inhibitor cocktail). The cell suspension was passed through a 20 G1/2 needle several times to break up the pellet. The suspension was rocked at 4^{o}C for 30 minutes and spun down for 30 minutes at 12,000 rpm. The supernatant was transferred to another microtube; this is the nuclear extract and it was stored at – 80^{o}C

2.3.4 ***Chromatin fractionation***- Cells were pelleted and washed 3x in 1XPBS. The cell pellet was re-suspended in 10x packed cell volume (PCV) of Buffer A (10mM HEPES pH7.9, 10mM KCl, 1.5mM MgCl2, 0.34M sucrose, 10% glycerol, protease inhibitors, 1mM DTT) +0.1% TritonX-100 and allowed to incubate on ice for 5 minutes without vortexing. The mixture was spun down at 3,600 rpm for 5 minutes at 4^{o}C and the supernatant was collected. This is the S1 (cytoplasmic) fraction. The pellet was washed and spun down at 3,600 rpm for 5 minutes at 4^{o}C in 2x in Buffer A. The pellet was then re-suspended in 1x PCV of Buffer B (3mM EDTA, 0.2mM EGTA and protease inhibitors)

and kept on ice for 30 minutes with vortexing every 5 minutes. The mixture was spun down at 4,000 rpm for 5 minutes at 4^{o}C and the supernatant was collected. This is the S2 (nuclear soluble) fraction. The remaining pellet was washed twice with Buffer B and spun down at 4,000 rpm for 5 minutes at 4^{o}C. The pellet was re-suspended in 2x PCV of Buffer B and was sonicated 3x for 30 seconds and 30 seconds rest intervals on ice and at high amplitude. This is the P3 (chromatin) fraction.

2.3.5 ***Western blot analysis –*** Protein samples were prepared in 6X protein sample buffer (0.12% Bromophenol blue, 0.1% SDS, 0.3% Glycerol in 4X Tris.Cl/SDS PH-6.8) or 4X protein sample buffer (4X NuPAGE Lithium Dodecyl Sulphate buffer, 20mM DTT). Samples prepared in 6X PSB were heated at 95^{o}C for 10 minutes and samples prepared in 4X NuPAGE buffer were heated at 70^{o}C for 10 minutes after which 1μl of 1M iodoacetamide (Sigma-Aldrich) was added to prevent re-ligation of di-sulfide bridges and protein aggregates. All samples were separated via 10% SDS-PAGE followed by an electro-transfer to nitrocellulose membrane. The membrane was blocked in 5% non-fat milk in a solution of 1XPBS/0.1% Tween 20 and was probed overnight at 4^{o}C. Washes were done with 1XPBS/0.1% Tween 20 solution. Secondary anti-mouse or anti-rabbit antibody (Sigma) was applied to the membrane for 1 hour at room temperature and the membrane was washed three times. Protein signal was activated by chemiluminescence using the Super signal kit (Pierce) and detected after exposure for autoradiography to Hyblot CL films (Denville Scientific).

2.3.6 ***Antibodies***- The following antibodies were used for western blot, immunoprecipitation, immunofluorescence or immunohistochemistry analysis: anti-p53 mouse monoclonal supernatant mix- 1801, 421 and 240 (N-terminus, Central and C-terminus regions respectively) (Bargonetti et al., 1993); anti-Mdm2 monoclonal supernatant mix- 4B2, 2A9 and 4B11 (N-terminus, Central and C-terminus regions respectively) (Chen et al., 1993), anti-Mdm2: SMP14 (Sigma), anti-Mdm2: N-20 (Santa Cruz), anti-Mdm2-C rabbit polyclonal immune serum, anti-Mdm2-C mouse polyclonal; rabbit pre immune serum, mouse pre immune serum; anti-Actin (Sigma); anti-eIF-4E (Cell signaling), anti-Nucleolin: C23 (Santa-Cruz); anti-hnRNPA1 (a generous gift from Dr. Karen Hubbard at City College of New york, CUNY); anti-HSP90 (Cell signaling) and anti-HSP70 (Cell Signaling).

2.4 ***Genomic DNA extraction-*** A875 (G/G *mdm2* SNP309/ wild-type *p53*) cells were lysed as per manufacturers instruction (Qiagen) and Genomic DNA was extracted and quantified.

2.4.1 ***RNA isolation and quantitative RT-PCR –*** Cells were pelleted at 1,100 rpm for 6 minutes at 4^{o}C, washed twice with ice-cold phosphate buffered saline (1XPBS), and cells were frozen at -80^{o}C overnight. The RNA was isolated using QIAshredder columns and the RNeasy Mini Kit (Qiagen) following manufacturer's protocol and the resulting RNA was stored at -80^{o}C. 5µg of RNA was used for cDNA synthesis using the High Capacity cDNA Archive Kit reagents and protocol (Applied Biosystems), where the

Reverse Transcription (RT) master mix (containing RT buffer, dNTPs, random primers and MultiScribe reverse transcriptase) along with the RNA was incubated at room temperature for 10 minutes and then at 37^{o}C for 2 hours. cDNA was stored at -20^{o}C. Gene transcripts were amplified by quantitative RT-PCR (qRT-PCR) with primer probes for *puma* (Hs00248075_m1), *mdm2* (Hs00242813_m1), *p21* (Hs00355782_m1) and *actin* (4352935E) from Applied Biosystems Assays on Demand primers. 150ng of cDNA was combined with Taqman Universal Master Mix and 1.25μl of 10μM primers for qRT-PCR. In addition, primers to *mdm2-C* (exon 4:10 Forward: $^{5'}$GAAAGAGGATCTTGATGCTGGTGTA$^{3'}$ and exon 12 Reverse: $^{5'}$GGGGGATTCATTTCATTGCATG$^{3'}$) were used in a Syber Green qRT-PCR reaction to quantify *mdm2-C* transcripts. cDNA was diluted 1:10 and 3μl (15ng) of cDNA was combined with Taqman Universal Master Mix and 0.125μl of 10μM primers for qRT-PCR. The PCR reaction was carried out following the program: one cycle, 2 minutes, 50^{o}C; one cycle, 10 minutes, 94^{o}C; and 40 cycles, 15 seconds, 94^{o}C and 1 minutes 60^{o}C in a 7500 Sequence Detection System (Applied Biosystems).

2.5 ***Preparation of radioactive probe for northern blot analysis-*** Plasmid DNA was combined with Taqman Universal Master Mix and primers flanking regions of *mdm2* exons 12 (forward: TTCGTGAGAATTTGGCTTCCT, reverse: GGCAGGGCTTATTCCTTTTC- both in the 5' to 3' direction) or GAPDH (forward: TGATAGCATCAAGAAGGTGGTGAAT, reverse: TCCTTGGAGGCCATGTGGGCCAT- both in the 5' to 3' direction) for PCR in a GeneAmp 5400 (Perkin Elmer, Waltham, Mass). The amplification steps were as follows: one cycle, 5 minutes- 50^{o}C, 10 minutes-

94^{o}C; 35 cycles, 30 seconds- 94^{o}C, 30 seconds- 58^{o}C (*mdm2*) or 55^{o}C (*GAPDH*), and 2 minutes- 72^{o}C; and one cycle, 10 minutes- 72^{o}C. The resulting PCR products were purified using the QiaQuick PCR Purification Kit (QIAGEN). 25ng of PCR templates were used for Random labeling with the High Prime Random Labeling Kit (Roche) and Easy Tag α-^{32}P dCTP (Perkin Elmer) was used as the radioactivity source. The resulting probes were cleaned using Sephadex^{TM} G-50 DNA Grade Nick Columns (GE Healthcare) and the count per minutes (CPM) was measured using the Scintillation counter (Perkin Elmer)**.**

2.5.1 ***Northern blot analysis-*** mRNA samples were purified from total RNA using the Oligotex mRNA Mini Kit (QIAGEN). Total RNA samples were separated using a 1.0% denaturing formaldehyde agarose gel followed by a 10X SSC capillary action transfer onto a BrightStar-Plus positively charged nylon membrane (Ambion) no more than 6 hours. RNA was cross-linked to the membrane via Ultra Violet exposure at the optimal setting for 1 minute. The membrane was then pre-hybridized in formamide pre-hybridization/hybridization solution for 3 hours at 42^{o}C after which the probe (heated at 95^{o}C for 10 minutes and placed on ice to cool) was added to the membrane for hybridization over night. The membrane was then washed three times for 10 minutes, each at different stringencies (2X SSC/0.1% SDS; 0.2XSSC/0.1% SDS and 2X SSC). Autoradiography was achieved by exposing the membrane to Kodax BioMax XAR films (KODAX) at room temperature and at – 80^{o}C with screen.

2.6 **In vitro *transcription/ translation-*** 100-1000ng of Xho1 linearized pcDNA3-mdm2-FL, pcDNA3-mdm2-C or PRK53 plasmid DNA was mixed with components of the wheat germ extract kit (Promega) [25μl Wheat germ extract, 1μl amino acid without Methionine mix, 1μl RNA polymerase II, 2μl of reaction buffer, 2μl of radiolabelled ^{35}S methionine (20.4μci of 1175ci/mmol)] (Promega) and the reaction was brought to 50μl with nuclease-free water and allowed to sit at 30^{o}C for 90 minutes. Radiolabelled ^{35}S methionine (Promega) was used as a radiolabel source. The resulting protein was resolved on a 10% polyacrylamide gel.

2.7 ***Immunoprecipitation –*** *In vitro* translated protein products or 0.75-4mg of MANCA whole cell extracts were incubated with 1-2μg (purified antibodies- SMP14) or 5-10μl (serum antibody- C410 and Pre-Immune- serum), in 300-500μl of 1X lysis buffer (0.1% Triton-X w/v, 50mM Tris.CL (P.H 7.5), 15mM Ethylene Glycol Tetraacetic Acid (EGTA), 100mM Sodium Chloride (NaCL), 1mM Phenylmethanesulfonyl Fluoride (PMSF), 2μg/ml Leupeptin and 10.3μg/ml Aprotonin). The mixture was placed at 4^{o}C over night and the next day, 30μl of 75% protein-A sepharose beads slurry was added for 3 hours. The protein-Antibody-beads mixtures were spun down at 3,000 rpm for 2 minutes and washed 3X with 1X PBS/0.1% TWEEN 20. The complex was re-suspended in 30μl 1X protein sample buffer with 20mM DTT (with addition of 1μl of 1M Iodoacetamide (Sigma) after heating). Samples were heated at 70^{o}C for 10 minutes and resolved on a 10% acrylamide gel. 1-10% of protein input was also run along side the pull down samples.

2.7.1 ***Immunofluorescence*** **–** Cells were seeded onto glass coverslips at 10% confluency and grown for 5 days with and without 10μM estrogen. Suspension cells were spun down and re-suspended in serum-free medium. Cells were transferred into 12-well plates containing poly-lysine coated cover slips and allowed to settle and stick to the cover slips. After indicated treatments, cover slips were washed once with 1X PBS and fixed with 4% paraformaldehyde in 1X PBS for 15 minutes at room temperature. The slides were washed three times with 1X PBS, permeabilized with 0.5% Triton-X-100 in 1X PBS/1% FBS for 10 minutes at room temperature and washed three times with 1XPBS/1% FBS. The cells were incubated for 1 hour at room temperature with 1:200 dilution of rabbit anti-human Mdm2 C410 serum or rabbit anti-human pre-immune serum, mouse anti-human monoclonal p53 DO-1, eIF-4E mouse anti-human monoclonal, hnRNPA1 mouse anti-human monoclonal, Nucleolin (C23)- mouse anti-human monoclonal, HSP90 rabbit anti-human monoclonal and HSP70 mouse anti-human monoclonal. The slides were washed three times with 1XPBS/1% FBS, incubated with 1:200 dilution of Alexa-conjugated goat anti-rabbit (Invitrogen) and FITC-conjugated goat anti-mouse (Jackson ImmunoResearch) secondary antibodies, and washed again three times with 1XPBS/1% FBS. Coverslips were then mounted onto slides using Vectashield mounting medium containing 4', 6-diamidino-2-phenylindole (DAPI) to visualize the nuclei. Images were collected with a Nikon fluorescent microscope at 60X magnification.

2.7.2 ***Spinning disk confocal microscopy-*** Cells were visualized using spinning disk confocal microscope. All confocal images were captured with the 60X objective. Images were visualized and captured under different channels: rhodamine (red), FITC (Goldstrohm et al.) and ultra violet light (Blue for DAPI). Single and double channel images were saved as TIFFS and analyzed for protein localization or protein:protein co-localization.

2.7.3 ***ImarisColoc for protein co-localization***- Images were captured with the spinning disk confocal microscope. Images were saved as OME.TIFF files and opened with the imariscoloc program. The rhodamine or FITC captured images for Mdm2-C were used for masking purposes in order to delineate the region of interest for co-localization analysis. The imaris slice software was used to determine the high and low signal threshold points for the two channels used to determine co-localization. The low signal threshold values were used to set the starting point parameters for co-localization detection. The imariscoloc percentages were calculated based on the area masked and the signal threshold parameters. Images were captured via screen capture and saved as TIFF files.

2.7.4 ***Immunohistochemistry-*** Paraffin embedded slides were de-paraffinized with xylene (2x 3 minutes) and xylene:100% ethanol (3 minutes). The slides were then hydrated in 100% ethanol (2x 3 minutes, 95% ethanol (3 minutes), 70% ethanol (3 minutes) and 50% ethanol (3 minutes). Slides were rinsed in water and placed in the

antigen retrieval buffer (10mM Tris base, 1mM EDTA and 0.05% Tween 20 PH 9.0) and boiled for 20 minutes after the solution had come to boiling. The slides were rinsed in cold water and washed 3x 5 minutes in 1X wash buffer (1X PBS/0.025% Triton X-100). Slides were blocked in blocker solution from the Vectastain ABC kit (Vector) for 1 hour at room temperature. The slides were rinsed in 1X wash buffer 3x 5 minutes. Primary antibody – C410 serum and pre-immune polyclonal serum were diluted to 1:100 in 1X PBS/1%BSA and incubated over night at 4^{o}C. The next day, slides were rinsed 3x 5 minutes in 1X wash buffer. The secondary antibody mixture was diluted in blocking solution and incubated fro 45 minutes at room temperature. The slides were washed 3x for 5 minutes in the wash buffer. The slides were developed for approximately one minute per slide using the peroxidase substrate kit, DAB (Vector). The slides were rinsed off with water immediately they began to develop. Slides were counterstained with Hams modified Hematoxylin (Mozzherin and Fisher) and washed in water 2x 5 minutes. The slides were then dehydrated as follows: 2x 95% ethanol, 2x 100% ethanol and 2x 100% xylene-. The slides were then mounted with Permount solution (Mozzherin and Fisher) and visualized under the Nikon bright upright microscope and pictures are taken at 20X and 40X magnification.

2.8 ***Annexin V-APC and PI staining for Fluorescence Activated Cell Sorting (FACS)*** - Cells were washed twice in cold 1X PBS and the supernatant was discarded. The cell pellet was re-suspended in cold 1X binding buffer to a concentration of $1x10^{5-6}$ cells/mL. Four tubes were labeled (A. unstained B. Annexin V-FITC only C. PI only D. Annexin V-FITC + PI) and 100µL of cells was added to each tube. 10µL of annexon V-

FITC was added to tubes B and D and the tubes were gently vortexed and incubated on ice for 15 minutes in the dark. After 15 minutes, 380µL of cold 1X binding buffer was added to all tubes and 10µL of PI was added into tubes C and D. The samples were then analyzed by flow cytometry.

2.9 ***Plasmid DNA transfection-*** Approximately 2-6x10^5 cells were plated per well in 6-well plates or at 50% confluence into 10cm plates per transfection. Cells were treated with Lipofectamin 2000 (Invitrogen) as per manufacturers instruction. 10ng of *Sn3* plasmid and 10-1000ng *pcDNA3.1-Fhdm2* or 10-1000ng *pcDNA3.1-P2mdm2-C,* were co-transfected with 10ng of *SN3* (Baker et al., 1990) plasmid and *p21-luciferase* plasmid (Datto et al., 1995). *PGL2* plasmid was used as a DNA control.

2.9.1 ***Luciferase assay-*** Cells were co-transfected with *Sn3*, *p2*1-luciferase reporter plasmid and pcDNA3.1-F*hdm2* or pcDNA3.1-P2*mdm2-C*. 48 hours after transfection, cells were lysed as stated above and assayed using the luciferase reporter assay (Promega) and activity was measured via luminoskan. Samples were normalized for the amount of protein.

2.9.2 ***DNA concentration curve for growth change-*** 6 x 10^5 cells were plated per well into 6-well plates in duplicates and transfected the next day. 48 hours after transfection, the numbers of cells were counted.

2.9.3 **siRNA transfection**- Cells were plated into 10cm plates at a 50% confluence. After 24 hours, the media was changed to DMEM/10% FBS media free of antibiotics. Cells were Lipofectamine 2000 (Invitrogen) treated as per manufacturers' with 10-16µl Lipofectamine and 10µM control (Dharmacon), *mdm2* (Smart pool from Dharmacon*)*, *mdm2-C* (Sense: AAAGAGGAUCUUGAUGCUGGUUU; Anti-sense: ACCCGCAUCAAGAUCCUCUUU) and *mdm2-C* scrambled (Sense: GAGGAAGGUUACGUGAUUCAUUU; Anti-sense: AUGAAUCACGUAACCUUCCUCUU) siRNA for 6 hours. DMEM Media containing 40% FBS was added to the cells for a total media volume of 10ml. The cells were allowed to grow for 48 hours with 5% CO_2 at 37^{o}C.

2.10 ***shRNA-mediated knockdown***: T47D and MCF-7 *mdm2* and empty vector (STGM) shRNA clones cells were plated at 50% confluence. After 24 hours, DMEM complete media containing 4µg/mL (T47D) or 2µg/mL (MCF-7) doxycycline was added to cells. The media was changed every other day to obtain maximum knockdown. After 6 days of doxycycline treatment and shRNA induction, cells were collected and examined for protein knockdown via microscopy (for GFP induction) and western blot (for protein knockdown).

2.11 ***Retroviral-mediated gene transfer- Preparation of retrovirus***: 293 Phoenix cells were transfected via Lipofectamine 2000 (Invitrogen) with pAAV-LAΔRAloxp (LA- left

arm, Δ- deleted region and RA- right arm) along aside VSV-G and gag-pol plasmids. Cells were incubated at 37^{o}C and virus was collected at 48, 72 and 96 hours.

2.12 ***Colony formation assay-*** H1299 and -/-MEF cells were transfected with 400ng of pBaBe-puro-*mdm2-FL* or pBaBe-puro-*mdm2-C* plasmids in the presence or absence of 10ng Sn3 plasmid. Five hours after transfection, the media was changed to complete RPMI/10%FBS or DMEM/10% FBS. 24 hours later cells were trypsinized and diluted. 2000 cells were plated into media with 2μg/ml puromycin on 10cm plates and allowed to grow for 2-3 weeks. Colonies were stained with methylene blue for 2 minutes (Sigma-Aldrich) and counted.

2.13 ***Trypan blue Staining-*** Cells were trypsinized and spun down at 1,100 rpm for 5 minutes. The cell pellet was re-suspended in serum-free DMEM and 0.4% Trypan blue dye (Sigma) was added to the cells at a 1:6 dilution ratio. The dye and cells mixture was allowed to sit at room temperature for 5 minutes and the total numbers of cells as well as the number of blue cells were counted.

2.14 ***Coomassie staining-*** Acrylamide gels were rinsed 3X with Milli-Q water for 15 minutes each and stained for an hour using Gelcode Blue (Thermo Scientific) as per manufacturers suggestions. The gel was de-stained with Milli-Q water and stored at 4^{o}C in water.

2.15 ***Liquid Chromatography tandem Mass Spectrometry (LC-MS/MS)*** - After comassie staining of proteins on the SDS-PAGE, protein bands were excised and trypsin was utilized for sample digestion. All samples were subjected to LC-MS/MS and the resulting data was uploaded onto a proteome software program, scaffold 3. Scaffold 3 analyses the MS/MS data and collates the information in a table format giving the identified peptides, their corresponding proteins, biological functions and classification based on biological function. The program identifies a protein based on the peptides observed and their frequency. The data obtained was put in a table format according to the frequency of peptides observed. N.B- The SDS-PAGE analysis was performed by the Mass spectrometry facility at Memorial Sloan Kettering Cancer Center (MSKCC).

CHAPTER 3:

mdm2-C Splice Variant Transcript, Endogenous Protein expression & Functions in the Non-canonical pathway of Mdm2

3.1:

Introduction

Although studies have shown that *mdm2* transcripts have the ability to form protein and alter the cellular processes when exogenously expressed, the presence of endogenous protein from *mdm2* spliced isoforms has not been documented. We hypothesized that endogenous Mdm2-C protein was responsible for oncogenic functions. Thus our goal was to determine the presence of the endogenously expressed Mdm2 isoform protein, Mdm2-C, its cellular location and the protein function. The *mdm2-C* transcript is missing exons 5 through 9, which contains a part of the p53 binding domain, the nuclear localization and export signals as well as a portion of the acidic domain. However, the transcript retains the coding sequences for the ZINC and RING finger domains.

Splicing is a naturally occurring process in which the cell expands its protein repertoire. The cell does this by eliminating some of its exons to generate a new form of protein with possibly, a function that is distinct and unique from its full-length protein. There are a number of transcripts that have splice variants with functions that are very important to cell survival such as BRCA1 and DNA methyl transferase (DNMT), whose alternative splice forms often are detrimental to the cell (Fackenthal and Godley, 2008). For example, the over-expression of two DNMT3B splice variant isoforms altered DNA methylation and increased cell proliferation (Ostler et al., 2007; Saito et al., 2002). The cellular function of DNMT is to catalyze DNA methylation. Therefore the alteration of DNA methylation in the presence of excess DNMT3B splice variant isoforms could indicate that the alternate forms of DNMT3B might promote aberrant cellular phenotypes.

The *mdm2* transcript undergoes alternative and alternative splicing. The *mdm2* gene possesses two promoters, P1 and P2, which are p53-independent and p53-dependent respectively. Transcription from the alternate promoters produces transcripts with: exons 1 and exon 3 spliced together with the exclusion of exon 2 (P1-derived transcript) or without exon 1 (P2-derived transcript). However, the resulting transcripts- P1: exons 1, 3-12 and P2: exons 2-12, produce the same protein product. This is because the reading frame of the polypeptide begins at exon 3. Mdm2 over-expression in cancers is often accompanied with the over-expression of alternatively spliced *mdm2* transcripts (Bartel et al., 2001b; Liang et al., 2004; Matsumoto et al., 1998; Sanchez-Aguilera et al., 2006; Sigalas et al., 1996). While over 40 *mdm2* alternatively spliced transcripts have been identified in multiple tumor types, (Bartel et al., 2002), only eight, Mdm2-A, A1, B, C, D, E, F and G have been shown to form protein *in vitro* (Anderson et al., 2007; Tamborini et al., 2001). Early studies showed that the expression of these five *mdm2* transcripts in NIH3T3 cells leads to foci formation (Sigalas et al., 1996). However, only two of these translatable isoforms, Mdm2-A and B, have been extensively studied to determine their biological functions.

Mouse studies with Mdm2-A showed that high expression of the protein caused an increase in tumorigenesis in a null or compromised p53 background and an altered tumor spectrum when compared to the control (Volk et al., 2009a; Volk et al., 2009b). Mdm2-B mouse studies showed a difference in the incidence of tumor formation in a *p53*-null background when compared to the control (Steinman et al., 2004). Interestingly, an Mdm2-B mouse in a wild-type *p53* background was found to be non-

viable. This could be due to cell death caused by the presence of active p53 that cannot be regulated by Mdm2-B (Sigalas et al., 1996).

We have documented that despite paradoxically high p53 protein levels, cells with Mdm2 over-expression through a single nucleotide polymorphism at position 309 (SNP309) in the *mdm2* gene have compromised p53 activity (Arva et al., 2005). The nucleotide changes from a thymine to a guanine, increases the affinity of the *mdm2* promoter region for Sp1 and promotes enhanced transcription from the *mdm2* P2 promoter therefore resulting in high levels of *mdm2* transcript and protein (Bond et al., 2004). After cellular stress via DNA damage, cells possessing two gene copies of the SNP (G/G *mdm2* SNP309), when compared to cells with the T/T *mdm2* SNP309 genotype, were unable to efficiently activate p53 target genes (Arva et al., 2005; Bond et al., 2004). The inability to activate p53 after cellular stress has been attributed to the persistent presence of the Mdm2:p53 complex on the chromatin (Arva et al., 2005). As a result, we postulated that: cells with Mdm2 over-expression might have an alternative form of Mdm2 protein that negatively influences p53 on the chromatin despite damage-induced modifications. We hypothesized that this might result from a different distribution of *mdm2* splice variant isoform messages, derived due to increased Mdm2 expression that produced Mdm2 isoform proteins with altered biological activity.

Although the canonical functions of Mdm2 (E3 ubiquitin ligase) towards p53 are more widely focused on, the promiscuity of Mdm2 in protein binding partners has lead to the discovery of Mdm2 function in several molecular pathways. The Mdm2 protein has been found to be involved in a plethora of p53-independent pathways such as

transcription, DNA repair, RNA binding, cell growth, etc. (Okoro et al., 2012). Some examples of proteins that bind to Mdm2 include (see Fig. 5 in introduction): E2F1, whose binding to Mdm2 results in its transcriptional stimulation and a possible increase in cell proliferation by an up-regulation of cell cycle specific proteins (Loughran and La Thangue, 2000; Martin et al., 1995); NBS1, a component of the Mre11/Rad50/NBS1 (MRN) complex (Alt et al., 2005), whose binding to Mdm2 results in a delay in DNA repair after a damage response (Bouska and Eischen, 2009a; Bouska et al., 2008) that is p53-independent (Bouska and Eischen, 2009b).

We have detected high levels of *mdm2-C* transcript, which correlates with Mdm2 over-expression. We have created an Mdm2 isoform specific polyclonal antibody, Mdm2 C410 that detects endogenous Mdm2-C. We have found that Mdm2-C does not function in the Mdm2 canonical pathway. In addition, we observed that estrogen treatment increased Mdm2-C expression and the over-expression of Mdm2-C protein increased colony formation. Our results show that Mdm2-C contributes to a non-canonical pathway of Mdm2 and may be important for tumor survival.

3.2:

Results

3.2.1 **Mdm2 and Its Splice Variant, *mdm2-C***

To begin to address our hypothesis, we performed *mdm2* cDNA cloning using a panel of cell lines with variable SNP309 genotypes (see Table 1), in order to examine the presence and species of *mdm2* alternatively spliced variants when Mdm2 was over-expressed. To survey what transcripts might contribute to the compromised p53 activity observed in G/G cancer cells, we assessed transcripts specifically from the internal *mdm2* P2 promoter. Primer sets to exon 2 and exon 12 were used in a PCR reaction to amplify all P2-derived transcripts (Fig. 12A). Derived transcripts were cloned (by TA cloning) and several clones (over 100) were screened. We discovered a number of splice variant *mdm2* cDNAs, which slightly differed among the panel of cells. We observed that some had previously been identified from the P1 promoter (Bartel et al., 2002).

CELL NAME AND CANCER TYPE	*mdm2* SNP309 STATUS	*p53* STATUS
MANCA (Burkitts' Lymphoma)	G/G	WT
SJSA-1 (Oesteosarcoma)	T/T*	WT
ML-1 (Myeloid Leukemia)	T/T	WT
K562 (Chronic Myeloid Leukemia)	T/G	NULL

Table 1: Panel of cells with different *mdm2* and *p53* statuses.
*SNP309 represents-Single Nucleotide Polymorphism at position 309 in the mdm2 gene. G represents Guanine, T represents Tyrosine and WT represent wild-type. * Represents genomic amplification of the mdm2 gene- 25 copies (Tovar et al., 2006).*

In order to determine whether a specific *mdm2* splice variant transcript stands out in Mdm2 over-expressing cells vs. other cell lines, we aligned the splice variant transcript sequences from the panel of cells to the full-length *mdm2* DNA sequence. The alternatively spliced *mdm2* transcripts from the panel of cells were aligned in order to determine which exons were excised and their relative frequency. We observed that cells that over-express Mdm2 possessed a high frequency of transcripts with large regions excised. This suggests that the increased transcription of *mdm2* could be driving the production of alternative splice variants of *mdm2.* One recurring *mdm2* transcript identified in Mdm2 over-expressing cells was the variant missing exons 5-9, *mdm2-C* (Fig. 12B).

The *mdm2-C* transcript is one of three major transcripts (in addition to *mdm2-A* and *mdm2-B)* often found over-expressed in cancers (Jeyaraj et al., 2009). *In silico* translation using the online translation tool, ExPasy showed that the *mdm2-C* transcript was translatable to protein and this had been previously proven *in vitro* and published (Anderson et al., 2007; Sigalas et al., 1996). The polypeptide sequence produced was observed to be spliced in-frame (apart from regions spliced out) to the full-length Mdm2 polypeptide sequence (Fig. 12C). However, while the transcript can be translated to protein *in vitro* and via exogenous expression, it has never been detected as an endogenous protein isoform.

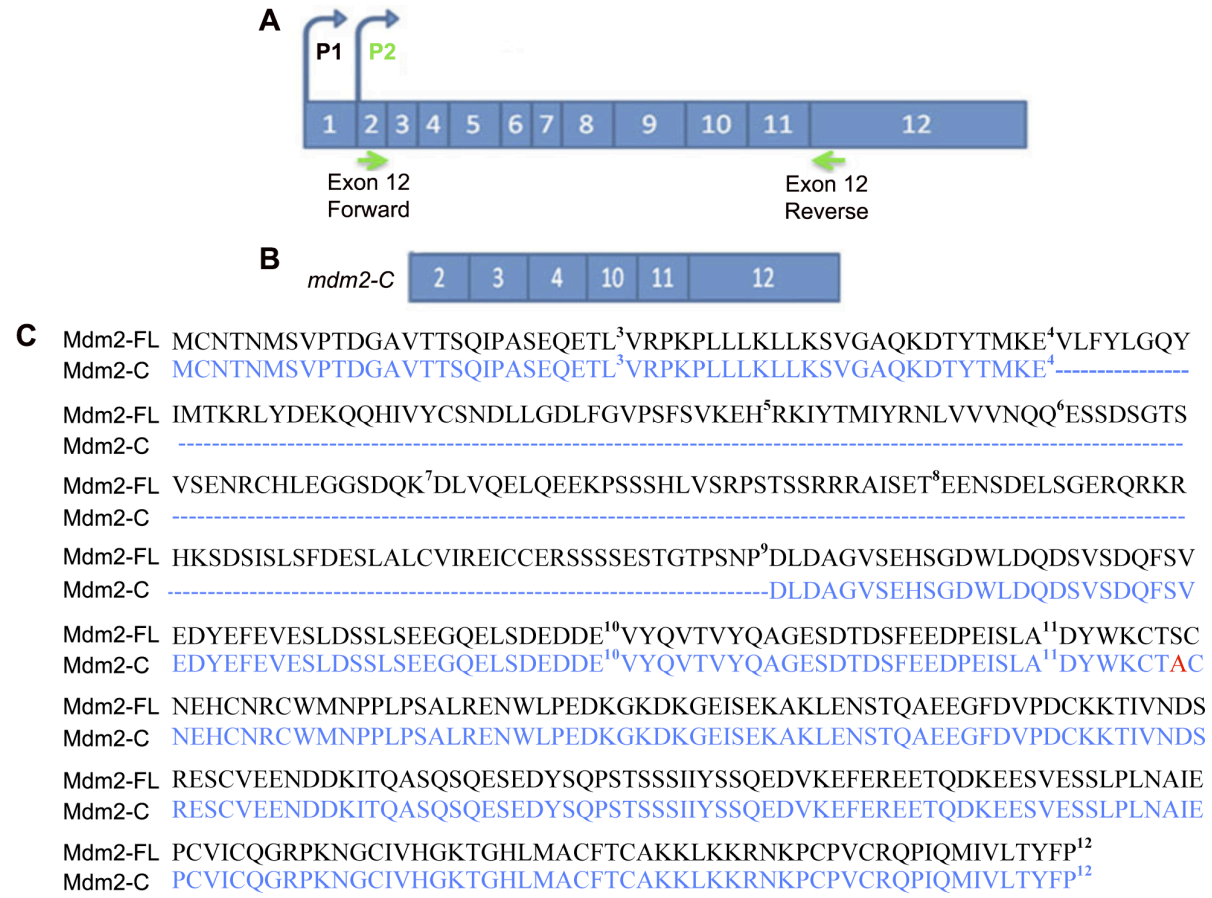

Figure 12: **The *mdm2-C* transcript is predominantly observed in Mdm2 over-expressing cells and the polypeptide is spliced in frame to full-length *mdm2*.**
A. *Schematic of* mdm2*, its exons and promoters. The primers used in cDNA cloning are depicted. The forward primer is specific to exon 2 and the reverse primer is specific to the beginning of exon 12.* **B.** *Schematic of the* mdm2-C *transcript derived from the mdm2 P2 promoter and the exons it retains.* ***C.*** *The polypeptide sequences of Mdm2-FL and Mdm2-C aligned after* in silico *translation using the computer tool found at www.ExPasy.org. The RED highlighted amino acid in the Mdm2-C polypeptide sequence represents a change in nucleotide that switched the amino acid from a serine to an alanine.*

The cDNA cloning revealed a higher apparent ratio of *mdm2-C* transcript to other transcripts in cells that over-express Mdm2. However, we did not know how the total *mdm2* levels compare in the panel of cells with different *p53* and *mdm2* statuses (Table

1). In order to determine the level of total *mdm2* RNA in the panel of cells, we began by performing a northern blot. We quantified *mdm2* transcripts via northern blot using a ^{32}P α-dCTP radiolabelled DNA probe amplified from exon 12 sequences (Fig. 13A). We observed that Mdm2 over-expressing cells- MANCA and SJSA-1- had high levels of *mdm2* transcript (Fig. 13B). We observed a predominant RNA species at approximately 8 kb in MANCA and K562 cells (Fig. 13B lanes 1 and 4). SJSA-1 cells showed a smear of RNA species between 9.49 kb and 1.35 kb (Fig 13B lane 2). The difference between SJSA-1 and MANCA cells is most likely due to the over-expression of Mdm2 because of gene amplification (25 *mdm2* gene copies) (Tovar et al., 2006). ML-1 cells did not show significant amount of *mdm2* transcript but with a along exposure, there were very faint smaller sized transcripts observed between 4.4 kb and 1.35 kb (data not shown). Thus suggesting that ML-1 cells produced truncated *mdm2* transcripts. The reason for very long *mdm2* transcripts is not understood. The coding mRNA for mdm2-FL is only 1.4 kb.

In order to determine the fold difference in *mdm2* transcript levels in the panel of cell lines, we compared all the samples to the *p53*-null K562 cell line. Image J quantitation of the radioactivity signal showed that SJSA-1 cells had the highest fold increase of *mdm2* transcript with a fold level increase of 4 (with the error bar deduction) (Fig. 13C). On the other hand, image J quantitation showed that MANCA cells had an *mdm2* transcript fold level increase of 3 (with the error bar deduction) while ML-1 cells had a fold level increase of 2 (Fig. 13C). Nonetheless, this quantitation did not distinguish between the different *mdm2* transcript species.

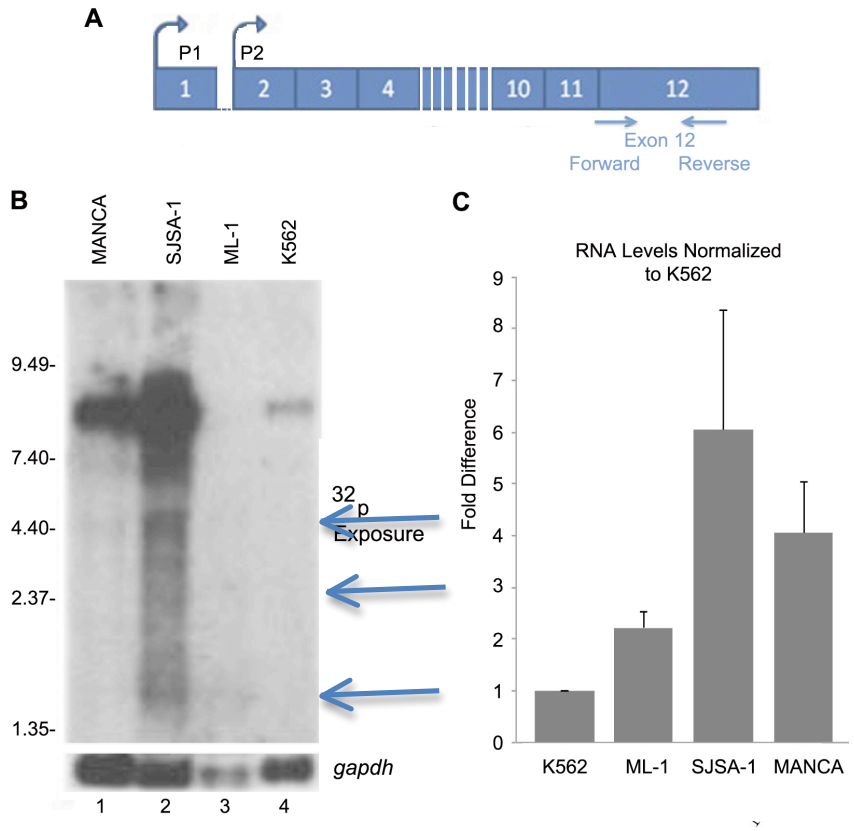

Figure 13: **Mdm2 over-expressing cells have high *mdm2* transcript levels.**
A. *Schematic of* mdm2*, its exons and promoters. The primers used in creating the probe for northern blot analysis is depicted. The forward and reverse primers are to sequences in exon 12. The product was random labeled with* ^{32}P *α-dCTP.* **B.** *Northern blot quantitation of total RNA from untreated MANCA, SJSA-1, ML-1 and K562 cells. RNA samples were electrophoresed onto a 1% denaturing formaldehyde agarose gel and transferred to a nylon membrane. The northern blot was probed with an exon 12-specific probe for* mdm2 *and exposed to film for transcript detection.* gapdh *was used as a normalizer for RNA levels. This is a representative of three independent experiments.* **C** *Quantitation using Image J after northern blot analysis of RNA from untreated MANCA, SJSA-1, ML-1 and K562 cell samples. Transcript levels were compared to K562 for basal expression and normalized for RNA levels to* gapdh*. An average of four independent experiments is shown. Error bars indicate standard error. Arrows depict RNA transcripts observed.*

To specifically quantify *mdm2-C* transcripts missing exons 5-9, we designed an exon 4:10 junction-specific forward primer and a reverse primer to exon 12 (Fig. 14A).

We also used a taqman quantitative probe to exon 6 and 7 to detect *mdm2* transcripts that retain exons 6 and 7. We referred to this transcript as *mdm2-FL*. However, this only represents *mdm2* transcripts that retain exons 6 and 7. All samples were normalized to the *p53*-null K562 cells. This was done in order to analyze the fold difference in basal transcripts produced from the *mdm2* P2 promoter above transcripts from the *mdm2* P1 promoter. In SJSA-1 cells, we observed that the *mdm2 (4:10-12)* primer set and the *mdm2 (6-7)* probe showed an equal ratio of *mdm2-C* and *mdm2-FL* transcripts (Fig. 14B). On the other hand, MANCA cells showed a higher ratio of *mdm2-C* transcript as compared to the *mdm2-FL* transcript (Fig. 14B). ML-1 cells showed very low basal *mdm2* transcripts for both the *mdm2-C* and *mdm2-FL* transcripts (Fig. 14B).

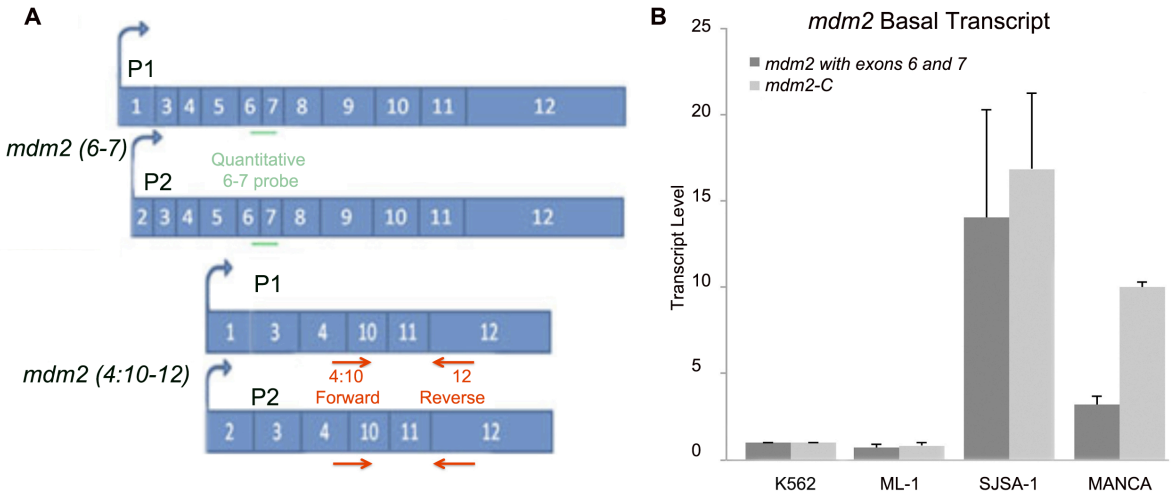

Figure 14: **MANCA cells have a higher ratio of basal *mdm2-C* transcript to other *mdm2* transcripts. A.** *Schematic of* mdm2 *messages detected using a Taqman probe for exons 6 and 7 (6-7 probe) or forward primer for 4:10 and reverse primer for 12 (4:10-12 primer) for* mdm2-C*.* **B.** *qRT-PCR with 4:10 forward and exon 12 reverse vs. Taqman probe to exon 6 and 7 of* mdm2 *were performed to detect* mdm2-C *and* mdm2 *(with exons 6 and 7) transcripts. The* mdm2-C *transcripts were detected via Syber Green and* mdm2 *(with exons 6 and 7) transcripts were detected via Taqman technology. Transcript levels were compared to K562 for basal expression and normalized for RNA levels to* gapdh*. An average of three independent experiments is shown. Error bars indicate standard error.*

To determine whether the ratio of *mdm2-C* to *mdm2-FL* transcript changes with DNA damage to the cell, we treated the panel of cells for three (3) hours with etoposide (etop), a topoisomerase II inhibitor. Etop inhibits the activity of topoisomerase II by preventing the resealing of DNA strands. This leads to DNA breaks that inhibit transcription in the cell (Ljungman and Zhang, 1996; Riou et al., 1993). Etop is known to activate p53 and induce the transcription of the cyclin dependent kinase inhibitor, *p21* in a time and dose-dependent manner (Arriola et al., 1999). Each cell line was normalized to its own untreated control sample. The control bars in the graphs (Fig. 15A and B-dark blue bars) signify the untreated control for the represented genes (*mdm2-C, mdm2-FL, p21* and *puma*). We observed that K562 cells, as expected, did not show damage-induced activation of *mdm2-FL or mdm2-C* (Fig. 15A). ML-1 cells showed a robust activation of *mdm2-FL* and *mdm2-C,* despite low basal levels for both transcripts (Compare Fig. 15B and Fig 15A). After DNA damage via etoposide, ML-1 cells showed a high ratio of *mdm2-C* to *mdm2-FL* transcripts (Fig. 15A). This suggests that the *mdm2-C* transcript can be induced by p53.

SJSA-1 cells showed activation of both *mdm2-FL* and *mdm2-C* transcripts (Fig. 15A). Similar to the basal *mdm2* transcript levels, SJSA-1 showed an equal ratio of *mdm2-C* to *mdm2-FL* transcripts (Compare Fig. 14B to Fig. 15A). On the other hand, MANCA cells showed a decrease in *mdm2-FL* transcript after etop treatment (Fig. 15A-red arrow). Previous work has shown that UV irradiation causes a decrease in *mdm2* transcription (Arriola et al., 1999; Wu and Levine, 1997). This decrease in *mdm2* transcript levels after DNA damage is attributed to the open conformation of the *mdm2* promoter region. This could increase the susceptibility of the *mdm2* promoter region to

DNA adducts caused by UV irradiation or at sites of DNA entanglements caused by an inactivation of topoisomerase II (Xiao et al., 1998). This is in contrast to reports that show an increase in *mdm2* transcription with DNA damage (Chen et al., 1994; Perry et al., 1993).

In order to determine how the ratio of *mdm2-C* to *mdm2-FL* transcripts affects p53 activity, we examined the induction of p53 target genes- *p21* and *puma* after etop treatment (Fig. 15B). We observed that ML-1 cells showed a robust activation of *p21* and *puma* transcripts after etop treatment. On the other hand, SJSA-1 showed compromised activation of *p21* and *puma* transcripts in contrast to the activation of *mdm2-FL* and *mdm2-C* transcripts previously observed (compare Fig. 15A vs. Fig. 15B- red arrows). The reason for *mdm2* induction in SJSA-1 cells can be ascribed to the amplification of the *mdm2* gene in these cells. In addition, MANCA cells were compromised in the activation of *p21* and *puma* transcripts after etop treatment (Fig. 15B- red arrows).

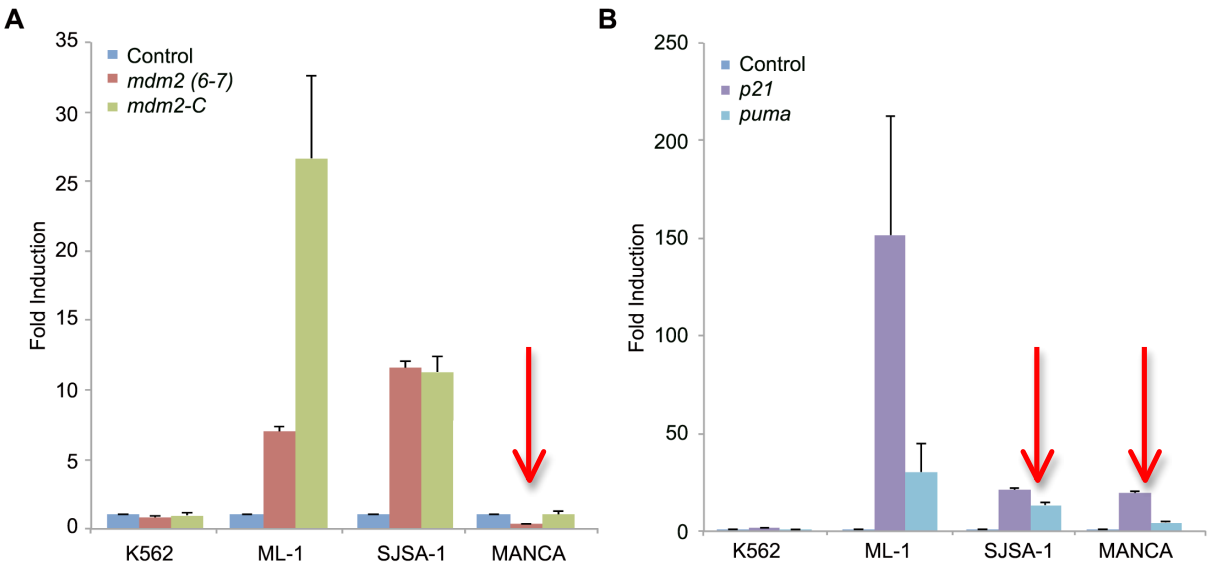

Figure 15: **Mdm2 over-expressing cells exhibit compromised DNA damaged induced activation of p53 target genes.** *qRT-PCR of RNA using Taqman and syber green technology for* **A.** mdm2 *with exons 6 and 7 and* mdm2-C respectively and **B.** *p53 target genes,* p21 *and* puma *after DNA damage treatment with 8μM etoposide for 3 hours. Data from each cell line is presented as normalized to its own untreated control sample for fold activation and normalized for RNA levels to gapdh. The control represents untreated samples for both genes per graph. An average of three independent experiments is shown. Error bars indicate standard error. Arrows depict decrease in transcript levels.*

3.2.2 **The *mdm2-C* Transcript is Translatable to Protein**

The endogenous protein expression of a specific Mdm2 isoform has never been documented. Prior assessment of the polypeptide sequence of Mdm2-C showed that despite missing exons 5 through 9, the transcript is translated in-frame (Fig. 12C). Mdm2-C and Mdm2-FL proteins have previously been translated into protein *in vitro* using rabbit reticulocyte lysates (Anderson et al., 2007; Sigalas et al., 1996). We translated Mdm2-C and Mdm2-FL proteins in wheat germ extract containing radiolabeled ^{35}S methionine (Fig. 16A). We reduced the protein samples with strong

reducing agents, dithiothreitol (DTT) and iodoacetamide, which prevents the re-ligation of disulfide bonds after protein denaturation. After reducing the samples, running an SDS-PAGE and subsequent ^{35}S signal exposure, Mdm2-C was observed to migrate at one predominant mass of 75 kDa (Fig. 16A lane 1). Mdm2-FL was observed to migrate at a predominant mass of 110 kDa (Fig. 16A lane 2). These molecular masses observed after protein reduction correlated with masses previously documented for Mdm2-FL and Mdm2-C, 90 kDa and 75 kDa respectively (Sigalas et al., 1996).

In the absence of strong reduction before SDS-PAGE, Mdm2-C and Mdm2-FL migrate at similar molecular masses above 98 kDa (Fig. 16B). The *in vitro* translated Mdm2-C protein migrated at several molecular masses, all of which were larger than the amino acid composite calculated mass of 36 kDa (Fig. 16B lane 1). The Mdm2-FL protein also migrated at several molecular masses, some of which were larger than the calculated mass of 55 kDa (Fig. 16A lane 2). We reasoned that the difference in protein migration in the presence and absence of reducing agents was due to the dissolution of disulfide bonds, which would retard the migration of the proteins in SDS-PAGE (Compare Fig. 16A to 16B). In addition, the difference in mass from the calculated size has been attributed to the major acidic domain region present in Mdm2, thus resulting in aberrant migration in SDS-PAGE (Chen et al., 1993).

It is important to note that the molecular masses did not revert to the calculated size after protein reduction. The reason for this might lie in the presence of other post-translational modifications such as glycosylation and myristoylation (See Fig. 4). Interestingly after SDS-PAGE of whole cell extracts, several protein bands of different

molecular masses can be seen ranging from 36 - 250 kDa (Bargonetti lab observation). The identities of these bands have not been confirmed and could represent artifacts, post-translationally modified Mdm2 proteins or Mdm2 splice variant protein products. We hypothesize that many of these protein molecular masses result from splice variant messages of *mdm2* and others are from variations in post-translational modifications.

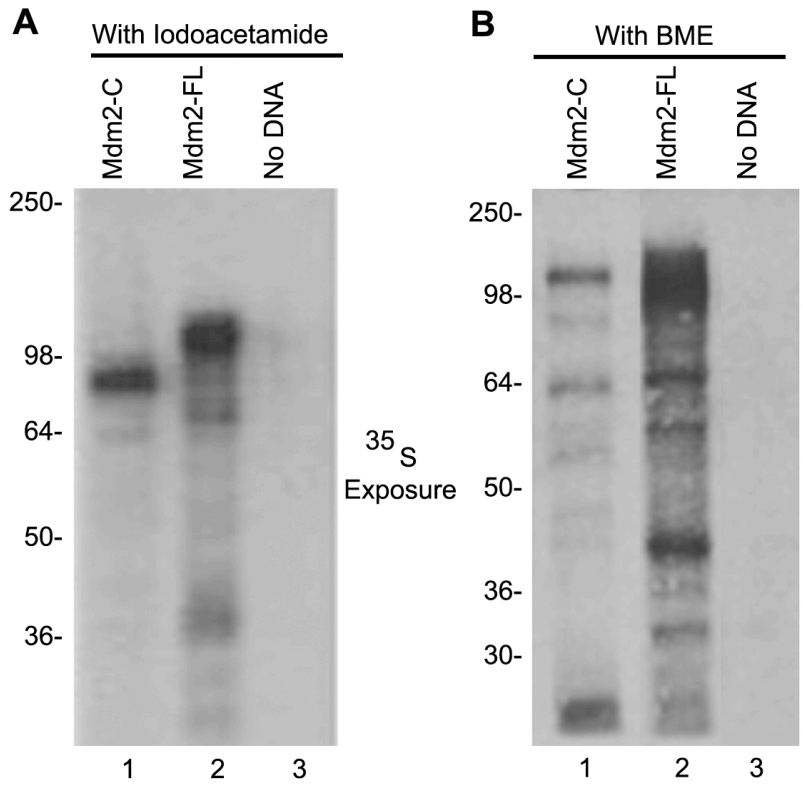

Figure 16**: SDS-PAGE and ^{35}S analysis of *in vitro* translated Mdm2-FL and Mdm2-C proteins.** *^{35}S methionine was used as a radioactivity source to label* in vitro *translated proteins. In vitro translations of* pcDNA3-mdm2-FL *and* pcDNA3-P2mdm2-C *using the TNT coupled wheat germ extract system. Resulting Mdm2-FL and Mdm2-C protein were electrophoresed on a 10% SDS-PAGE in a 5:1:1 ratio. The gel was transferred to a nitrocellulose membrane and exposed to film for significant Mdm2-C protein product detection. Wheat germ lysate without DNA was used as a negative control. Samples in* **A.** *were prepared at 1X from 4X protein sample buffer with 20mM dithiothreitol (DTT) and heated for 10 minutes at 70^{0}C. After heating, the samples were allowed to cool to room temperature and then 1% 1M iodoacetamide was added to the samples. The samples in* **B.** *were prepared at 1X from 6X protein sample buffer with 12% β-mercaptoethanol (BME) and heated for 10 minutes at 95^{0}C.*

3.2.3 **An Mdm2 Isoform Specific Antibody is Made**

In order to detect endogenous Mdm2-C protein, an Mdm2-C specific polyclonal antibody was produced. Rabbits were immunized with a peptide sequence containing the exon 4 and exon 10 splice junction sequence (Fig. 17A). The specificity of the antibody was validated via western blot using wheat germ extract *in vitro* translated Mdm2-C and full-length Mdm2 (Mdm2-FL) protein products (Fig. 17B). The Mdm2 C410 polyclonal antibody detected only Mdm2-C protein (Fig. 17B lane 1) and did not detect Mdm2-FL protein despite its high levels after immunoblot with the Mdm2 monoclonal antibody, 4B11 (Fig. 17B compare lanes 2 and 8). The Mdm2 C410 antibody detected several molecular masses for the Mdm2-C protein with masses between- 250 and 98 kDa (Fig. 17B lane 4). This was unlike the single mass detected by the Mdm2 monoclonal antibody mix (Fig. 17B compare lanes 1 and 7). The pre immune serum showed no signal indicating that the proteins observed were valid (Fig. 17B lanes 4 - 6).

To further validate the Mdm2-C specific antibody, *in vitro* translated Mdm2-C and Mdm2-FL protein products were used in an immuno-precipitation (IP) experiment for Mdm2-C protein pull-down. The protein pull down experiment was carried out using ^{35}S radiolabeled *in vitro* translated Mdm2-C and Mdm2-FL protein products incubated with the Mdm2-C specific antibody. The resulting radiolabeled immuno-precipitated protein was electrophoresed via SDS-PAGE and exposed for autoradiography. The Mdm2-C antibody pulled down Mdm2-C protein (Fig. 17C, compare lanes 3 and 8) but did not pull down Mdm2-FL protein (Fig. 17C, compare lanes 4 and 9). Furthermore, Mdm2 C410 IP and subsequent antibody detection using the Mdm2 monoclonal antibody mix

showed that only the Mdm2-C protein (indicated by arrow) and not the Mdm2-FL protein was pulled-down with the Mdm2 C410 antibody (Fig. 17D, compare lanes 2 and 3). Interestingly, the molecular mass detected after western blot differed from the mass detected in IP (compare Fig. 17B lane 1 to Fig. 17C lane 3 and Fig. 17D lane 2). The reason for this might be because the Mdm2 C410 antibody detects different Mdm2-C protein species based on their conformation statuses i.e. native vs. denatured.

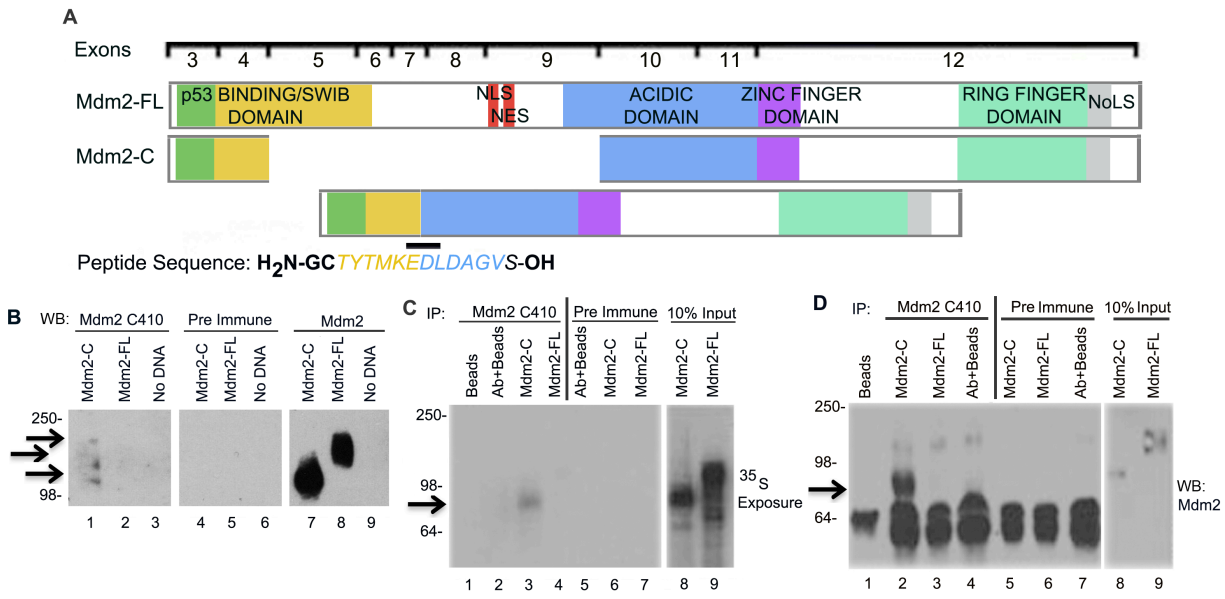

Figure 17**: The Mdm2 C410 antibody is specific to human Mdm2-C protein**
A. *Schematic of full-length Mdm2 (Mdm2-FL) and Mdm2-C. The retained proteins' biochemical functional domains are shown as color codes. The peptide sequence used as an immunogen containing the splice junction of human Mdm2-C is shown. Glycine (G) and Cysteine (C) residues were added to the N-terminus of the peptide to facilitate conjugation to an immunoreactive protein, keyhole limpet hemocyanin (KLH).* **B.** *Western blot detection of in vitro translated Mdm2-FL and Mdm2-C protein products from* pcDNA3-mdm2-FL *of* pcDNA3-mdm2-C *plasmids. Samples were electrophoresed on a 10% SDS-PAGE gel at a ratio of 5:1:1 (Mdm2-C: Mdm2-FL: No DNA). Mdm2 C410 immune and pre-immune polyclonal serum and Mdm2 monoclonal antibody mix (4B2, 2A9, 4B11)- lanes 1 – 3, lanes 4 – 6 and lanes 7 – 9, respectively, were utilized as antibodies for protein identification. Wheat germ lysate without DNA was used as a negative control.* **C.** *Immunoprecipitation of* ^{35}*S methionine radioactive-labeled* in vitro *translated Mdm2-FL and Mdm2-C proteins using Mdm2 C410 and pre-immune polyclonal serum antibodies. Protein ratios as shown in* **B** *were used in the pull down assay. Samples were electrophoresed on a 10% SDS-PAGE gel transferred to a nitrocellulose membrane and exposed to film for protein detection. This is representative of three independent experiments.* **D.** *Immunoprecipitation of* in vitro *translated Mdm2-FL and Mdm2-C proteins using Mdm2 C410 and pre-immune polyclonal serum antibodies. Mdm2 monoclonal antibody mix (4B2, 2A9, 4B11) was utilized for protein identification. Wheat germ lysate without plasmid DNA was used as a negative control. HRP-conjugated anti-mouse and anti-rabbit were used as secondary antibodies. This is a representative of three independent experiments. Arrows depict protein bands.*

To further validate the Mdm2-C protein and the epitope regions missing in the protein, we examined via western blot whether the Mdm2-C protein, compared to the full-length Mdm2 protein could be detected by different Mdm2 monoclonal antibodies. We used Mdm2 monoclonal antibodies specific to different epitopes of the Mdm2 protein (Chen et al., 1993). We generated Mdm2 proteins in two *in vitro* translation systems, rabbit (RRL) and wheat germ (WGE). Using the C-terminal Mdm2 antibody, 4B11, whose epitope of recognition lies within amino acids 383 – 491 (Chen et al., 1993). This epitope region is present in majority of the putative Mdm2 proteins made in the cell (Bartel et al., 2002). We detected the Mdm2-C and Mdm2-FL proteins with the Mdm2 4B11 antibody (Fig. 18 lanes 1 - 4, upper panel). Interestingly, there were three molecular mass proteins (75kDa, 98kDa and above 98kDa) made in the RRL system compared to the single molecular mass protein made in the WGE system (98kDa) (Fig. 18 compare lane 1 to 3, upper panel). The reason for this might lie in a difference in post-translational modifications or RNA processing of the *mdm2-C* RNA in the different eukaryotic systems. Surprisingly, the Mdm2-FL protein made in the different systems remained the same (Fig. 18 compare lanes 2 and 4). This suggests that the difference observed with the Mdm2-C protein is unique to the *mdm2-C* transcript. Next we used the Mdm2 monoclonal antibody, 2A9, whose epitope of recognition lies with in amino acids 153 – 222 (Chen et al., 1993), a region missing in the Mdm2-C protein (See Fig. 12C). We observed that Mdm2-C was not detected while Mdm2-FL protein was detected in both *in vitro* systems (Fig. 18 compare lanes 1 and 3 to 2 and 4). This confirms that the Mdm2-C protein has the designated regions spliced out and is indeed a truncated protein despite its unusually high molecular mass.

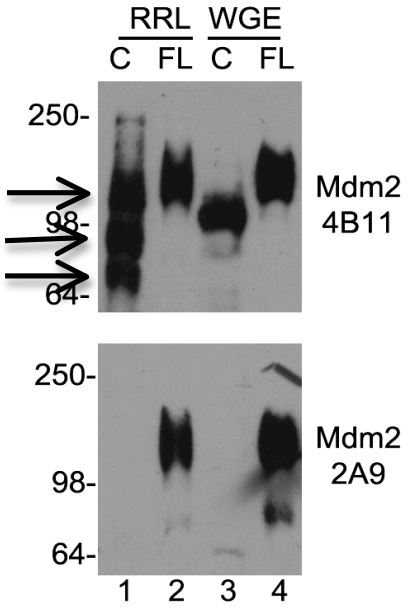

Figure 18: **Mdm2-C protein is not detected by Mdm2 monoclonal antibody, 2A9**. *Mdm2-C (C) and Mdm2-FL (FL) proteins were made in two* in vitro *translation systems, rabbit reticulocyte (RRL) and wheat germ extracts (WGE). SDS-PAGE was run and the proteins were detected using the Mdm2 monoclonal antibodies to the Mdm2 C-terminus, 4B11 or to the central region, 2A9. HRP-conjugated anti-mouse and anti-rabbit were used as secondary antibodies. Arrows depict protein bands.*

3.2.4 **Mdm2-C Protein is Endogenously Expressed**

In order to determine if high levels of *mdm2-C* transcript correlates to endogenous Mdm2-C protein expression, we examined a panel of cell lines (Table 1) with the Mdm2-C specific antibody, Mdm2 C410. We compared total Mdm2 expressions using the Mdm2 monoclonal antibody 4B11 to Mdm2-C protein expression using the Mdm2 C410 antibody (Fig. 19A). Using the Mdm2 C410 polyclonal antibody, we observed three (3) major molecular mass protein bands above 98kDa, in the cell lines examined (Fig. 19A lanes 1 - 4). MANCA cells showed the highest level of Mdm2-C protein (Fig. 19A lane 1). The comparative level of Mdm2-C protein endogenously

expressed in MANCA cells directly correlated with the mRNA data (Fig. 13B and 14B). SJSA-1 cells showed low level of Mdm2-C protein, which did not correlate with the *mdm2-C* mRNA data (Compare Fig. 19A lane 2 to Fig. 13B and 14B). SJSA-1 cells have 25 copies of the *mdm2* gene due to gene amplification and this gives an increase in high *mdm2-C* transcript, however why this does not translate to high Mdm2-C protein is unclear. Interestingly, K562 cells showed moderate levels of Mdm2-C protein compared to SJSA-1 cells (Fig. 19A compare lanes 2 to 4) that did not correlate with the RNA levels (see Fig. 13B and 14B).

Next we examined Mdm2 protein levels using the Mdm2 monoclonal antibody, 4B11. We observed that MANCA and SJSA-1 cells possessed high Mdm2 protein levels (Fig. 19A lanes 9 – 10), which correlated with the *mdm2* transcript levels (see Fig. 13B and 14B). ML-1 cells did not show Mdm2 protein with molecular mass above 98 kDa (Fig. 19A lane 11). In contrast, we detected smaller molecular mass proteins between 50 kDa and 36 kDa (data not shown). We detected a moderate level of Mdm2 protein in K562 cells after a long exposure (Fig. 19A lane 12). This did not correlate with the Mdm2-C protein, which showed a moderate level of Mdm2-C protein (Fig 19A lane 4); neither did it correlate with the *mdm2* transcript level (Fig. 14B). This might be because the K562 cells are heterozygous for the *mdm2* SNP309 allele.

We compared the proteins detected after Mdm2 C410 and 4B11 immunoblots and observed that all the molecular mass protein products detected with the Mdm2 C410 antibody aligned with the protein bands observed with the 4B11 antibody (Compare Fig. 19A lanes 1 - 4 and lanes 9 - 12). This therefore suggests that the

proteins detected after Mdm2 C410 immunoblot are indeed Mdm2-C. We also observed a predominant molecular mass band between 64 and 90 kDa after Mdm2 C410 immunoblot but this band did not align with any band observed after immunoblot with the Mdm2 4B11 antibody (data not shown). Nonetheless, the Mdm2-C molecular mass protein between 64 and 90 kDa is specific to the Mdm2 C410 antibody and could represent an Mdm2-C form that is not detected by the 4B11 antibody due to epitope masking. Interestingly, the Mdm2-C protein has been documented to migrate at a molecular mass of 85 kDa (Anderson et al., 2007). The pre-immune serum was used as a negative control and showed a very low background protein signal in all cell lines examined (Fig. 19A lanes 5 - 8).

Previous work has shown the Mdm2 isoforms, Mdm2-A and Mdm2-B, localize to the cell nucleus after exogenous protein expression in mouse and human cells (Schuster et al., 2007). This is despite the fact that the regions encoding to the nuclear localization and export signals are spliced out. Similarly, Mdm2-C has the nuclear localization and export signal regions spliced out. We examined the cellular localization of Mdm2-C in MANCA cells by performing a chromatin fractionation that separates the proteins in the cells based on their cellular compartments into chromatin bound, nuclear soluble and the cytoplasmic fractions. The S1 fraction represents the cytoplasmic proteins while the P3 fraction represents the chromatin bound proteins, which are present in the nucleus of the cell. We performed immunoblot on proteins extracted from MANCA cells using the Mdm2 C410 and 4B11 antibodies. We observed that when compared to whole cell extracted proteins (WCE), Mdm2-C protein was equally present in the cytoplasmic extract fraction (S1) and in the chromatin extract fraction (P3) (Fig.

19Bi lanes 1 – 3). In addition, there were three molecular mass bands observed between 98 and 250 kDa. The two bands closest to 250 kDa were present in both the S1 and P3 fractions but the fastest migrating band at 98 kDa was only present in the WCE and P3 fractions (Fig. 19Bi lane 3). This suggests that this molecular mass protein of Mdm2-C could have functions that are localized to the nucleus. Using the Mdm2 4B11 antibody, we observed that Mdm2 was predominantly located in the SI fraction (Fig. 19Bi lane 8). Furthermore, after a longer exposure, Mdm2 was detected in the P3 fraction (Fig. 19Bi lanes 9). Intriguingly, most of the Mdm2 present in MANCA cells appears to be present in the S1 fraction but after Mdm2 C410 immunoblot, it was observed that a substantial amount of Mdm2-C protein was localized in the P3 fraction (Fig. 19Bi compare lanes 2 and 3 to 8 and 9). This suggests that in MANCA cells, the nuclear localized Mdm2 protein might be predominantly Mdm2-C. We performed immunoblots for nuclear and cytoplasmic markers (Fibrillarin and Tubulin, respectively) to confirm proper fractionation of the cell extracts (Fig. 19Bii).

In order to further confirm the localization of Mdm2-C in MANCA cells, we performed immunofluorescence (IF) via spinning disk confocal microscopy. Using the Mdm2 C410 specific antibody, we found via IF that Mdm2-C localized to the cytoplasm and what we think are nucleoli of the cells based on DAPI staining (Fig. 19Cii). The distribution of Mdm2-C protein did not change with DNA damage treatment via etoposide for 3 hours (data not shown). The p53 protein localized to the cytoplasm and nucleus of the cells (Fig. 19Civ). The protein products of Mdm2 splice isoforms, Mdm2-A and Mdm2-B have not been observed to interact with p53 (Fridman et al., 2003; Schuster et al., 2007) because they splice out majority of the p53-binding domain

(Bartel et al., 2002). Interestingly, p53 and Mdm2-C were observed to co-localize in the cytoplasm and nucleoli as indicated by the yellow color change due to protein co-localization after the merge of the different laser channels (Fig. 19Cv). The pre-immune serum showed only low background staining, thus further confirming the specificity of Mdm2 C410 for Mdm2-C protein (Fig. 19Cvii).

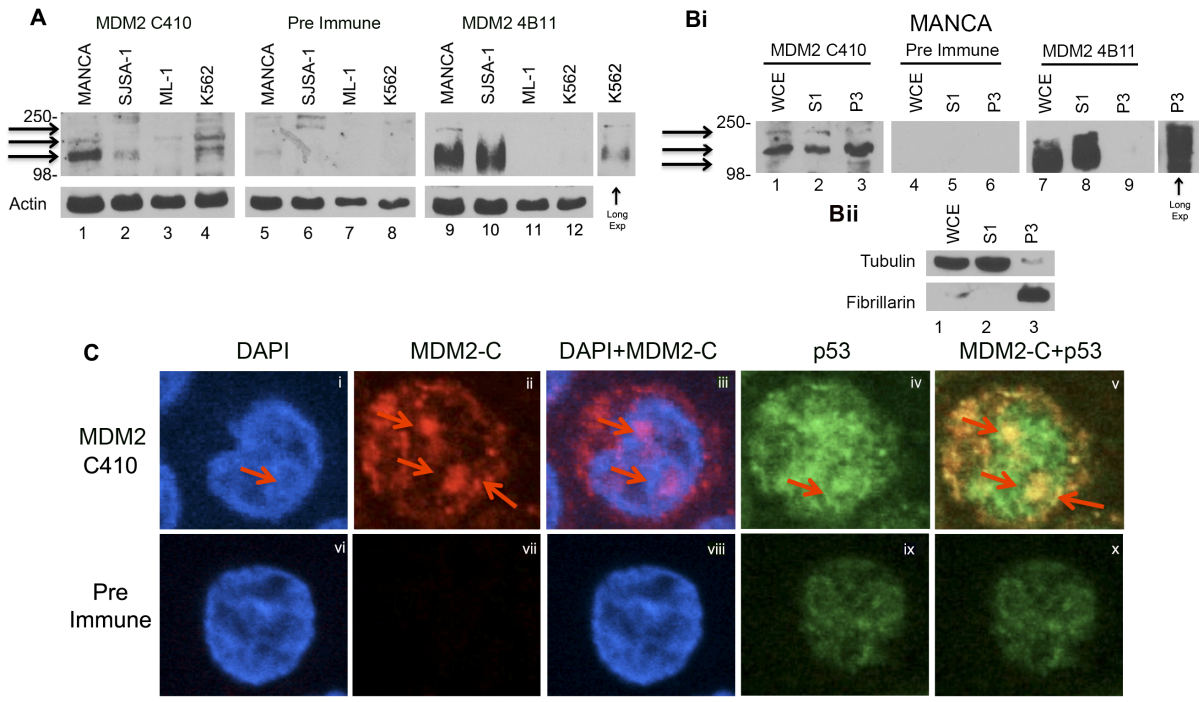

Figure 19: **High expression of endogenous Mdm2-C protein in G/G *mdm2* SNP309 human Mdm2 over-expressing cancer cells.** *Western blot analysis of whole cell extracts from: MANCA, SJSA-1, ML-1 and K562 cells. 50μg protein was subjected to SDS-PAGE and total Mdm2 and Mdm2-C protein levels were analyzed via* **A***. Mdm2 polyclonal antibody- Mdm2 C410, Pre immune polyclonal serum was used as a control (lanes 1 – 4 and 5 – 8 respectively) and Mdm2 monoclonal antibody, 4B11 (lanes 9 – 12). Actin was used as a loading control. HRP-conjugated anti-mouse and anti-rabbit were used as secondary antibodies. This is representative of three experiments. Bi. MANCA cells were lysed either as whole cell extracts (WCE) or into cellular compartments- cytosolic (S1) and Chromatin (P3). Proteins were detected as in* ***A****.* ***Bii****. Tubulin and Fibrillarin were used to show efficient cellular fractionation.* **C.** *Spinning disk confocal microscopy of MANCA cells. Cells were fixed, permeabilized and incubated with p53, Mdm2 C410 and pre-immune polyclonal serum antibodies. Slides were incubated with secondary Alexa-conjugated goat anti-rabbit and FITC-conjugated goat anti-mouse. DAPI was used to stain the cell nuclei. Pictures were taken at 60X magnification. Arrows depict protein bands or protein localization regions.*

3.2.5 **Mdm2-C Does Not Function in the Canonical Pathway of Mdm2**

Over-expression of Mdm2-A or B in BJ cells (human fibroblasts) with wild-type p53 results in a decrease in cell proliferation. Over-expression of these Mdm2 isoforms

in *p53-null* mouse embryonic fibroblasts does not halt growth and these growth inhibitory functions are dependent on p53 activity (Sanchez-Aguilera et al., 2006). To determine the effect of Mdm2-C on the cellular proliferation of human cells, Mdm2-C was expressed in human *p53*-null lung carcinoma cells, H1299, in the presence and absence of exogenously expressed p53. Western blot analysis showed an increase in Mdm2 protein expressed with increasing DNA transiently transfected (Fig. 20A, Mdm2 panel). Interestingly, with exogenous expression of Mdm2-C and Mdm2-FL in H1299 cells, Mdm2 protein from both transfected cells was observed to migrate at a similar molecular mass, comparable to the endogenous proteins (Compare Fig. 19A to 20A).

Previous work established by other laboratories has shown that the over-expression of full-length Mdm2 and p53 in *p53*-null H1299 cells results in a decrease in p53 protein due to Mdm2-mediated proteasome degradation (Haupt et al., 1997). We checked for the levels of p53 protein and observed that with increased *mdm2-C* transiently transfected, p53 protein levels did not decrease as dramatically as they did with the addition of *mdm2-FL* (Fig. 20A compare p53 panel, lanes 3 - 8 vs. lane 9 – 14). Image J quantification of the bands after 400ng *mdm2-FL* showed 0.02 p53 protein levels compared to 0.3 in cells transfected with *mdm2-C* (Fig. 20A, p53 panel).

Mdm2-A and Mdm2-B have been shown to bind to Mdm2-FL and they sequester it to the cytoplasm and promote p53 activation (Evans et al., 2001; Volk et al., 2009b). To determine the effect of Mdm2-C on p53 transcriptional activity, luciferase assay experiments were performed. Results showed that increasing Mdm2-FL protein (Fig. 20A lanes 9 - 14) drastically reduced the transcriptional activity of p53 (Fig. 20B, red arrow) but increasing Mdm2-C protein did not (Fig. 20B, blue arrow). These data imply

that Mdm2-C does not function in the canonical pathway of Mdm2. To assess the effect of increased Mdm2-C on cell proliferation, H1299 cells were transiently transfected in the presence or absence of with increasing amounts of *mdm2-C*. The number of cells was determined after 48 hours of transfection. In the presence of p53, there was no effect of *mdm2-C* transfection (Fig. 20C). Alternatively, increased *mdm2-C* DNA transfected showed a slight growth advantage over Mdm2-FL expressing cells in the absence of p53 (Fig. 20C).

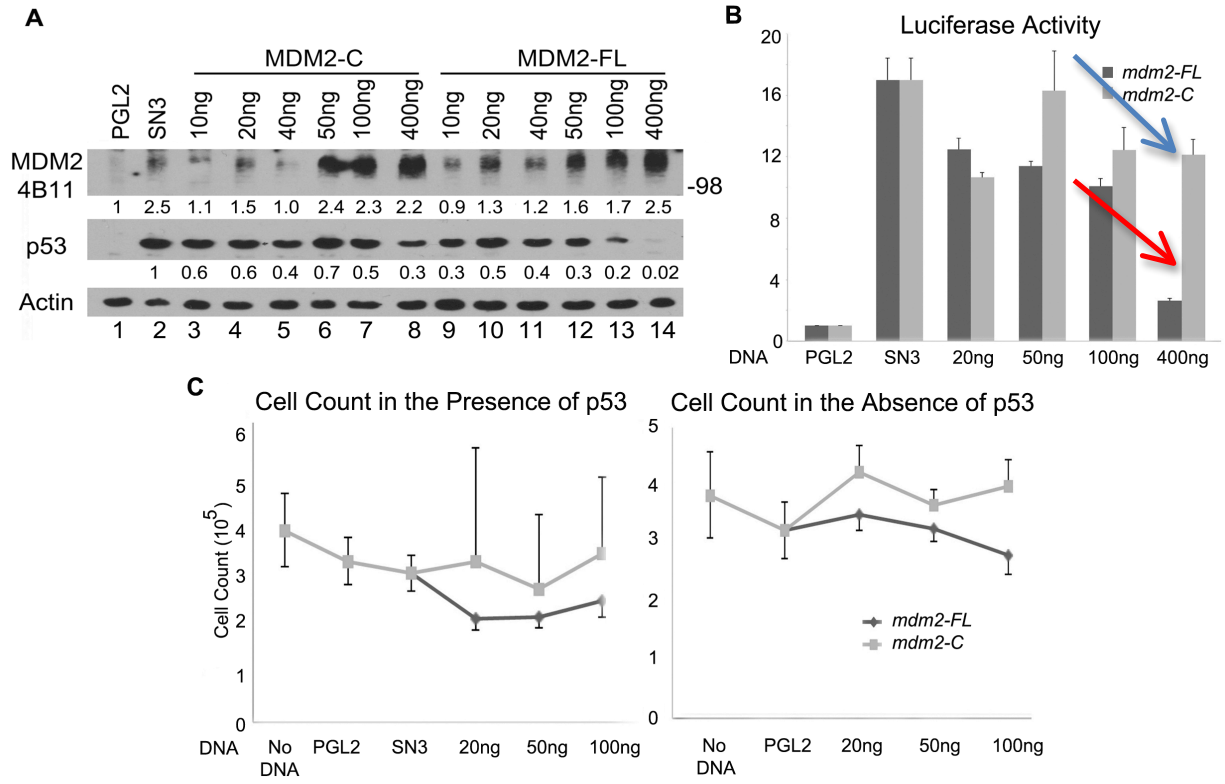

Figure 20**: Mdm2-C protein does not function in the canonical p53 degradation pathway. A.** *Analysis of exogenously expressed Mdm2-FL or Mdm2-C with p53 via western blot. Increasing amount of* pcDNA3-mdm2-FL *and* pcDNA-mdm2-C *plasmid DNAs were transiently transfected with a constant amount of* sn3 *plasmid (p53) into H1299* p53*-null cells.* PGL2 *plasmid was used as a DNA normalizer. Cells extracts were prepared 48hours after transfection and analyzed for protein expression using the Mdm2 monoclonal antibody mix (4B2, 2A9, 4B11) and p53 monoclonal antibody mix (240, 1801, 421). Actin was used as a loading control. The numbers below the Mdm2 and p53 blots are image J quantifications of the bands normalized to actin.* **B.** *48 hours after transfection, cells were lysed and protein extracts were utilized in a luciferase assay reaction. Samples were compared to PGL2 and normalized for amount of protein. An average of three independent experiments is shown. Error bars represent standard error.* **C.** *Cell counts after mdm2-FL and mdm2-C transient transfection in the presence and absence of p53. Equal amounts of cells were plated a day before transfection. 48 hours later, cells were counted. An average of three independent experiments shown. Error bars represent standard error. Red arrow depicts drastic decrease in transcription while the blue arrow depicts minor decrease in transcription.*

To further examine the effect of Mdm2-C on cell proliferation, we performed colony formation assays. Human *p53*-null lung carcinoma cells, H1299 and *mdm2/p53* double null mouse embryonic fibroblasts (-/- MEF) were transiently transfected with 400µg of *mdm2-C* or *mdm2-FL* with and without *p53*. Cells were plated into drug selection medium at 2000 cells per 10cm plate and allowed to grow for a period of two to three weeks. After the incubation time, compared to the vector control and *mdm2-FL* transiently transfected cells, *mdm2-C* transiently transfected H1299 cells showed more colonies formed (Fig. 21A). The numbers of colonies were counted and the values were graphed. The highest number of H1299 colonies, irrespective of the absence or presence of p53, was observed in cells with Mdm2-C over-expression (Fig. 21B blue and red bars). Regardless of the presence or absence of p53, when compared to the vector control, this increase in the number of colonies with Mdm2-C expression was found to be significant (Fig. 21B). Western blot analysis from the transiently transfected H1299 cells after puromycin drug selection showed that Mdm2-C and Mdm2-FL proteins were expressed (Fig. 21C lanes 2 and 3; compare to Fig. 21A lanes 1, 8 and 14). Mouse embryonic fibroblasts null for *p53* and *mdm2* (-/- MEF) were also assessed for the effect of exogenously expressed Mdm2-C on cell growth. Compared to *mdm2-FL* and vector control, MEFs transfected with *mdm2-C* showed more colonies formed (data not shown). The colonies were counted and the numbers were plotted. Although the number of colonies were not as high compared to the H1299 cells (data not shown), we observed that regardless of the presence or absence of p53, compared to the vector control and *mdm2-FL, mdm2-C* transiently transfected cells showed more colonies (data not shown).

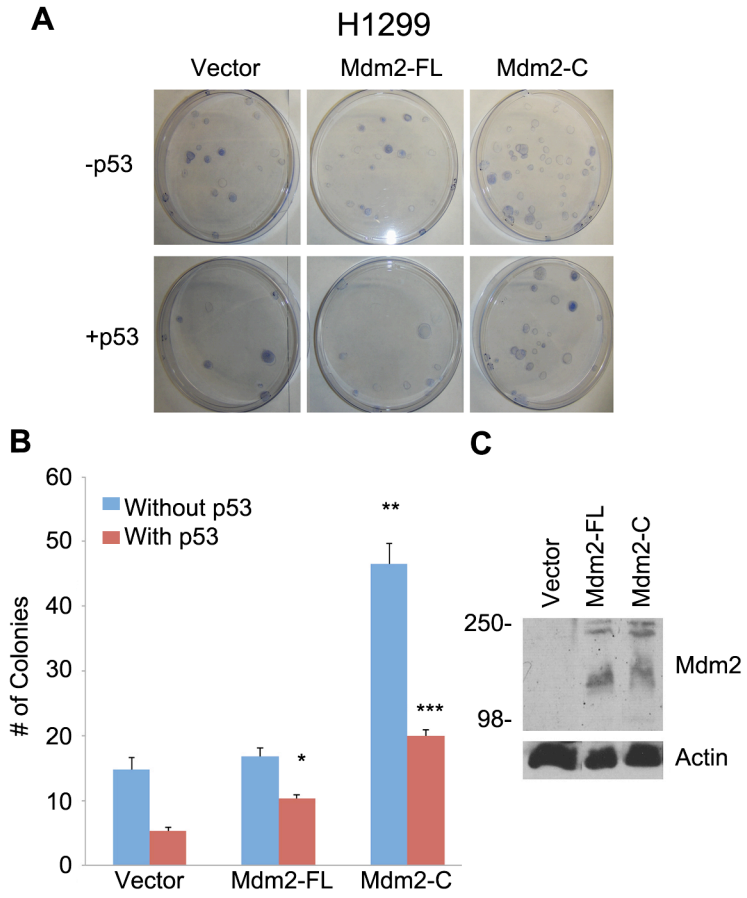

Figure 21**: Mdm2-C increases colony-forming units in the presence and absence of p53. A.** *Colony formation assay in H1299 cells. Cells were transfected with* pBABE-puro/mdm2-FL *and* pBABE-puro/mdm2-C *plasmids and after 24 hours, 2000 cells were plated into selection media (RPMI / DMEM with 2μg/ml puromycin). Cells were allowed to grow for 3 weeks. Picture represents one experiment. Two experiments were carried out in duplicates.* **B.** *Colony counts after colony formation assay. An average of two experiments carried out in duplicates is shown. Error bars represent standard error. * Represents significance compared to vector control. Where asterisks (*) represent: *> 0.05, ** > 0.005 and ***> 0.0005.* **C.** *Western blot analysis of samples from H1299 cells with exogenously expressed Mdm2-C and Mdm2-FL proteins. 24 hours post transfection cells were plated into medium containing 2μg/ml puromycin for the selection of transformed cells. The cells were allowed to grow for 5-7 days. Cells were lysed and proteins were extracted for western blot analysis. Mdm2 monoclonal antibody mix (4B2, 2A9, 4B11) was used for protein detection and Actin was used as a loading control.*

3.2.6 **Mdm2-C Endogenous Expression Increases with Estrogen Treatment and the Mdm2-C Protein Localizes to Distinct Speckled Foci in the Cytoplasm and Nucleoli of ER+ Breast Cancer Cells**

We have shown that in estrogen receptor positive (ER+) breast cancer cells after estrogen treatment, Mdm2 is over-expressed (Brekman et al., 2011). Furthermore, *mdm2* knockdown results in a decrease in cell growth independent of p53; thus providing evidence for the importance of an estrogen driven, Mdm2-mediated, p53-independent, cell proliferation program. Since *mdm2* spliced variant transcripts are also over-expressed with the over-expression of Mdm2 (Bartel et al., 2001b; Liang et al., 2004; Matsumoto et al., 1998; Sanchez-Aguilera et al., 2006; Sigalas et al., 1996), we examined the expression of Mdm2-C protein and *mdm2-C* transcript in two ER+ breast cancer cells, MCF-7 and T47D, possessing different genotypes for *mdm2* SNP309 (T/G vs. G/G) and *p53* (wild-type vs. mutant respectively) statuses. We observed a slight increase in Mdm2-C protein after estrogen treatment of MCF-7 and T47D cells (Fig. 22A lanes 2 and 4). Interestingly, there were two molecular masses- 98 and above 98 kDa, for the Mdm2-C protein in both breast cancer cell lines examined (Fig. 22A), which could represent differentially modified Mdm2-C protein forms in the different cell lines. The pre-immune serum was used as a background control for the Mdm2 C410 antibody and very low protein was detected (Fig. 22A lanes 5 - 8). We checked for the effect of estrogen treatment on the *mdm2-C* message. We observed a slight increase of the *mdm2-C* message in T47D cells after estrogen treatment (Fig. 22B). Therefore, we can conclude that the *mdm2-C* transcript and protein levels are up regulated in an estrogen-mediated manner.

To determine the localization of Mdm2-C in MCF-7 and T47D breast cancer we performed chromatin fractionation. Immunoblot with Mdm2 C410 showed that there were three predominant molecular mass protein bands between 98 kDa and 250 kDa in MCF-7 and T47D cells (Fig. 22Ci lanes 1 - 6). Interestingly, the different species of Mdm2-C protein present in the both cell lines as observed in Fig. 22A, are represented in different proportions in two cell lines (Fig. 22Ci compare lanes 2 and 3 to 5 and 6). In MCF-7 and T47D cells, we observed that the Mdm2-C protein mass closest to 98 kDa appeared somewhat more prevalent in the P3 fractions than in the S1 fractions (Fig. 22Ci compare lanes 2 and 3 and 5 and 6). Interestingly, in T47D cells, the molecular mass protein at 250 kDa was largely present in the S1 and P3 fractions examined but was absent in the P3 fraction of MCF-7 cells (Fig. 22Ci compare lanes 2 and 3 to lanes 5 and 6); the reason for this is unclear. The Pre immune antibody showed no background signal, thus confirming that the protein bands observed were Mdm2-C (Fig. 22Ci lanes 7 - 12).

We also performed an immunoblot using the Mdm2 4B11 antibody for Mdm2. We observed that in MCF-7 cells, the majority of the Mdm2 protein was localized to the S1 fraction (Fig. 22Ci compare lanes 14 and 15). Conversely, in T47D cells, there was a similar level of Mdm2 protein observed in the S1 and P3 fractions (Fig. 22Ci compare lanes 17 and 18). However, these levels were not definite because the markers that ascertain proper fractionation did not depict an efficient S1 and P3 fractionation in T47D cells (Fig. 22Cii lane 6). Unlike in T47D cells, there was no tubulin observed in the P3 fraction of the MCF-7 fractionation sample (Fig. 22Cii compare lanes 3 to 6). Therefore,

it is possible that the P3 fraction of the T47D samples contained some S1 localized proteins, hence the seemingly equal levels of Mdm2 protein in the S1 and P3 fractions.

In order to further confirm the localization of Mdm2-C in the presence and absence of estrogen treatment in MCF-7 and T47D cells, IF was performed. In the absence of estrogen treatment, MCF-7 cells showed a spatial cytoplasmic and nucleoplasmic presence of Mdm2-C (Fig. 22Cii), while in T47D cells, Mdm2-C was observed predominantly cytoplasmic and in the nucleoli (Fig. 22Cxii). We also examined whether Mdm2-C could be found co-localized with p53 in these cells. MCF-7 cells showed a predominant co-localization of Mdm2-C with p53 in the cytoplasm and partially in the nucleus (Fig. 22Cv). However, T47D cells did not show the same co-localization (Fig. 22Cxv). The reason for this might lie in the fact that the p53 in the MCF-7 cells is wild-type while the p53 protein in T47D cells is mutant- a missense mutation at position 194 in the zinc-binding domain that is important for DNA binding.

In the presence of estrogen treatment, MCF-7 cells showed an altered localization of Mdm2-C (Fig. 22Cvii) to a more cytoplasmic and speckled/punctate appearance. Note that the increased speckle formation was not limited to the cytoplasm but extended to the nucleus (Fig. 22Cvii). We observed that compared to before estrogen treatment, p53 was localized primarily to the nucleus (Fig. 22C compare iv to ix). However, any cytoplasmic p53 present was co-localized with Mdm2-C (Fig. 22Cvii). Although, T47D cells did not exhibit the same extreme re-localization pattern of Mdm2-C distribution compared to MCF-7 cells, the Mdm2-C staining appeared slightly more speckled after estrogen treatment (Fig. 22Cxvii). In addition, after estrogen treatment as

compared to MCF-7 cells, we did not find significant co-localization of p53 with Mdm2-C (Fig. 22C compare x to xx).

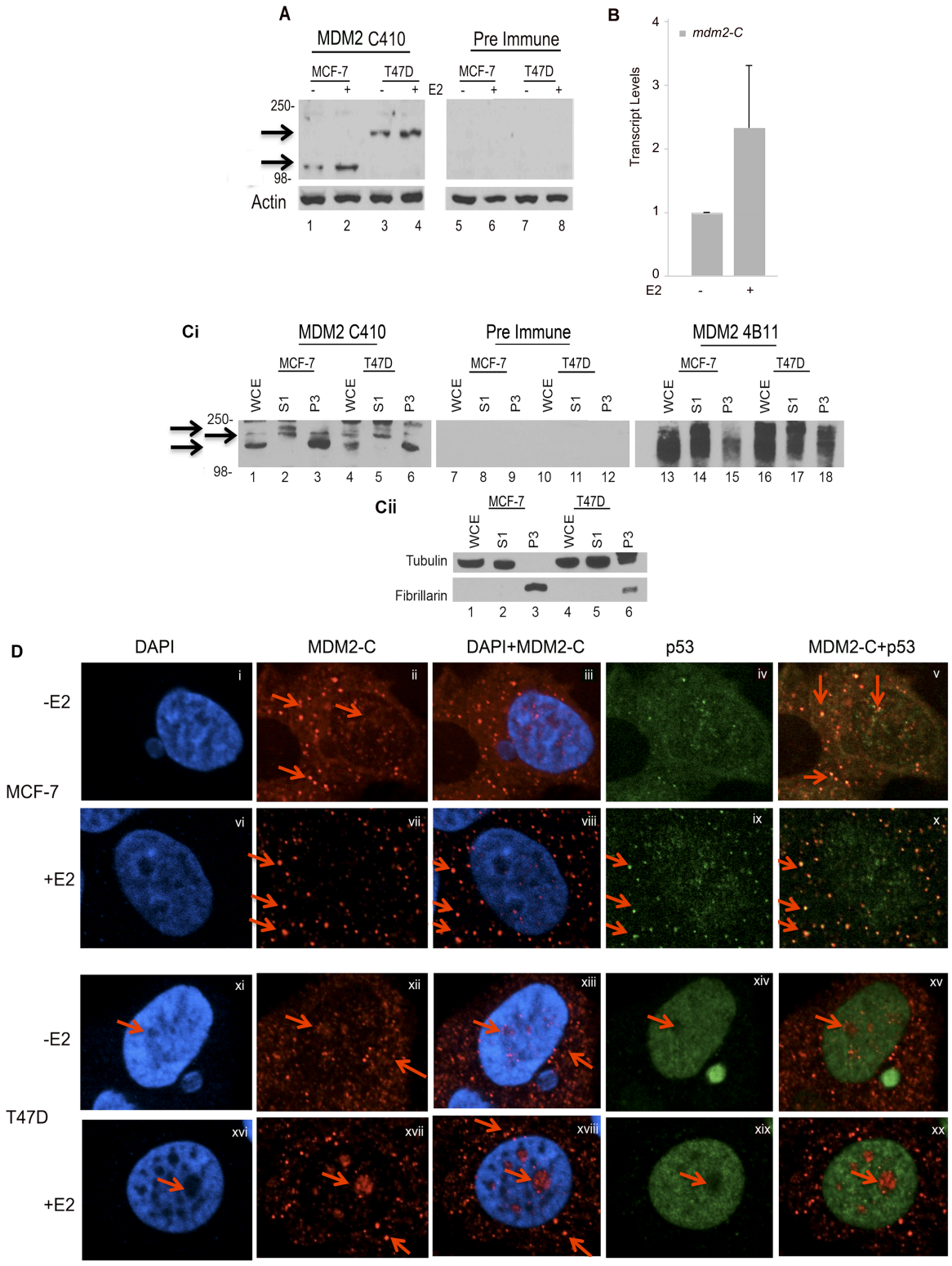

Figure 22: **Mdm2-C increases with estrogen treatment in ER+ breast cancer cells and is located in the cell nucleoli. A.** *MCF-7 and T47D cells were grown and treated*

with 10nM estrogen (E2) for five days. Cells were lysed and 50μg sample was subjected to SDS-PAGE and proteins were analyzed via western blot. Mdm2 C410 polyclonal serum anti-rabbit antibody (lanes 1 – 4) was used for protein detection. Pre-immune polyclonal serum was used to detect background signal (lanes 5 – 8). HRP-conjugated anti-mouse and anti-rabbit were used as secondary antibodies. Actin was used as a loading control. This is representative of three independent experiments. **B**. *T47D cells were grown for three days in the presence and absence of estrogen treatment. Cells were lysed and RNA was extracted for qRT-PCR of mdm2-C transcript. Samples were normalized to –E2 control for fold induction and normalized for RNA levels with gapdh. Average of three independent experiments is represented. Error bars indicate standard error*. **Ci.** MCF-7 and T47D cells were lysed for whole cell or chromatin fractionation extracts. 50μg samples were resolved on 10% SDS-PAGE and Mdm2 C410 polyclonal sera (lanes 1 – 6) and Mdm2 monoclonal antibody, 4B11 (lanes 13 – 18) were used for protein detection. Pre immune was used to detect background signal (lanes 7 – 12). Secondary antibodies used were same as in **A**. **Cii**. Tubulin and Fibrillarin were used as controls for cellular compartment specification. **D.** *Spinning disk microscopy of MCF-7 and T47D cells. Cells were grown on coverslips and treated with 10nM E2 for five days. Cells were fixed and incubated with p53 antibody and Mdm2 C410 polyclonal antibody for protein detection. Pre-immune serum was used as a negative control for staining. Slides were incubated with secondary Alexa-conjugated goat anti-rabbit and FITC-conjugated goat anti-mouse. DAPI was used to stain the nuclei. Cells were visualized at 60X magnification. Arrows depict protein bands or protein localization regions.*

3.2.7 **Mdm2-C Minimally Co-localizes With nucleolin and eIF-4E**

Mdm2 has been shown to bind to nucleolin (Bhatt et al., 2012; Saxena et al., 2006)**.** In order to confirm the nucleoli localization of Mdm2-C, we used IF to check for co-localization of the Mdm2-C protein with the nucleolar marker, nucleolin in MANCA and T47D cells. We did not observe any obvious co-localization of Mdm2-C and nucleolin (Fig. 23- MANCA v and T47D v). In some nuclei of T47D cells, in addition to being present in the nucleus, nucleolin appears to form a pore-like distribution around the membrane edges of the nucleoli in regions distinct from where Mdm2-C is found (Fig 23B compare iii to iv). We are not sure why this is the case since nucleolin is a nucleolar marker and should be present in the nucleolus. Interestingly, this nucleolar

membrane localization of nucleolin was mostly absent after estrogen treatment (Fig. 23 T47D-x). Therefore, the reason for the speckle formation by Mdm2-C in MANCA cells and both breast cancer cell lines before and after estrogen remains under investigation.

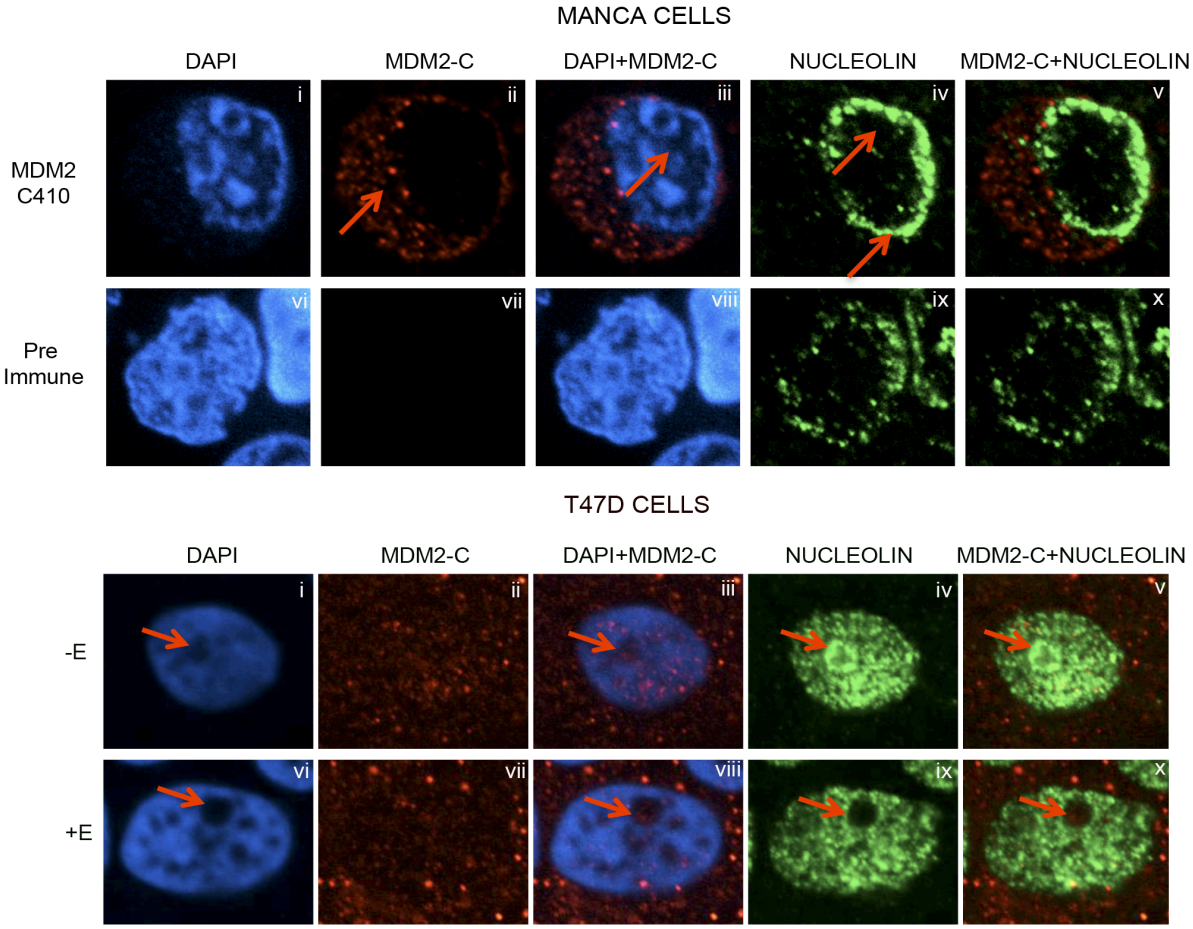

Figure 23**: Mdm2-C does not co-localize with nucleolin in MANCA and T47D cells.** *Spinning disk microscopy of MANCA and T47D cells. Cells were either spun down onto (MANCA) or grown on coverslips and treated with 10nM E2 for five days (T47D). Cells were fixed and incubated with Nucleolin antibody and Mdm2 C410 polyclonal antibody for protein detection. Slides were incubated with secondary Alexa-conjugated goat anti-rabbit and FITC-conjugated goat anti-mouse. DAPI was used to stain the nuclei. Cells were visualized at 60X magnification. Arrows depict protein localization regions.*

Due to the speckled cytoplasmic localization of Mdm2-C in all the cells examined (See Fig. 19C and 22D), we checked for the co-localization of Mdm2-C with RNA binding proteins eIF-4E and hnRNPA1 in MCF-7 and T47D cells. We did not observe any obvious co-localization in the presence or absence of estrogen treatment, between Mdm2-C and eIF-4E or hnRNPA1 proteins (Fig. 24 and data not shown). We concluded that the lack of co-localization observed was due to poor analysis caused by the using the color observation of color change after dual (Rhodamine and FITC) channel overlay.

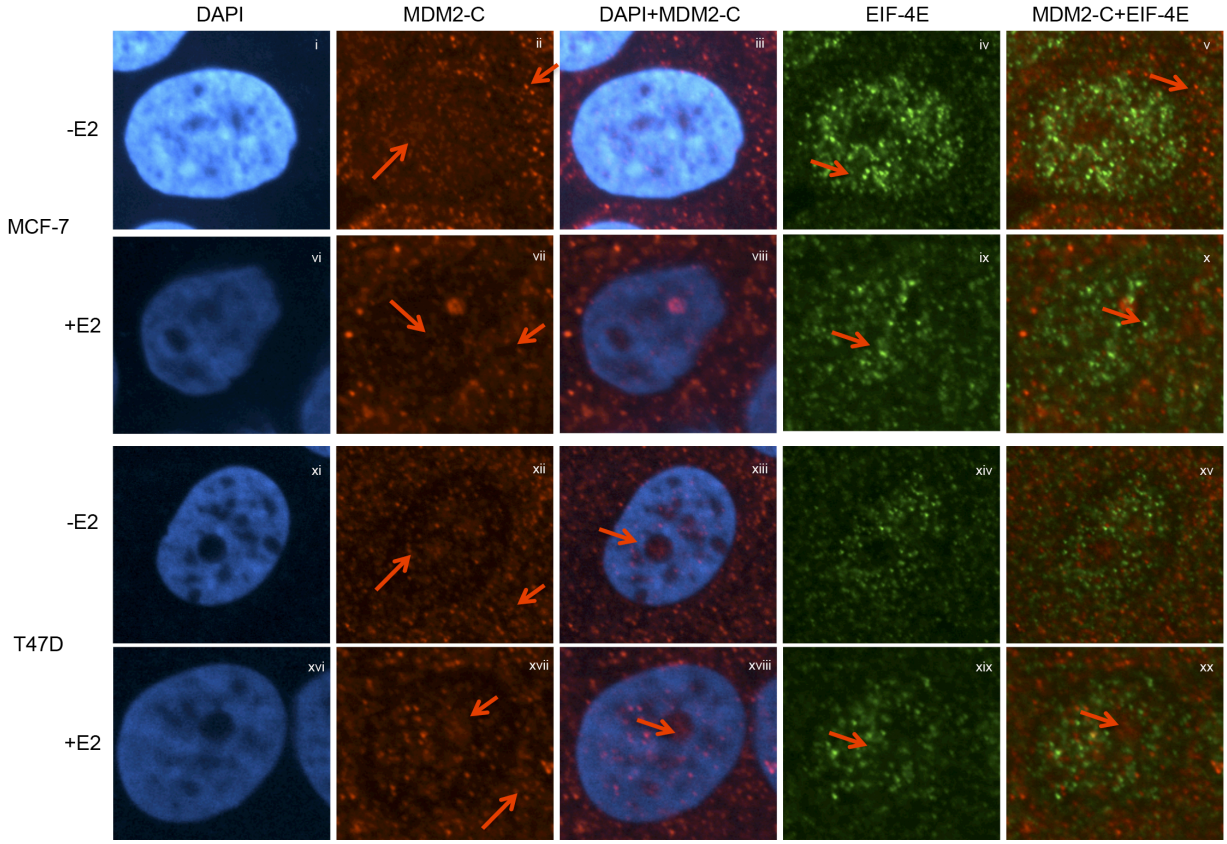

Figure 24**: Mdm2-C does not co-localize with eIF-4E.**
Spinning disk confocal microscopy of MCF-7 and T47D cells. Cells were grown on coverslips and treated with 10nM estrogen for 5 days. Cells were fixed and incubated with eIF-4E monoclonal antibody and Mdm2 C410 polyclonal serum antibody for protein detection. Slides were incubated with secondary Texas Red -conjugated donkey anti-rabbit antibody and FITC-conjugated goat anti-mouse antibody. DAPI was used to stain the nuclei. Cells were visualized at 40X magnification. Arrows depict protein localization regions.

In order to detect the presence or absence of co-localization, we used the co-localization specific program, imarisColoc. We discovered minor co-localizations of Mdm2-C to nucleolin, eIF-4E and hnRNPA1. The imariscoloc software works by quantifying regions of signal co-distribution under threshold parameters that are chosen based on the source signals being examined. Using the software, a new channel is

created in which the areas of co-localization are discovered and highlighted with the color of choice (in our case- yellow). We were able to confirm the co-localization of Mdm2-C to p53 in MANCA cells (Fig. 25i). We also observed some co-localization of Mdm2-C with nucleolin although, not at a high percentage- 0.43% of the total signal for both proteins (Fig. 26ii). The software calculates the percentage as a factor of the amount of co-distributed signal detected to the amount of signal present from the two channels-Rhodamine and FITC. A low percentage could indicate that majority of the Mdm2-C and nucleolin proteins were not found co-distributed in the sample.

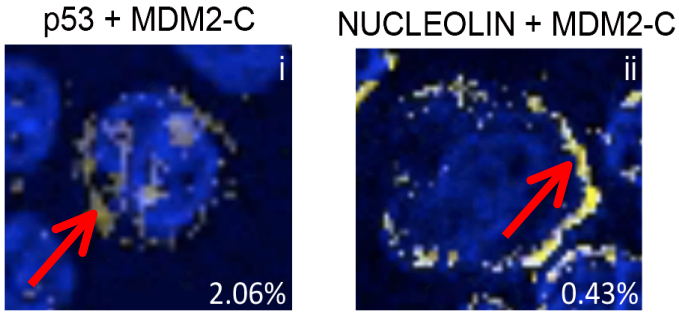

Figure 25: **Mdm2-C co-localizes with p53 and nucleolin in MANCA cells.**
Pictures taken with the spinning disk microscope were examined with the ImarisColoc software. The Mdm2-C channel was used for masking to delineate the area of focus for co-localization. Percentages represent the amount of co-localization. Arrows indicate regions of co-distribution of proteins

We also examined T47D cells for Mdm2-C co-localization. We observed that unlike previously observed in T47D cells, Mdm2-C co-localizes with mutant p53 (Compare Fig. 22xv and xx to Fig. 26i and iv). The reason we did not observe co-localization before might have been due to the strength of the Mdm2-C (rhodamine) signal channel, which was over-saturated and thus masked the presence of co-distribution. We also saw that

in T47D cells, there was some co-distribution of Mdm2-C and nucleolin (Fig. 26ii and v) as well as Mdm2-C and EIF-4E (Fig. 26iii and vi). In addition, we saw co-distribution of Mdm2-C and hnRNPA1 (Fig. 27).

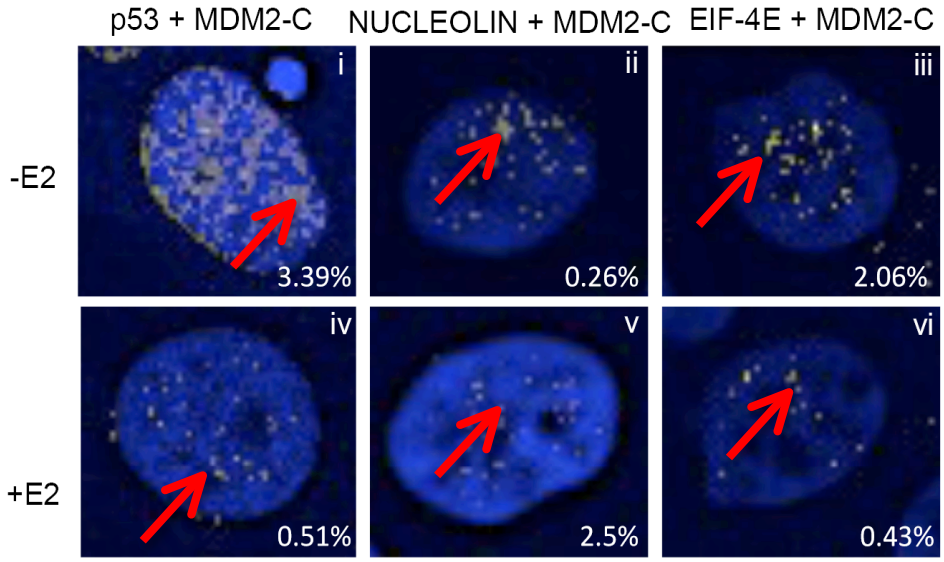

Figure 26: **Mdm2-C co-localizes with p53, nucleolin and eIF-4E in T47D cells.** *Pictures taken with the spinning disk microscope were examined with the ImarisColoc software. The Mdm2-C channel was used for masking to delineate the area of focus for co-localization. Percentages represent the amount of co-localization. Arrows indicate regions of co-distribution of proteins.*

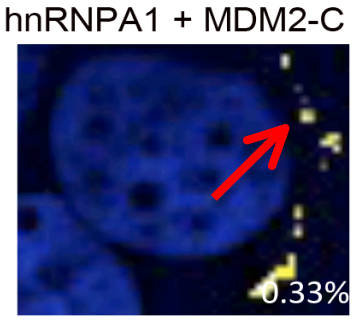

Figure 27: **hnRNPA1 is found minimally co-distributed with Mdm2-C.**
Pictures taken with the spinning disk microscope were examined with the ImarisColoc software. The Mdm2-C channel was used for masking to delineate the area of focus for co-localization. Percentages represent the amount of co-localization. Arrows indicate regions of co-distribution of proteins.

3.2.8 **Knockdown of *mdm2-C* in ER+ cells results in increased cell death**

We have observed that the over-expression of Mdm2-C in *p53*-null H1299 cells increased colony formation in the presence and absence of p53 (Fig. 21). Our data suggested that the influence of Mdm2-C was not dependent on wild-type p53. In addition, previous work in the laboratory has shown that the knockdown of total *mdm2* in mutant *p53* T47D breast cancer cells decreased cell proliferation (Brekman et al., 2011) but did not increase cell death via trypan blue staining (Bargonetti Lab observation). Therefore, we examined whether the decrease of total *mdm2* via shRNA-mediated knockdown in T47D and MCF-7 cells (Brekman et al., 2011) would also lead to the reduction of *mdm2-C* transcript and protein. The *mdm2* shRNA is specific to portions of exon 12 in the *mdm2* transcript and should cause a decrease in *mdm2* transcripts that retain this region. Using *mdm2* knockdown clones, two (2) from T47D and one (1) from MCF-7 cells, we examined the levels of *mdm2-C* transcript and protein after doxycycline treatment for six (6) days. We observed that the *mdm2-FL* (transcript with exons 6 and 7) and *mdm2-C* transcripts were reduced after *mdm2* knockdown in T47D and MCF-7 clones (Fig. 28A).

Next, we wanted to know if the decrease in *mdm2* transcripts correlated with a decrease in Mdm2 proteins. Using the C-terminal specific Mdm2 antibody, 4B11 in immunoblot, we examined the level of total Mdm2 protein in T47D and MCF-7 cells with or without (-/+) doxycycline treatment after six (6) days. We observed a decrease in Mdm2 protein after Mdm2 4B11 immunoblot in all the clones, including the STGM vector control (Fig. 28B lanes 2, 4, 6, 8, 10- indicated by the arrow). However, there was a marked decrease in Mdm2 protein in the *mdm2* shRNA clones compared to the vector

(Fig 28B compare lanes 2 to 4 and 6; 10 to 8). This showed that in the absence of *mdm2* shRNA, doxycycline treatment causes a slight reduction in Mdm2 protein in T47D and MCF-7 breast cancer cells.

Next we checked whether the decrease in *mdm2-C* transcript after doxycycline-mediated *mdm2* knockdown correlated with a decrease in Mdm2-C protein. Using the Mdm2-C specific antibody, Mdm2 C410, we examined Mdm2-C protein levels in T47D and MCF-7 cells with and without (-/+) doxycycline after six (6) days. We observed a decrease in Mdm2-C protein- indicated by the arrow, in all samples treated with doxycycline (Fig 28C lanes 2, 4, 6, 8, 10). However, the decrease was concluded to be due to the doxycycline treatment and not *mdm2* knockdown. This is because there was no dramatic difference in Mdm2-C protein levels seen among all the samples including the STGM vector treated with doxycycline (Fig. 28C compare lanes: T47D: 2 to 4 and 6 and MCF-7: 8 to 10). This is in contrast to the marked decrease observed in Mdm2 protein after the Mdm2 4B11 immunoblot in the *mdm2* knockdown clones (Fig 28B). Although there was a marked decrease in *mdm2-C* transcript after total *mdm2* knockdown, the Mdm2-C protein was not reduced. Therefore, fact that we were able to get rid of the *mdm2-C* message but not protein suggests that the Mdm2-C protein is very stable.

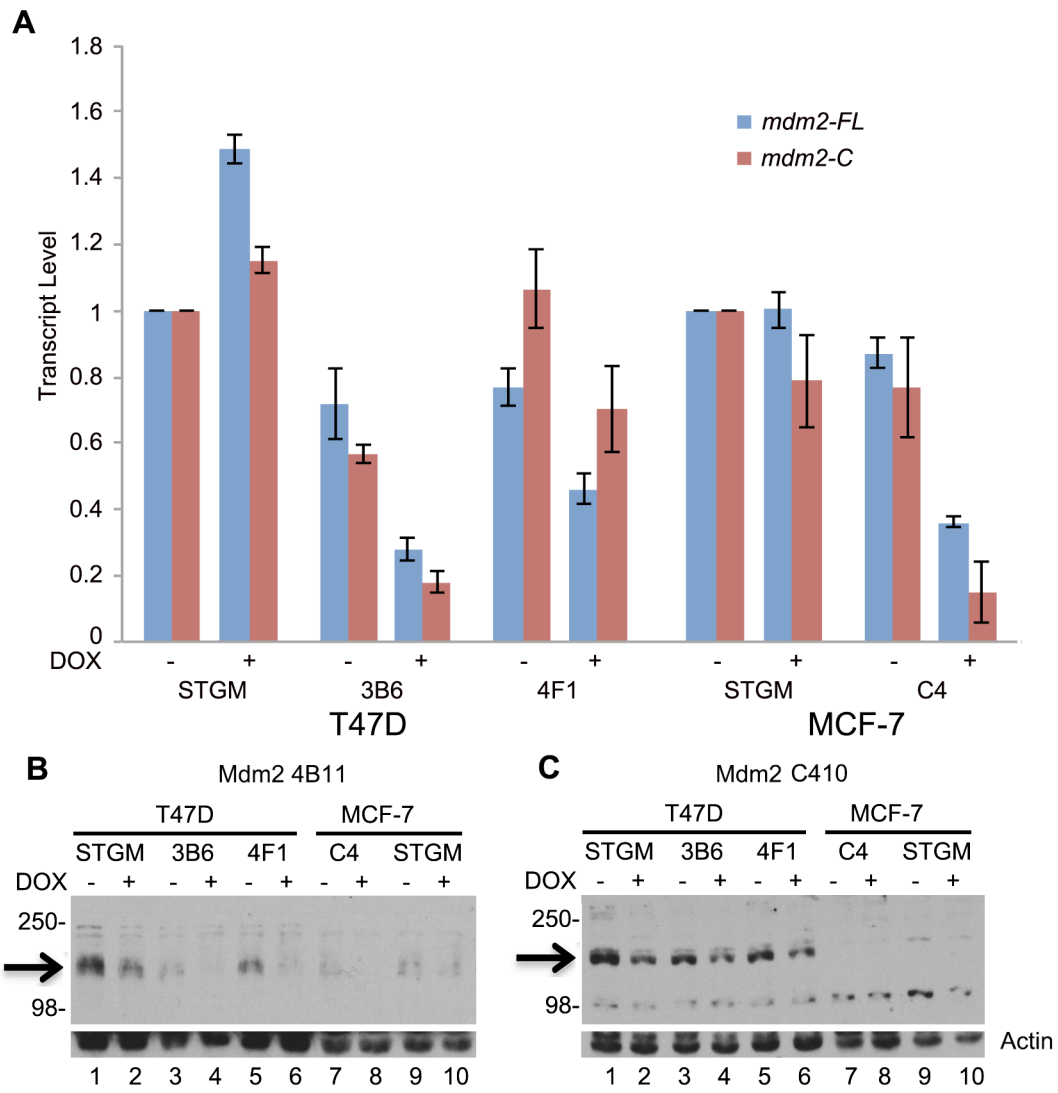

Figure 28: **Total *mdm2* knockdown in T47D and MCF-7 breast cancer cells decreases *mdm2-C*. A.** *qRT-PCR of* mdm2-C *and* mdm2 *(with exon 6 and 7) transcript. RNA was extracted from T47D and MCF-7 cells 6 days after (-/+) doxycycline treatment (4μg/mL or 2μg/mL respectively). Transcripts were quantified via Syber-green and Taqman technology detection (Same as in Fig. 15B). All samples are normalized to STGM vector (-) dox control for knockdown and normalized to actin for RNA levels. An average of two independent experiments is shown. Error bars represent standard error. Western blot analysis of protein extracted from doxycycline treated cells. Proteins were detected using* **B.** *the Mdm2 monoclonal antibody, 4B11 and* **C.** *the Mdm2-C specific polyclonal antibody, C410. Actin was used as a loading control. Arrows represent protein bands.*

Since we could not see a knockdown of Mdm2-C protein in MCF-7 or T47D breast cancer cells, we assumed this could contribute to the reason for the decrease in proliferation but lack of cell death observed in the breast cancer cells (Brekman et al., 2011). Therefore we sought to specifically knockdown *mdm2-C* transcript and consequently Mdm2-C protein and examine its effect on the survival of T47D cells. In order to knockdown the Mdm2-C protein, we generated a siRNA specifically targeted to the *mdm2-C* transcript and compared it to siRNA to total *mdm2* in the cell. The siRNA to *mdm2-C* was designed to the exon 4:10 splice junction of the *mdm2-C* transcript.

We transiently transfected T47D cells with siRNA to *mdm2* -using a smart pool library with four siRNA targets to: exons three, five, and twelve or specifically to *mdm2-C*. Quantitative RT-PCR from siRNA transiently transfected cells showed a partial decrease in *mdm2-C* transcript after *mdm2* and *mdm2-C* knockdown (Fig. 29A). We also observed a decrease in *mdm2* (with exons 6 and 7*)* transcript after *mdm2* smart pool and *mdm2-C* siRNA treatments. However, *mdm2-C* siRNA transiently transfected cells showed somewhat less knockdown of the *mdm2* (with exons 6 and 7) transcript compared to the *mdm2* smart pool treated cells (Fig. 29A). Western blot analysis using the Mdm2 C410 antibody showed a slight decrease in Mdm2-C protein after *mdm2* and *mdm2-C* knockdown, indicated by the arrow (Fig. 29B lanes 3 and 4). However, Image J analysis of the depicted western blot showed a similar decrease in Mdm2-C protein after treatment of the T47D cells with the control siRNA (Fig. 29B compare lanes 2 and 4). We also checked for the level of total Mdm2 protein in the cells after siRNA treatment using the Mdm2 monoclonal mix antibody. We observed that there was a

similar decrease in Mdm2 protein observed in the *mdm2* and *mdm2-C* siRNA treated samples (Fig. 29B lanes 7 and 8).

After siRNA treatment, we examined the cells via microscopy and observed that there were fewer cells after *mdm2* and *mdm2-C* knockdown (Fig. 29C panels iii and iv). Compared to the control and *mdm2* siRNA transiently transfected cells, *mdm2-C* knockdown cells showed more detached cells, often indicative of dead cells (compare Fig. 29Ciii and iv). Interestingly, although the *mdm2-C* transcript and protein were also decreased after *mdm2* knockdown (Fig. 29A and Fig. 29B lane 3), there was no change in cell death observed via trypan blue staining (Fig. 29D). This difference might be due to a reduction in more than one species of *mdm2* transcript when the *mdm2* smart pool siRNA is used, thus resulting in a balance of the ratio of *mdm2* transcripts present in the cell. Conversely, in the *mdm2-C* siRNA transiently transfected cells, there could be an imbalance in the ratio of *mdm2* transcripts, which thus leads to an increase in dead cells (Fig. 29D). To confirm that this increase in death was not due to an off-target effect caused by the *mdm2-C* siRNA, a control scrambled *mdm2-C* siRNA was created. This siRNA contains the same nucleotide sequence as the *mdm2-C* siRNA but is in a rearranged format. The treatment of T47D cells with the *mdm2-C* scrambled siRNA, and trypan blue staining did not show a substantial increase in cell death (Fig. 29D). The cell death observed after *mdm2-C* scrambled siRNA treatment was comparable to the no siRNA, *control* and *mdm2* siRNA treated samples. This confirmed that the increase in cell death observed in the T47D cells was due to the specific knockdown of *mdm2-C*. Additionally, we examined the levels of transcripts of genes involved in cell cycle arrest- *p21* and cell death- *puma*. qRT-PCR of *p21* after *mdm2-C* knockdown showed a slight

increase (two fold) in transcript levels that was p53 independent; but *puma* was unaffected (Fig. 30).

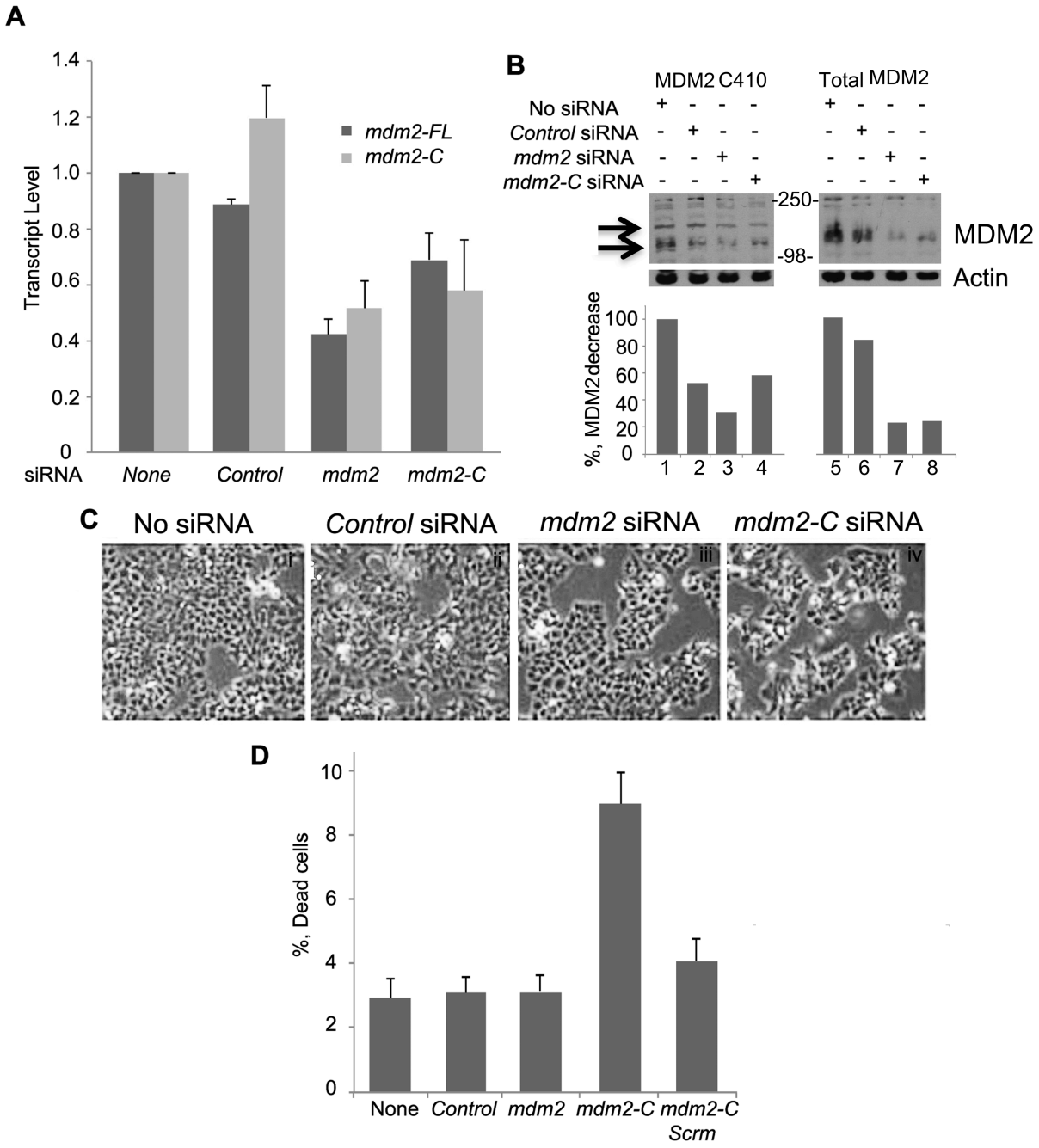

Figure 29**: *mdm2-C* knockdown in T47D breast cancer cells increases cell death. A.** *qRT-PCR of* mdm2-C *and* mdm2 *(with exon 6 and 7) transcript. RNA was extracted from siRNA treated cells and transcripts were quantified via Syber-green and Taqman technology detection (Same as in Fig. 15B). All samples are normalized to no siRNA*

control for knockdown and normalized to gapdh *for RNA levels. An average of three independent experiments is shown. Error bars represent standard error.* **B.** *Western blot analysis of protein extracted from siRNA treated cells. Proteins were detected using the Mdm2 C410 polyclonal sera antibody and the Mdm2 monoclonal antibody mix (4B2, 2A9, 4B11). Actin was used as a loading control. The bar graph represents image J quantitation of the representative western blot shown after siRNA transient transfection. Samples were normalized to no siRNA control for knockdown and Actin for protein levels*. **C.** *T47D cells were plated at 50% confluence and treated the next day with siRNA to mdm2 (smart pool with four exon targets- three, five (2) and twelve) and mdm2-C. Pictures were taken after 48 hours*. **D.** *siRNA treated cells were trypsinized and treated with Trypan blue staining to count the number of all cells and dead cells. The percent dead cells were plotted. An average of three independent experiments is shown. Error bars represent standard error. Arrows represent protein bands.*

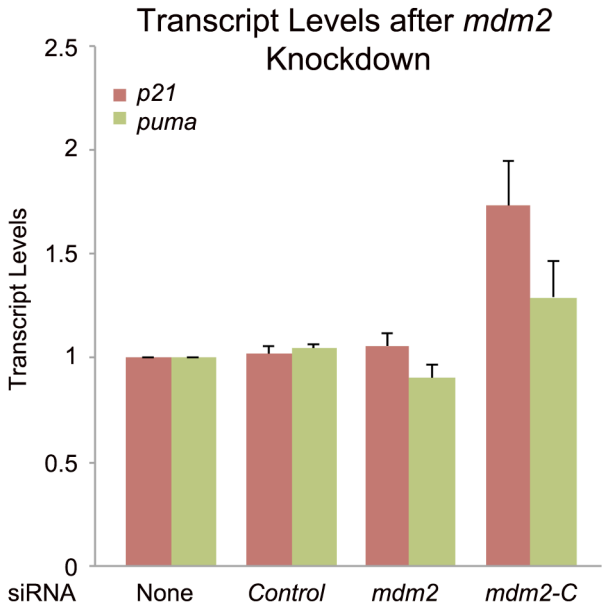

Figure 30**: The cyclin-dependent kinase inhibitor 1 transcript, p21, increases slightly after *mdm2-C* knockdown in T47D ER+ breast cancer cells.** *Quantitative RT-PCR of* p21 *and* puma *transcripts on RNA from siRNA treated T47D samples. All samples are normalized to the no siRNA sample for knockdown and* gapdh *for RNA levels. An average of three independent experiments is shown. Error bars represent standard error.*

3.2.9 **Mdm2-C is Highly Expressed in Liposarcoma and Breast Cancer Tissues**

Mdm2 expression is often observed in liposarcoma (Adachi et al., 2001; Nakayama et al., 1995; Schneider-Stock et al., 1998; Tamborini et al., 2001). In order to determine whether the Mdm2-C protein was expressed in human liposarcoma tumor tissues, we performed immunohistochemistry (IHC) using the Mdm2 C410 polyclonal antibody. Positive staining was observed for two out of three sample sets analyzed (Fig. 31iii). The pre immune serum only detected low background staining in the liposarcoma tissues (Fig. 31ii). A higher magnification picture of the liposarcoma tissue showed that was high expression of Mdm2-C protein (Fig. 31viii). Lipoma tissues were also stained with the Mdm2 C410 antibody and showed very low staining as compared to the liposarcoma tissue (Fig. 31vi). The pre immune serum was also used to show background staining and we detected low staining in both tissues examined (Fig. 31ii and iv). Hematoxylin and Eosin staining was used to show the nuclear and cytoplasmic regions in the tissue sample (Fig. 31i, iv and vii).

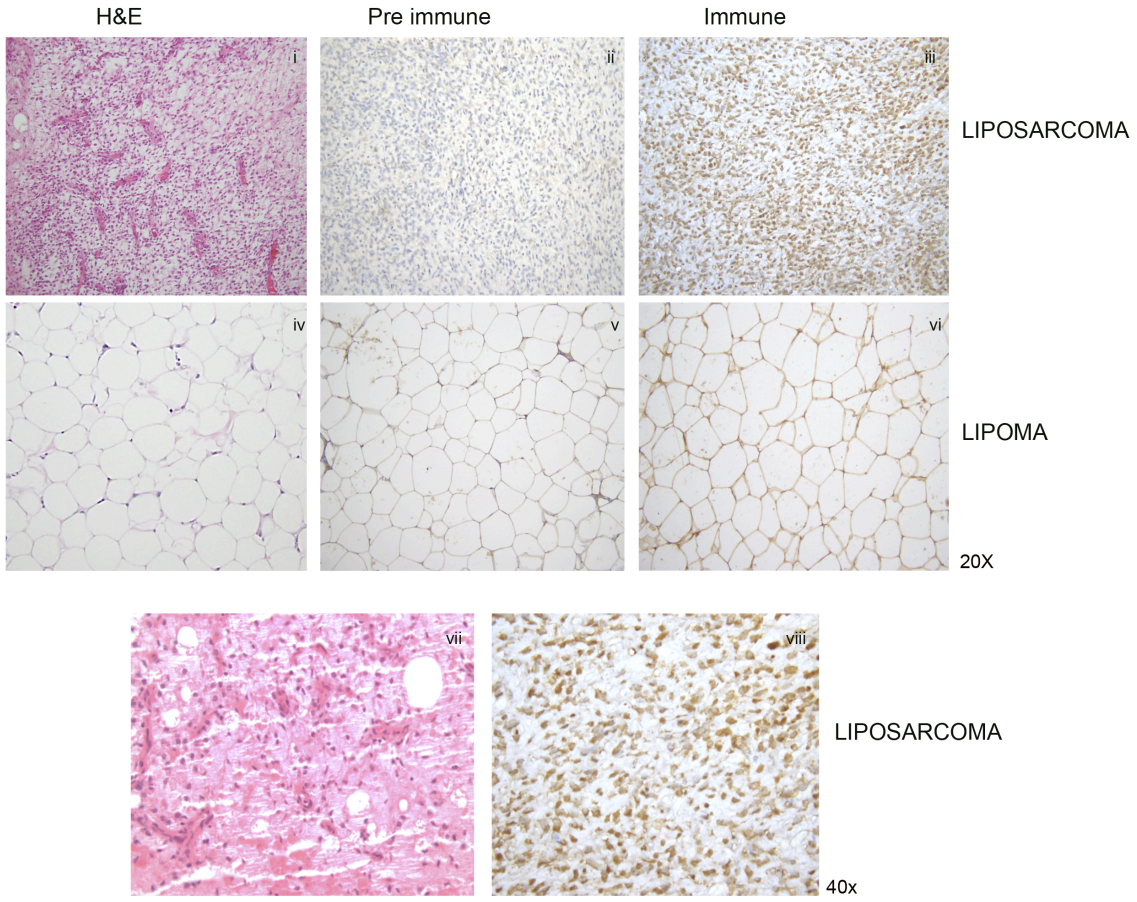

Figure 31: **Mdm2-C is highly expressed in liposarcoma tissues.**
Immunohistochemistry of lipoma and liposarcoma tissues using Mdm2 C410 and pre-immune polyclonal serum antibodies. Secondary antibody mix from Vector kit was used. Pictures were obtained at 20X and 40x magnification. H&E refers to Hematoxylin and Eosin stainings, which were performed by Dr. Nicole Arva.

We also examined a ductal carcinoma breast cancer tissue for Mdm2-C protein expression. Using IHC, we observed that Mdm2-C was highly expressed in the tissue (Fig. 32). The tissue sample showed that Mdm2-C was predominantly expressed in ductal regions of the tissue (Fig. 32i and ii). A closer examination of the tissue at a higher magnification showed that majority of the surround cells in the tissue sample

expressed low or no Mdm2-C compared to the cells in the ductal region (Fig. 32iii and iv).

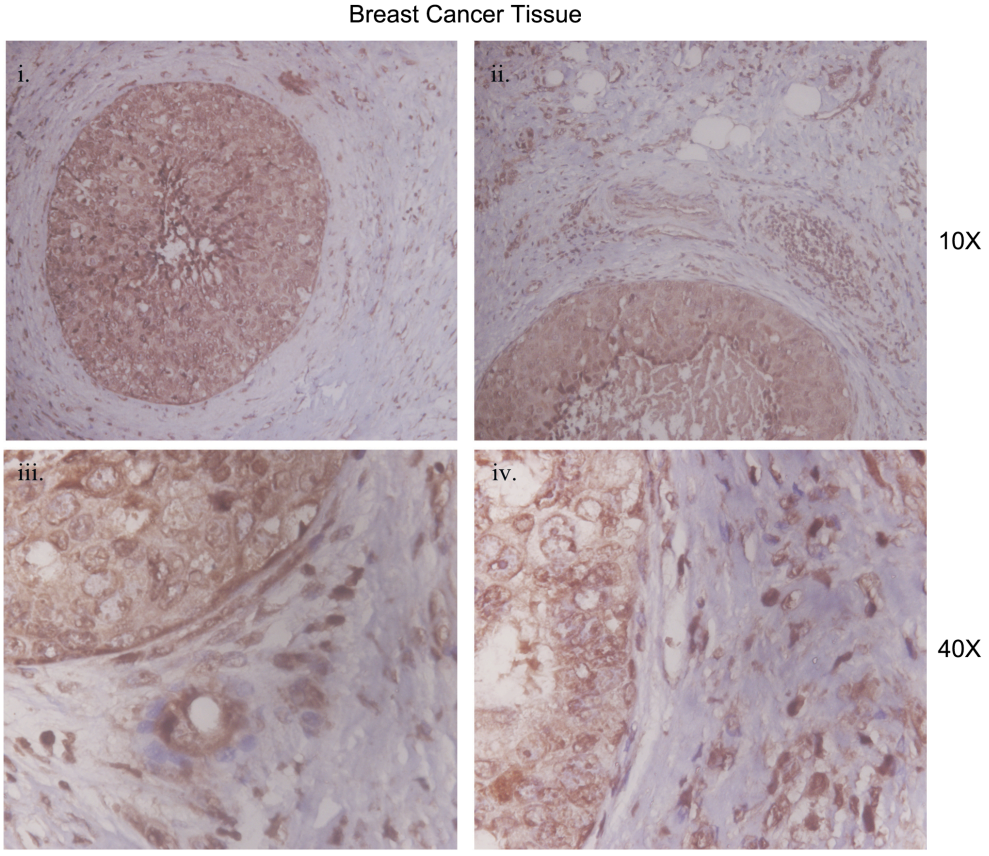

Figure 32**: High Mdm2-C expression is observed in breast cancer tissue.** *Immunohistochemistry of breast cancer tissue #11 using Mdm2 C410 immune polyclonal antibody. Pictures were obtained at 10X and 40X magnification.*

CHAPTER 4:

Discussion

The *mdm2-C* isoform is one of 3 most expressed alternatively spliced variants of *mdm2*. The *mdm2-C* transcript is missing exons 5 through 9 and can be translated into protein (Anderson et al., 2007; Sigalas et al., 1996). All works with Mdm2 isoforms such as studies with Mdm2-A and Mdm2-B have been carried out with exogenously expressed proteins. The exogenous expression of Mdm2-C results in the transformation of NIH3T3 cells (Sigalas et al., 1996) but no further work has been performed to determine the biological function of the Mdm2-C protein. In addition, although Mdm2 isoforms have been studied for some years now, the endogenous detection of a specific isoform has remained elusive. We report here the development of an Mdm2-C specific antibody, Mdm2 C410 that spans the exon 4 and exon 10 splice junction of the Mdm2-C polypeptide (Fig. 17). In this study, we examined a panel of cell lines to determine the comparative levels of *mdm2-C* transcript and Mdm2-C protein. We also assessed the biological functions of the Mdm2-C protein. We also report that like the Mdm2-A and Mdm2-B isoforms, Mdm2-C has non-canonical Mdm2 cellular functions.

We identified the endogenous expression of *mdm2-C* transcript (Fig. 14B) and Mdm2-C protein (Fig. 19A). Transcript levels of *mdm2-C* in the panel of cells differed based on the status of Mdm2 protein expression. We observed that SJSA-1 cells compared to MANCA cells, showed less Mdm2-C protein despite higher *mdm2-C* transcript levels (Compare Fig. 14B to 19A lanes 1 and 2). The reason for this discrepancy between mRNA and protein levels is unclear. Conversely, MANCA cells, which over-express Mdm2 via the *G/G mdm2 SNP309*, compared to *mdm2-FL* transcripts, showed a seven-fold increase in *mdm2-C* transcript (Fig. 14B). MANCA cells are a Burkitts' lymphoma derived cancer cell line, which have compromised p53

activity and are resistant to stress-dependent death (Arva et al., 2005; Arva et al., 2008). This high *mdm2-C* transcript level correlated with high Mdm2-C protein detected (Fig. 19A lane 1) and compromised p53 activity in the damage-induced activation of p53 target genes, *p21* and *puma* (Fig. 15B). SJSA-1 cells, like MANCA cells had high basal levels of *mdm2-C* transcript compared to ML-1 and K562, also showed compromised p53 activity (Fig. 15B) and (Fig 15B). Interestingly, It has been documented that a two and a half fold increase in *mdm2* transcript due to the *mdm2* SNP309 causes a change in tumor spectrum and damage-induced response observed in mice (Post et al., 2010). Therefore, this suggests that the levels of individual *mdm2* transcripts matter and could influence the nature of proteins produced in the cell. It also suggests that a higher level of one *mdm2* transcript over others could give the cell a selective advantage against tumor suppression. In the case of Mdm2 in MANCA cells, it might be the inactivation of the tumor suppressor protein, p53.

We found endogenous Mdm2-C protein in the cytoplasm and in the nucleolus in a punctate pattern (Fig. 19C and 22D). We confirmed localization of Mdm2-C to the organelles by checking for co-localization of Mdm2-C and nucleolin. We observed that in T47D cells with estrogen treatment, the condition at which Mdm2 protein is highest and MANCA cells, nucleolin only moderately co-localized with Mdm2-C with percentages of 2.5% and 0.43% respectively (Fig. 25ii-MANCA and Fig. 26v-T47D). The reason for a low percentage value for co-localization could be as a result of an indirect interaction between Mdm2-C and nucleolin.

The punctate pattern of Mdm2-C suggested that unlike the other Mdm2 isoforms, Mdm2-C might function in an alternate pathway that is related to its manner of cellular

distribution. Often times, punctate protein localization in the cytoplasm represents sites of RNA processing. Therefore, it is possible that the presence of Mdm2-C in the nucleolus could be involved in splicing, ribosome biogenesis or translation. To address the cytoplasmic speckled localization of Mdm2-C, we examined two RNA binding proteins involved in splicing and translation, Eukaryotic translation initiation Factor 4 (eIF-4E) and heterogeneous ribonucleoprotein A1 (hnRNPA1), for their interaction with Mdm2-C. We observed minor co-localization of Mdm2-C with eIF-4E and hnRNPA1 proteins with percentages of 0.43% and 0.33% respectively (Fig. 26vi and Fig. 27). Nonetheless, the strength of overall co-localization observed was not striking (with percentages between 0.1 - 4.3%). Therefore, the reason behind the speckled localization of Mdm2-C still needs to be explored by looking at other RNA binding and processing proteins as well as their cellular interaction with Mdm2-C.

We have also observed that in cells with Mdm2 over-expression, there are more alternatively spliced *mdm2* variants than non-*mdm2* over-expressing cells (Arva et al., 2008). This suggests that Mdm2 could be involved in processing its own RNA transcripts and possibly other target transcripts either directly or through binding of proteins associated with RNA processing. The ability of Mdm2-C to bind RNA has not been confirmed, however, the protein still possesses the RNA binding region similar to full-length Mdm2 (Candeias et al., 2008; Naski et al., 2009; Ofir-Rosenfeld et al., 2008; Takagi et al., 2005).

We found that exogenous expression of Mdm2-C in *p53*-null H1299 cells did not inhibit p53 transactivation ability nor did it significantly target p53 for proteasome-

mediated degradation. The reason for this must lie in absence of portions of the p53-binding domain, which is critical in facilitating the Mdm2-p53 interaction and p53 degradation (Poyurovsky et al., 2010). Additionally, most Mdm2 variant isoforms have been documented to be unable to bind to p53 (Fridman et al., 2003; Schuster et al., 2007). So this result is not surprising. Rather, the oncogenic influence of Mdm2-C appears to be independent of p53.

We show data that supports the involvement of Mdm2-C in cell proliferation. Colony formation assay after exogenous expression of Mdm2-C resulted in increased cell colony forming units (Fig. 21). The increase in colony units observed was p53-independent because in the presence of p53, compared to the vector control and Mdm2-FL expressing cells, Mdm2-C over-expression resulted more colonies albeit at a lower penetrance (Fig. 21). This is akin to studies that have shown that Mdm2 promotes cell proliferation independent of p53 (Brekman et al., 2011; Deb, 2003). In addition, the partial knockdown of *mdm2-C* in T47D breast cancer cells with mutant p53 caused a modest increase in cell death (Fig 29). To validate the type of cell death observed, Annexin-V/PI staining was performed. We observed that the cells did not die via apoptosis because there was no difference in the amount of Annexin-V only stained cells. However, there was a slight increase in PI only stained cells, which is indicative of compromised plasma membrane and necrotic cell death (data not shown). However to confirm this, more experiments need to be done where the specific cell death markers are examined.

Our data suggests that the ratio of *mdm2* isoforms may indicate variable regulatory outcomes (Fig. 14B and Fig. 15B). The difference in cell death observed in T47D cells when *mdm2* is knocked down vs. when *mdm2-C* is knocked down might be due to a reduction in more than one species of *mdm2* transcript after *mdm2* knockdown. This is interesting because the knockdown of *mdm2* using the shRNA to exon 12 of *mdm2* or the smart pool siRNA with a number of mRNA epitope targets to- exons 3, exon 5 (2) and exon 12- did not show an increase in cell death (data not shown and Fig. 29D). Conversely, the knockdown of *mdm2-C* could have resulted in an imbalance in the ratio of *mdm2* transcripts and Mdm2 proteins, which caused cell death. This suggests that Mdm2-C might be important for estrogen-mediated cell survival of ER+ breast cancer cells.

Additionally, we saw an estrogen-dependent and p53-independent increase of Mdm2-C in two ER+ *mdm2* SNP309 breast cancer cells (Fig. 22). This suggests that the over-expression of Mdm2-C could have a survival role in cells without functional p53, and could possibly influence non-p53 related pathways.

Mdm2 has the potential to serve as a cancer biomarker. It is amplified or overexpressed in over 30% of sarcomas, 80% of well-differentiated liposarcomas (WDLPS), and 60% of myxoid liposarcomas (Sandberg, 2004). The Mdm2 C410 antibody detected endogenous Mdm2-C in human cancer cell lines (Fig. 19) and using immunohistochemistry, we observed high expression of Mdm2-C in liposarcoma tissues compared to lipoma tissues (de-differentiated vs. differentiated tissues respectively) (Fig. 31) and in breast cancer tissue (Fig. 32). This suggests that Mdm2-C can be a

prognostic tool in pathology and could also be used as a cancer biomarker in liposarcoma and breast cancer tissues as well as other cancers with high Mdm2-C expression. Thus the creation of this antibody and subsequent monoclonal antibodies will make the future study of the Mdm2-C protein isoform easier and more productive.

We have observed that unlike Mdm2-A and Mdm2-B, Mdm2-C promotes growth in the absence and presence of p53 (Fig. 21) and does not activate p53 transactivation activity (Fig. 20). We have also detected endogenous Mdm2-C protein, something that has not been observed with the other Mdm2 isoforms. These data point to the identification of a putative growth promoting protein, which regardless of the presence or absence of p53, helps in the propagation of cancer. Further experiments to determine the pathway in which Mdm2-C operates is important. This will help facilitate the development and testing of targeted treatment options for cancer patients with Mdm2-C over-expression. Taken together, increased expression and the knockdown of *mdm2-C* caused a change in cell growth; thus suggesting that the Mdm2-C protein has roles in the proliferation and cell survival. The major proteins involved in cell proliferation and cell cycle control are E2F1 and RB proteins. The regulation of these proteins are very important in cancer (Nevins, 2001) and Mdm2 maintains functional interactions with both proteins (Trinh et al., 2001; Udayakumar et al., 2010; Xiao et al., 1995). Therefore, whether the Mdm2-C protein functions in the E2F/RB pathway, increases cell cycle-related proteins or participates in RNA processing, are questions that remain to be addressed.

CHAPTER 5:

Preliminary Data and Future Directions

5.1:

Preliminary Data

5.1.1 **Introduction**

We have reported data that showed non-canonical functions of Mdm2-C. We observed that Mdm2-C increased cell proliferation (Fig. 21) and had a role in cell survival (Fig. 29). We observed that these functions of Mdm2-C occurred independent of the presence or absence of wild-type p53. Therefore, unlike the well-characterized Mdm2 isoforms, Mdm2-A and Mdm2-B, the Mdm2-C isoform has p53-independent growth promoting functions. We also detected Mdm2-C in the cytoplasm and nucleolus, which was contrary to what has been documented for Mdm2-A and Mdm2-B, thus suggesting that the functions of Mdm2-C might lie in its localization and protein-binding partners. Our preliminary work showed that, either through direct or indirect associations, Mdm2-C might have a wide range of interacting proteins. And these Mdm2-C interactions may have cellular roles that classify the Mdm2-C protein as a cancer biomarker.

5.1.2 **Mdm2-C as a Cancer Prognostic Tool**

We showed that Mdm2-C is highly expressed in liposarcoma tissues and in one breast cancer tissue (Fig. 31 and 32). However, we need a larger cohort of samples to correlate this incidence to a constant prognostic phenotype that can be utilized as a tool for pathology. Also, to implicate Mdm2-C expression in a variety of cancer types, we need to perform more studies showing Mdm2-C expression in other cancer tissues. We are in the process of generating monoclonal Mdm2-C antibodies and the preliminary data with sera from five (5) immunized mice shows promise (Fig. 33 see lanes 3, 10, 16,

23 and 29). Unlike the rabbit polyclonal (Fig. 17C lane 3 vs. 4), the mouse polyclonal did not show any background with the Mdm2-FL protein after IP with the monoclonal antibody (Fig. 33 see lanes 4, 11, 17, 24, 30). The pre immune sera from the mice did not show any background protein (Fig. 33 lanes 6 – 8, 13 -15, 19 – 21, 26 – 28 and 32 - 34).

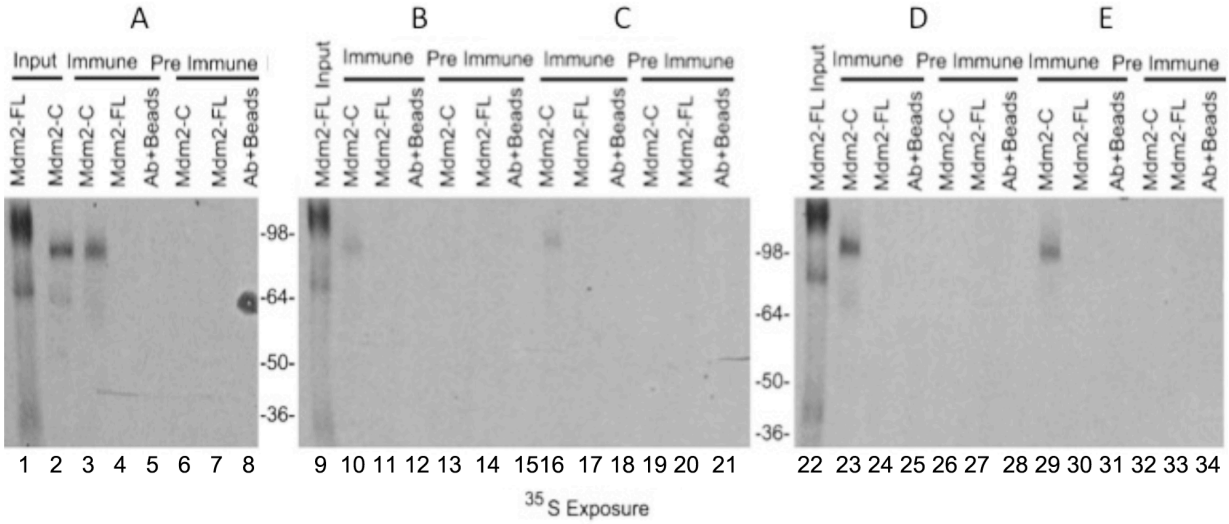

Figure 33: **The Mdm2 C410 peptide is highly immunoreactive and the mouse polyclonal Mdm2 C410 antibody is specific to Mdm2-C**. *Five mice were immunized with immunoreactive Mdm2 C410 peptide and antibody was generated. The antibody generated was used in an immunoprecipitation for Mdm2-C pull down using ^{35}S radio labeled in vitro translated Mdm2-C and Mdm2-FL proteins.*

We have preliminary immunohistochemistry data of an array of seventy-five (75) breast cancer tissue samples using polyclonal Mdm2 C410 from rabbit and mouse origins (Fig. 34). We observed that the mouse polyclonal antibody showed less protein staining (Fig. 34, middle panel) and this could be as a result of a lower antibody titer in the mouse. Further work is being performed to determine the percentage of Mdm2-C protein positive samples, the correlation between Mdm2-C protein expressions and the

stages and grade of the cancers. A closer observation of some of the tissue sections on the array showed that the polyclonal rabbit antibody had a higher protein signal as compared to the mouse polyclonal (Fig. 35 row iii vs. iv). But both proteins showed a similar staining pattern (Fig. 35 row iii vs. iv). The lower signal with the mouse polyclonal produced a better image for analysis. Thus this suggests that the monoclonal antibody when generated could serve as a better tool in Mdm2-C protein studies compared to the rabbit polyclonal due to less background staining and specificity for Mdm2-C protein.

Figure 34**: Mdm2 C410 mouse and rabbit polyclonal antibodies show reactivity to endogenous Mdm2-C protein in breast cancer tissue array.** *Breast Cancer tissue array with 75 paraffin embedded blocks in duplicates were purchased from protein biotechnologies and IHC was performed at memorial Sloan Kettering cancer center using polyclonal rabbit and mouse Mdm2 C410 antibodies and mouse IGG antibody. Picture of the slides was taken with a 10X Nikon camera.*

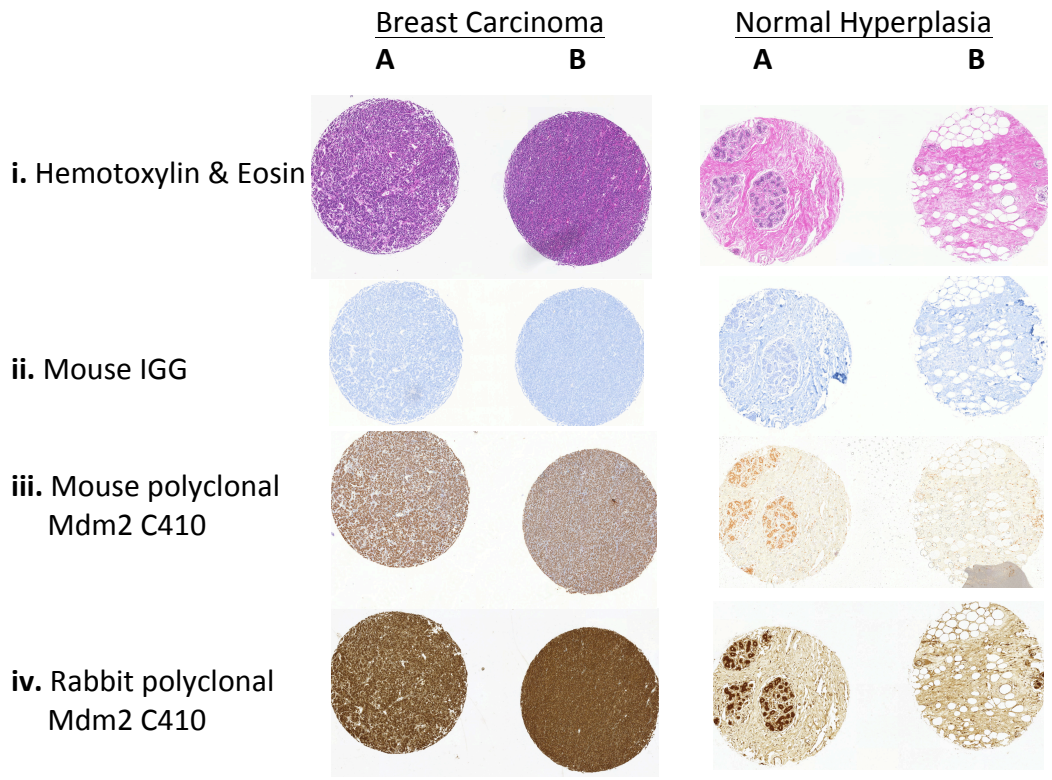

Figure 35: **Mdm2 C410 mouse monoclonal antibody detects Mdm2-C protein in a breast cancer array**. *The samples were stained with the polyclonal rabbit and mouse antibodies by the immunohistochemistry facility at Cornell University. Hemotoxylin and Eosin were used to show the cell morphology in the tissue section and Mouse IGG was used to show background from the mouse antibody. A and B represent duplicate samples of the same tissue section. The pictures were zoomed in at 5X and the image was captured using the panoramic viewer software*.

5.1.3 **Mdm2-C Binds to Full-length Mdm2 and Other Proteins *in vivo***

The functions of a protein in the cell are in part dependent on its cellular binding partners. Therefore in investigating the mechanism through which Mdm2-C influences growth, experiments that involve looking at the interacting proteins of Mdm2-C are critical. Mdm2 isoforms A and B have been shown to bind to Mdm2-FL but not to p53 *in vitro* (rabbit reticulocyte) (Sigalas et al., 1996) and in the cell (Schuster et al., 2007; Volk

et al., 2009b). To determine if Mdm2-C binds to Mdm2-FL, we performed protein pull-down assays from MANCA cell extracts. Antibodies used in the protein pull-down were the Mdm2-C specific antibody**,** Mdm2 C410 polyclonal serum antibody and the monoclonal antibody, SMP14, whose epitope of recognition lies within the nuclear localization and export signals region. SMP14 was used to detect full-length Mdm2 because Mdm2-C does not retain the epitope region specific to SMP14 (Bartel et al., 2002). Western blot detection using the Mdm2 C410 antibody showed that SMP14 immunoprecipitated Mdm2-C protein of three masses: above 98 kDa (Fig. 36A lane 2). These bands correlate to protein bands observed previously (See Fig. 19).

We examined the reverse protein pull-down using the Mdm2 C410 as bait to further confirm the binding of Mdm2-FL and Mdm2-C proteins. Immunoprecipitation with Mdm2 C410 antibody and protein detection with the Mdm2 SMP14 antibody did not detect a substantial pull down of Mdm2-FL protein (data not shown). This could be due to an alteration in the structural orientation of the protein complex that masks the epitope for the Mdm2 C410 antibody; thus preventing adequate pull-down of the Mdm2-C protein and consequently, Mdm2-FL. Alternatively, we performed an immunoblot using the C-terminal Mdm2 antibody 4B11 after Mdm2 C410 IP. We observed a major band close to 250 kDa (Fig. 36A lane 6). The pre immune showed some background detection, however, the immune IP showed a stronger protein detection signal (Fig. 36A compare lanes 6 and 8). In order to determine whether the band observed after 4B11 immunoblot was Mdm2-C or a combination of Mdm2-FL and Mdm2-C, we performed an immunolot using the central region specific Mdm2 antibody, 2A9. We observed

additional bands at 98 kDa and in between 98 kDa and 250 kDa (Fig. 36A lane 6, 2A9 lower panel). This thus supported that Mdm2-C bound to Mdm2-FL.

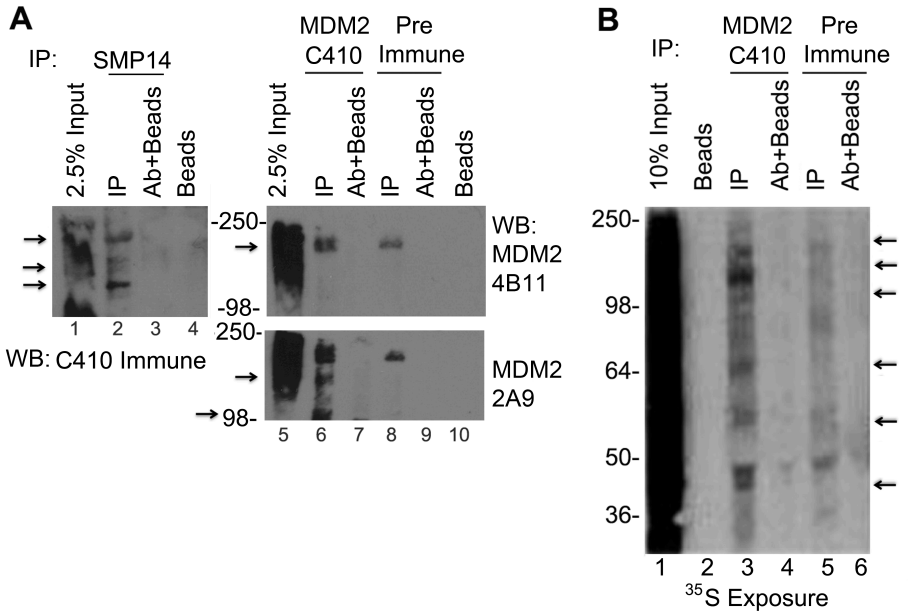

Figure 36**: Mdm2-C interacts with Mdm2-FL and other cellular proteins *in vivo***
A. *Immunoprecipitation from MANCA whole cell extract using SMP14 antibody. Samples were electrophoresed on a 10% SDS-PAGE gel, transferred to a nitrocellulose membrane and probed with Mdm2 C410 polyclonal serum antibody. Immunoprecipitation was also performed with the Mdm2 C410 and pre immune antibodies. Samples were electrophoresed on a 10% SDS-PAGE gel, transferred to a nitrocellulose membrane and probed with Mdm2 4B11 monoclonal serum antibody. The membrane was sequentially re-probed with Mdm2 2A9 monoclonal antibody. HRP-conjugated anti-mouse and anti-rabbit were used as secondary antibodies. This is a representative gel of three independent experiments*. **B.** *Immunoprecipitation of ^{35}S Methionine radioactive labeled MANCA whole cell extracts using Mdm2 C410 and pre-immune antibodies. Samples were electrophoresed on a 10% SDS-PAGE gel, transferred to nitrocellulose membrane and exposed to film for protein detection. Arrows represent protein bands.*

To assess whether other proteins bound to Mdm2-C *in vivo*, additional Mdm2 protein pull-down assays were performed from MANCA cells. Cultured cells were grown in media lacking methionine and every protein in the cell was radiolabeled with ^{35}S

methionine over night. The protein lysate obtained from the radiolabeled cells was used in an Mdm2 C410 protein pull-down assay. A number of bands were visualized after autoradiography (Fig. 36B lane 3). The detection of other bands implied that Mdm2-FL was not the sole protein that bound to Mdm2-C. Interestingly, some of the proteins observed correlated with the sizes of bands seen after immunoblot for Mdm2-C (see Fig. 36A lane 1 and 5).

In order to identify some of the radiolabelled proteins immunoprecipitated with the Mdm2 C410 antibody from MANCA cells, we performed liquid chromatography-mass spectrometry (LC/MS/MS). Six distinct bands were observed after coomassie blue staining (Fig. 37A). Western blot analysis showed that full-length Mdm2 was pulled down as one of the proteins after immunoprecipitation using the Mdm2 C410 specific antibody (Fig. 37B lane 2). The six bands were cut out and processed for protein identification and LC/MS/MS identified a number of proteins with functions in: splicing, transcription, translation and metabolism (See Table 2). Examples of some of the strongly identified proteins include: Nucleolin, Heat Shock Cognate 71 Protein (HSP7C), 2-oxoglutarate dehydrogenase mitochonadrial (ODO1), Heat Shock protein HSP90β (HS90B) and serine/threonine-protein kinase (Nek9). Other detected proteins that have been found to bind to Mdm2 include: DNA endonuclease (RBBP8), transcription intermediary factor 1 Beta (Trim28/KAP1/TIF1B) (Wang et al., 2005), CDKN2A-interacting protein (CARF) (Kamrul et al., 2007) and probable ATP-dependent RNA helicase (DDX5) (Table 2- proteins highlighted in red). Interestingly, we also identified a few proteins that were identified after specific pull-down of Mdm2 using the SMP14 antibody. They include: protein KIAA1967, RNA binding protein EWS and RNA-binding

protein FUS (Table 2- bolded proteins). However, the impact of Mdm2-C binding to these proteins *in vivo* is not known. In addition, we do not know whether the proteins pulled down maintain direct or indirect interactions with Mdm2-C.

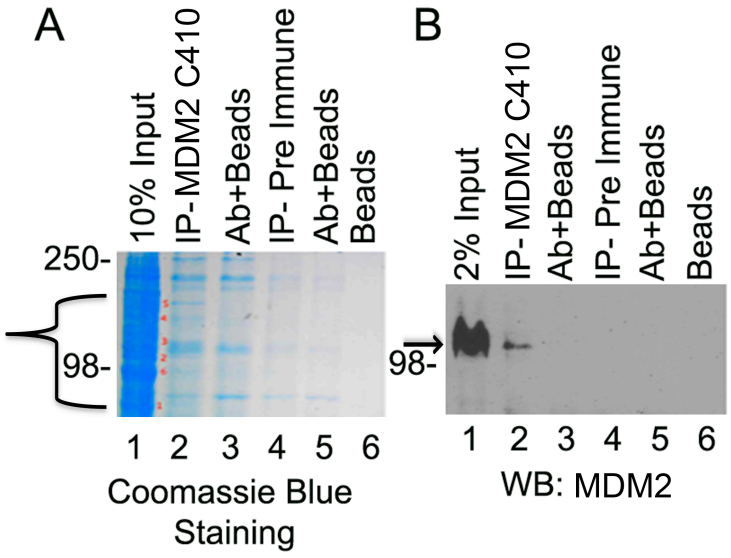

Figure 37**: Mdm2-C interacts with a variety of proteins *in vivo*.**
Immunoprecipitation from MANCA whole cell extracts using Mdm2 C410 and pre-immune polyclonal serum antibodies. Samples were electrophoresed onto a 10% SDS-PAGE gel in duplicate. **A.** *One half was stained with coomassie blue for protein detection. Protein bands were excised and sequenced via LC/MS/MS.* **B.** *The other half was transferred to nitrocellulose membrane and Mdm2 protein was detected using the Mdm2 monoclonal antibody mix (4B2, 2A9, 4B11). HRP-conjugated anti-mouse and anti-rabbit were used as secondary antibodies. Arrows indicate bands cut out for* ***A.*** *LC/MS/MS and* ***B.*** *Mdm2.*

Table 2: List of LC/MS/MS identified proteins after Mdm2-C IP from MANCA

Identified Proteins	Accession Number	Molecular Weight	Functioning Pathways	Unique peptides				% Total coverage
Nucleolin OS=Homo sapiens GN=NCL PE=1 SV=3	**NUCL_ HUMAN**	**77 kDa**	**Nucleolus**	22	11			**42.9**
2-oxoglutarate dehydrogenase, mitochondrial OS=Homo sapiens GN=OGDH PE=1 SV=3	ODO1_ HUMAN	116 kDa	Citric acid cycle	28	9	3	3	37.1
Dihydrolipoyllysine-residue acetyltransferase component of pyruvate dehydrogenase complex, mitochondrial OS=Homo sapiens GN=DLAT PE=1 SV=3	ODP2_ HUMAN	69 kDa	Links glycolysis to citric cycle	15	6	2		33.3
Minor histocompatibility protein HA-1 OS=Homo sapiens GN=HMHA1 PE=1 SV=2	HMHA1_	125 kDa	GTPase activator for Rho-type GTPases	27	11	2		32
Heat shock cognate 71 kDa protein OS=Homo sapiens GN=HSPA8 PE=1 SV=1	**HSP7C_ HUMAN**	**71 kDa**	**Chaperone**	**19**	**1**			**28.2**
Heat shock protein HSP 90-beta OS=Homo sapiens GN=HSP90AB1 PE=1 SV=4	HS90B_ HUMAN	83 kDa	Chaperone-constitutive	20	1			25.3
Serine/threonine-protein kinase Nek9 OS=Homo sapiens GN=NEK9 PE=1 SV=2	NEK9_ HUMAN	107 kDa	Mitosis progression	15	5	3	3	24.3
DNA endonuclease RBBP8 OS=Homo sapiens GN=RBBP8 PE=1 SV=2	**COM1_ HUMAN**	**102 kDa**	**DNA repair**	**18**	**5**			**22.6**

(Table 2 cont'd) **X-ray repair cross-complementing protein 6 OS=Homo sapiens GN=XRCC6 PE=1 SV=2**	**XRCC6_ HUMAN**	**70 kDa**	**Helicase**	**12**				**17.1**
Isoleucyl-tRNA synthetase, cytoplasmic OS=Homo sapiens GN=IARS PE=1 SV=2	SYIC_ HUMAN	145 kDa	Translation	22				15.2
Extended synaptotagminutes-1 OS=Homo sapiens GN=ESYT1 PE=1 SV=1	ESYT1_ HUMAN	123 kDa	Calcium-regulated intrinsic membrane	17				13.8
Lysyl-tRNA synthetase OS=Homo sapiens GN=KARS PE=1 SV=3	SYK_ HUMAN	68 kDa	Translation	9				13.2
Probable ATP-dependent RNA helicase DDX5 OS=Homo sapiens GN=DDX5 PE=1 SV=1	**DDX5_ HUMAN**	**69 kDa**	**RNA helicase & pre-mRNA splicing**	8				**11.6**
Heterogeneous nuclear ribonucleoprotein M OS=Homo sapiens GN=HNRNPM PE=1 SV=3	HNRPM_ HUMAN	78 kDa	Ribosome	9				11.5
Alkyldihydroxyacetonephosphate synthase, peroxisomal OS=Homo sapiens GN=AGPS PE=1 SV=1	ADAS_ HUMAN	73 kDa	Peroxisomes- energy metabolism	8				10.96
ATP-dependent DNA helicase Q1 OS=Homo sapiens GN=RECQL PE=1 SV=3	RECQ1_ HUMAN	73 kDa	Helicase-DNA repair	8				10.96
Transitional endoplasmic reticulum ATPase OS=Homo sapiens GN=VCP PE=1 SV=4	TERA_ HUMAN	89 kDa	Transitional ER	9				10.1
DNA topoisomerase 1 OS=Homo sapiens GN=TOP1 PE=1 SV=2	TOP1_ HUMAN	91 kDa	DNA unwinding	9				9.9

(Table 2 cont'd)								
Arginyl-tRNA synthetase, cytoplasmic OS=Homo sapiens GN=RARS PE=1 SV=2	SYRC_ HUMAN	75 kDa	Ribosome	7				9.3
Splicing factor, proline- and glutamine-rich OS=Homo sapiens GN=SFPQ PE=1 SV=2	SFPQ_ HUMAN	76 kDa	Splicing	7				9.2
General transcription factor II-I OS=Homo sapiens GN=GTF2I PE=1 SV=2	**GTF2I_ HUMAN**	**112 kDa**	**Transcription & signal transduction**	**10**				**8.9**
Eukaryotic translation initiation factor 2-alpha kinase 1 OS=Homo sapiens GN=EIF2AK1 PE=1 SV=2	E2AK1_ HUMAN	71 kDa	Translation inhibition in response to stress	6				8.5
Insulin-like growth factor 2 mRNA-binding protein 3 OS=Homo sapiens GN=IGF2BP3 PE=1 SV=2	IF2B3_ HUMAN	64 kDa	RNA binding	5				7.8
Heterogeneous nuclear ribonucleoprotein U OS=Homo sapiens GN=HNRNPU PE=1 SV=6	HNRPU_ HUMAN	91 kDa	Pre-mRNA processing and metabolism	7				7.7
Interleukin enhancer-binding factor 3 OS=Homo sapiens GN=ILF3 PE=1 SV=3	ILF3_ HUMAN	95 kDa	Found in ribosomes. Interacts with FUS	7				7.4
Aldehyde dehydrogenase family 16 member A1 OS=Homo sapiens GN=ALDH16A1 PE=1 SV=2	A16A1_ HUMAN	85 kDa	Uses NADP as a cofactor	6				7.1
ATP-dependent RNA helicase A OS=Homo sapiens GN=DHX9 PE=1 SV=4	DHX9_ HUMAN	141 kDa	DNA un-winding & transcription activator	9				6.4
Splicing factor 3B subunit 1 OS=Homo sapiens GN=SF3B1 PE=1 SV=3	SF3B1_ HUMAN	146 kDa	Splicing	9				6.2

(Table 2 cont'd)								
Heat shock protein HSP 90-alpha OS=Homo sapiens GN=HSP90AA1 PE=1 SV=5	**HS90A_ HUMAN**	**85 kDa**	**Chaperone-induced**	**5**				**5.9**
RNA-binding protein EWS OS=Homo sapiens GN=EWSR1 PE=1 SV=1	**EWS_ HUMAN**	**68 kDa**	**RNA binding (TET family protein like FUS)**	**4**				**5.9**
Protein KIAA1967 OS=Homo sapiens GN=KIAA1967 PE=1 SV=2	**K1967_ HUMAN**	**103 kDa**	**Inhibits SIRT1 deacetylase**	**6**				**5.8**
Gamma-interferon-inducible protein 16 OS=Homo sapiens GN=IFI16 PE=1 SV=3	IF16_ HUMAN	88 kDa	Modulates p53 function and inhibits cell growth in the Ras/Raf pathway	5				5.7
Heat shock 70 kDa protein 1A/1B OS=Homo sapiens GN=HSPA1A PE=1 SV=5	HSP71_ HUMAN	70 kDa	Chaperone	4				5.7
Protein arginine N-methyltransferase 5 OS=Homo sapiens GN=PRMT5 PE=1 SV=4	ANM5_ HUMAN	73 kDa	Ribosome	4				5.5
Enhancer of mRNA-decapping protein 4 OS=Homo sapiens GN=EDC4 PE=1 SV=1	EDC4_ HUMAN	152 kDa	mRNA decapping	7	1			5.3
2-oxoglutarate dehydrogenase-like, mitochondrial OS=Homo sapiens GN=OGDHL PE=2 SV=3	OGDHL_ HUMAN	114 kDa	Citric acid cycle	6				5.3
X-ray repair cross-complementing protein 5 OS=Homo sapiens GN=XRCC5 PE=1 SV=3	**XRCC5_ HUMAN**	**83 kDa**	**Dsbreak repair during HNEJ and chromosome translocation**	**4**				**4.8**
Protein LYRIC OS=Homo sapiens GN=MTDH PE=1 SV=2	LYRIC_ HUMAN	64 kDa	Endocytic membrane fusion and membrane trafficking of recycling endosome. Activator of NF-kappaB	3				4.7

(Table 2 cont'd)								
Nucleolar RNA helicase 2 OS=Homo sapiens GN=DDX21 PE=1 SV=5	DDX21_ HUMAN	87 kDa	Nucleolus	4				4.6
cAMP-specific 3',5'-cyclic phosphodiesterase 4A OS=Homo sapiens GN=PDE4A PE=1 SV=3	PDE4A_ HUMAN	98 kDa	Citric acid cycle	4				4.1
Serine/threonine-protein kinase SRPK1 OS=Homo sapiens GN=SRPK1 PE=1 SV=2	**SRPK1_ HUMAN**	**74 kDa**	**Splicing (SR protein)**	**3**				**4.1**
Stress-70 protein, mitochondrial OS=Homo sapiens GN=HSPA9 PE=1 SV=2	GRP75_ HUMAN	74 kDa	Ribosome	3				4.1
Elongation factor 1-alpha 1 OS=Homo sapiens GN=EEF1A1 PE=1 SV=1	**EF1A1_ HUMAN (+2)**	**50 kDa**	**Chaperone**	**2**				**4**
ATP-dependent RNA helicase DDX18 OS=Homo sapiens GN=DDX18 PE=1 SV=2	DDX18_ HUMAN	75 kDa	RNA helicase	3				4
RNA-binding protein FUS OS=Homo sapiens GN=FUS PE=1 SV=1	**FUS_ HUMAN**	**53 kDa**	**Transport between ER and golgi**	**2**				**3.8**
Ribosome-releasing factor 2, mitochondrial OS=Homo sapiens GN=GFM2 PE=1 SV=1	RRF2M_ HUMAN	87 kDa	Mitochondrial protein synthesis	3				3.5
TNF receptor-associated factor 6 OS=Homo sapiens GN=TRAF6 PE=1 SV=1	TRAF6_ HUMAN	60 kDa	Signal transduction from TNF and toll receptors	2				3.3
CDKN2A-interacting protein OS=Homo sapiens GN=CDKN2AIP PE=1 SV=3	**CARF_ HUMAN**	**61 kDa**	**Membrane cytoskeleton and binds to calmodulin**	**2**				**3.3**
Thrombospondin-1 OS=Homo sapiens GN=THBS1 PE=1 SV=2	TSP1_ HUMAN	129 kDa	Mediates cell-cell and cell-matrix interaction	4				3.1

(Table 2 cont'd)								
Importin subunit beta-1 OS=Homo sapiens GN=KPNB1 PE=1 SV=2	IMB1_ HUMAN	97 kDa	Nuclear pore transport	3				3.1
Rab GTPase-binding effector protein 1 OS=Homo sapiens GN=RABEP1 PE=1 SV=2	RABE1_ HUMAN	99 kDa	Proliferation, stress response and maintenance of mitochondria	3				3.03
Pescadillo homolog OS=Homo sapiens GN=PES1 PE=1 SV=1	PESC_ HUMAN	68 kDa	Ribosome biogenesis	2				2.9
ATPase WRNIP1 OS=Homo sapiens GN=WRNIP1 PE=1 SV=2	WRIP1_ HUMAN	72 kDa	DNA synthesis and sensor of damage during replication	2				2.8
Alpha-adducin OS=Homo sapiens GN=ADD1 PE=1 SV=2	ADDA_ HUMAN	81 kDa	Membrane-cytoskeleton-associated protein that promotes the assembly of the spectrin-actin network. Binds to calmodulin.	2				2.5
Ribosomal RNA processing protein 1 homolog B OS=Homo sapiens GN=RRP1B PE=1 SV=3	RRP1B_ HUMAN	84 kDa	Transcription initiation	2				2.4
Glycogen [starch] synthase, muscle OS=Homo sapiens GN=GYS1 PE=1 SV=2	GYS1_ HUMAN	84 kDa	Glucose metabolic process	2				2.4
Leucine-rich repeat flightless-interacting protein 1 OS=Homo sapiens GN=LRRFIP1 PE=1 SV=2	LRRF1_ HUMAN	89 kDa	Transcription repressor, which preferentially binds CG-rich seqs (5'-AGCCCCCGGCG-3')	1				2.3
TFIIH basal transcription factor complex helicase XPB subunit OS=Homo sapiens GN=ERCC3 PE=1 SV=1	ERCC3_ HUMAN	89 kDa	Basal transcription and repair	2				2.3
Structural maintenance of chromosomes protein 1A OS=Homo sapiens	SMC1A_ HUMAN	143 kDa	Interacts with BRCA1 and p-ATM. Might be	3				2.1

(Table 2 cont'd) GN=SMC1A PE=1 SV=2			involved in DNA repair					
Glycogen phosphorylase, brain form OS=Homo sapiens GN=PYGB PE=1 SV=5	PYGB_ HUMAN	97 kDa	Important in carbohydrate metabolism	2				2.1
Splicing factor 3B subunit 2 OS=Homo sapiens GN=SF3B2 PE=1 SV=2	SF3B2_ HUMAN	100 kDa	Splicing	2				2
26S proteasome non-ATPase regulatory subunit 2 OS=Homo sapiens GN=PSMD2 PE=1 SV=3	**PSMD2_ HUMAN**	**100 kDa**	**Regulatory subunit of 26S UPP and binds TNFR1**	**2**				**2**
Zinc finger protein 318 OS=Homo sapiens GN=ZNF318 PE=1 SV=2	ZN318_ HUMAN	251 kDa	Transcription regulator during meiosis	5				1.99
Exosome component 10 OS=Homo sapiens GN=EXOSC10 PE=1 SV=2	EXOSX_ HUMAN	101 kDa	RNA exosome and processing	2				1.98
Methionyl-tRNA synthetase, cytoplasmic OS=Homo sapiens GN=MARS PE=1 SV=2	SYMC_ HUMAN	101 kDa	Protein synthesis	2				1.98
Insulin-like growth factor 2 mRNA-binding protein 1 OS=Homo sapiens GN=IGF2BP1 PE=1 SV=2	IF2B1_ HUMAN	63 kDa	mRNA localization, export, stability & translation	1				1.6
Coatomer subunit alpha OS=Homo sapiens GN=COPA PE=1 SV=2	COPA_ HUMAN	138 kDa	Cell proliferation and cell transformation	2				1.5
Cullin-associated NEDD8-dissociated protein 1 OS=Homo sapiens GN=CAND1 PE=1 SV=2	CAND1_ HUMAN	136 kDa	Transcription regulation	2				1.5
DNA replication licensing factor MCM7 OS=Homo sapiens GN=MCM7 PE=1 SV=4	MCM7_ HUMAN	81 kDa	Component of pre-Replication Complex, binds cyclin D/cdk4	1				1.2

(Table 2 cont'd)								
Mannosyl-oligosaccharide glucosidase OS=Homo sapiens GN=MOGS PE=1 SV=5	MOGS_ HUMAN	92 kDa	Cleavage during translation	1				1.1
Transcription intermediary factor 1-beta OS=Homo sapiens GN=TRIM28 PE=1 SV=5	**TIF1B_ HUMAN**	**89 kDa**	**Transcription repressor of transcription factors (p53 via Mdm2), by recruiting HDACs & HMTs**	**1**				**1.1**
Ribonucleases P/MRP protein subunit POP1 OS=Homo sapiens GN=POP1 PE=1 SV=2	POP1_ HUMAN	115 kDa	Ribosome biogenesis	1				0.87
N-acetyltransferase 10 OS=Homo sapiens GN=NAT10 PE=1 SV=2	NAT10_ HUMAN	116 kDa	Acetyltransferase of histones and microtubles	1				0.86
Replication factor C subunit 1 OS=Homo sapiens GN=RFC1 PE=1 SV=4	RFC1_ HUMAN	128 kDa	DNA replication and repair	1				0.78

Table 2: *Proteins are ranked according to the number of unique peptides identified during the MS/MS analysis. The larger the number of unique peptides, the higher the amount of peptide fragments observed.* The following represent some abbreviations used in the table: **ER**- Endoplasmic reticulum, **SIRT1**- Sirtuin 1, **NADP-** Nicotinamide adenine dinucleotide phosphate, **TNF**- Tumor Necrosis Factor, **UPP**- Ubiquitin proteasome pathway, **cyc** - Cyclin, **cdk**- Cyclin dependent kinase, **HDAC**- Histone deacetylases, **HMAT**- Histone methyltransferase. ***Percent coverage*** *is assessed by looking at the number of unique peptides related to the size of the protein [# of Unique peptides / Protein size (kDa)].* **BOLDED** *proteins represent previously identified proteins by LC/MS/MS using alternate Mdm2 antibodies (SMP14). Proteins in* ***RED*** *are proteins found to interact with Mdm2 via an online tool: http://string83.embl.de/*

In order to confirm the pull-down of HSP90 after Mdm2-C IP, we performed IF and using the imariscoloc program, we checked for co-localization of the proteins. We observed that in MANCA cells, there was not much co-distribution observed between

Mdm2-C and HSP90 (Fig. 38i-MANCA cells). However, in T47D cells compared to MANCA cells, we observed a higher level of Mdm2-C and HSP90 co-localization (Fig. 38i- T47D cells). The reason for this might lie in the fact that T47D cells have mutant p53 and HSP90 has been shown to cause the stabilization of the mutant protein (Li et al., 2011). We also checked for the co-localization of Mdm2-C and HSP70 and saw some co-localization (Fig. 38ii MANCA cells). This indicates that the pull down of these HSP proteins after the specific IP of Mdm2-C was valid. However, the direct interaction of Mdm2-C to either HSP70 or HSP90 cannot be concluded from this result. Further co-IP experiments will need to be performed to confirm the interaction of Mdm2-C to these proteins.

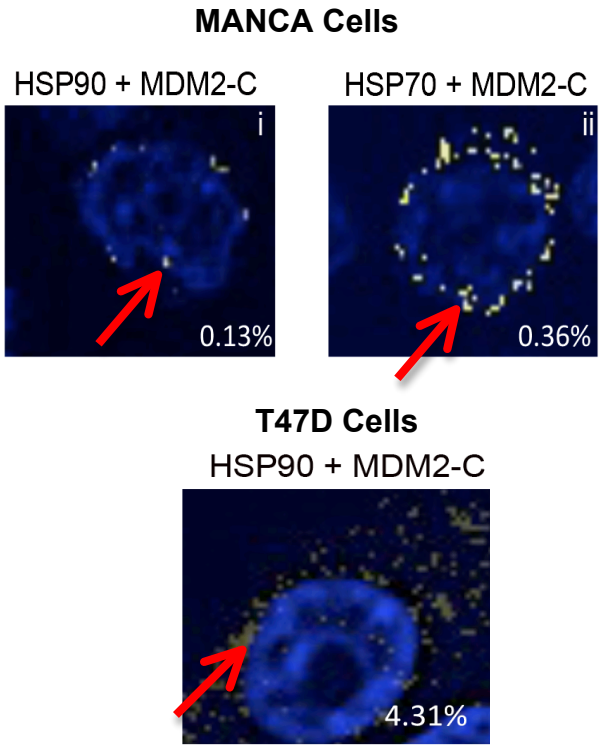

Figure 38: **Mdm2-C is found co-distributed with HSP90 and HSP70 in MANCA and T47D cells**. *Pictures taken with the spinning disk microscope were examined with the ImarisColoc software. The Mdm2-C channel was used for masking to delineate the area of focus for co-localization*. Arrows indicate regions of co-distribution of proteins. Percentage represents degree of co-localization.

5.1.4 **Mdm2-C and Chromatin Functions**

In order to more carefully examine the localization of Mdm2-C, we extracted proteins from MANCA cells by cellular fractionation that separates the different compartments of the cell into compartments. We observed high levels of Mdm2-C protein in the chromatin fraction (P3) (Fig. 19B lane 3). This implicated Mdm2-C in a chromatin-based function. We also separated MANCA proteins into 2 compartments - nuclear and cytosol. After immunoblot using the Mdm2 C410 antibody, we observed several molecular mass bands present in both fractions (N- five bands and C- four bands) (Fig. 39 lanes 1 and 2). Interestingly, the nuclear fraction possessed a molecular mass band above 250kDa (band #1) that was not present in the cytoplasmic fraction (Fig. 39 lane 2). The reason for this is unclear. It is possible that this Mdm2-C form represents a differentially modified Mdm2-C protein whose function differs in the nuclear compartment. Also, some of the protein bands observed were present in different amounts (Fig. 39 lanes 1 and 2, protein bands #2 and #3). The pre immune sera showed low background protein detection thus confirming that the proteins observed after Mdm2 C410 immunoblot were Mdm2-C (Fig. 39 lanes 3 and 4). Immunoblot using the Mdm2 4B11 antibody (for Mdm2 that retains the C-terminal region of the Mdm2 protein) detected more Mdm2 present in the cytoplasmic fractions as compared to the nuclear fractions (Fig. 39 compare lanes 5 and 7 to lanes 6 and 8); and this is comparable to what was observed previously (Fig. 19Bi lanes 8 and 9). Thus suggests that majority of the Mdm2 present in MANCA cells resides in the cytoplasmic region.

Similarly, immunoblot using the Mdm2 2A9 antibody (for all Mdm2 proteins that retain epitope region between amino acids 153 and 222, which is absent in Mdm2-C) detected more Mdm2 protein in the cytoplasmic fraction compared to the nuclear fraction (Fig. 39 lanes 7 and 8). Interestingly, the amount of Mdm2 protein detected after 4B11 immunoblot was greater than the amount detected after 2A9 immunoblot (Fig. 39 compare lanes 5 to 7 and 6 to 8). The reason for this could lie in the fact that the Mdm2 4B11 antibody detects most of the Mdm2 present in the cell because its epitope of recognition lies in the C terminus of Mdm2, a region majorly present in *mdm2* splice variant transcripts. On the other hand, the Mdm2 2A9 antibody detects an epitope region missing from the Mdm2-C polypeptide. The 4B11 antibody detects a combination of all the Mdm2 proteins in the cell while the 2A9 antibody recognizes only Mdm2 proteins that retain the central region. However, it is possible that the difference in protein amount after immunoblot could be attributed to a difference in the titer of the antibodies used for detection.

In order to determine whether the protein bands observed after C410 immunoblot were Mdm2, we aligned the molecular weight marker to the protein bands across each lane and immunoblot. We observed that protein bands #2 – 5 fell within the boundaries that correspond to the 4B11 immunoblot (Fig. 39 compare lanes 1 and 2 to lanes 5 and 6), while Protein band #1 did not. This suggests that protein bands, #2 - #5 represent Mdm2, while protein band #1 is not Mdm2. Nonetheless, this higher molecular weight protein form of Mdm2-C could be modified differently; and its identification by the Mdm2 4B11 antibody is impeded due to epitope masking. Therefore, the different forms of

Mdm2-C protein could represent differentially modified proteins with activities that are specific to the nucleus and nuclear-resident proteins.

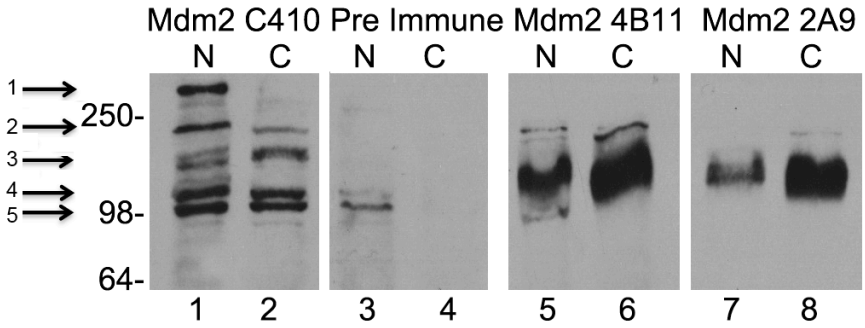

Figure 39: **Mdm2-C can be found in the nuclear and cytoplasmic cellular compartments of MANCA cells.** *MANCA cells were lysed and protein samples were electrophoresed via SDS-PAGE. Proteins were analyzed using Mdm2 monoclonal antibodies- 4B11 and 2A9 and Mdm2 polyclonal antibody- Mdm2 C410. Pre immune polyclonal serum was used as a control and. HRP-conjugated anti-mouse and anti-rabbit were used as secondary antibodies. Where N- Nuclear extracts and C- Cytoplasmic extracts. Arrows represent protein bands.*

5.1.5 **p53, Mdm2 and Translation**

In an attempt to observe an *in vitro* protein-protein interaction between Mdm2-C and p53, we co-translated Mdm2-FL or Mdm2-C with p53 (Fig. 40). We did not observe any interaction between Mdm2-C or Mdm2-FL and p53 in the TnT wheat germ assay system when Mdm2 was immunoprecipitated (Fig. 40A lane 3) or when p53 was immunoprecipitated (Fig. 40B lane 3). Mdm2 interacts with p53, however in the absence of RNA, the Mdm2-p53 interaction is not very stable (Burch et al., 2000). Our result suggests the need for a tertiary factor for an efficient interaction between Mdm2 and p53. Although we did not observe Mdm2-FL or Mdm2-C bound to p53 *in vitro*,

interestingly, we observed that in the presence p53, the translation of Mdm2-FL was enhanced as compared to its single translation (Fig. 40A compare lane 9 to 12).

The influence of p53 on *mdm2* translation does not equally apply to different splice variants. Immunoprecipitation of Mdm2 using the Mdm2 monoclonal antibody, N-20, revealed that the protein observed was predominantly Mdm2-FL (Fig. 40A compare lanes 3 and 9). Conversely, co-translation of p53 and Mdm2-C did not show an enhancement in Mdm2-C translation (Fig. 40A compare lanes 4 to 10). Immunoprecipitation of p53 after co-translation with Mdm2-FL or Mdm2-C protein (Fig. 40B) showed a larger ratio of Mdm2-FL to p53 protein present compared to Mdm2-C to p53 protein (Fig. 40 compare lanes 3A to 3B vs. 4A to 4B). In addition, an increase in Mdm2-FL protein translated resulted in a decrease in p53 protein made (Fig. 40A lane 9). In the presence of Mdm2-C, the translation of p53 was not drastically affected compared to p53 alone (Fig. 40A lane 10 and 40B lane 9).

The p53 protein binds RNA in a non-specific manner (Samad and Carroll, 1991). The interaction was confirmed after purifications in the same cells and in the absence of p53, did not reveal bound RNA (Fontoura et al., 1992). The p53 protein has been shown to possess anti-helicase activity that enhances the re-annealing of RNA-RNA duplexes (Oberosler et al., 1993), which facilitates translation inhibition of RNAs such as its own, cyclin dependent kinase 4 (cdk4) and fibroblast growth factor 2 (FGF-2) in transfection and *in vitro* experiments (Galy et al., 2001; Miller et al., 2000; Mosner et al., 1995). Therefore, these experiments showed that although p53 binds RNA non-specifically, it is involved in translation repression. These data suggest that there is a distinct interaction between Mdm2-FL and p53 that is deficient with Mdm2-C. The translation of

p53 appears to be interrupted greatly in the presence of Mdm2-FL compared to Mdm2-C. The reason for this difference might lie in the exon spliced out of the *mdm2-C* transcript and the resulting secondary/tertiary structure of the Mdm2-C polypeptide. It is known that Mdm2 binds to the p53 mRNA and enhances translation (Candeias et al., 2008; Naski et al., 2009). However, the influence of p53 on *mdm2* translation is a novel idea. Based on our findings in this experiment, we can propose that the exons 5 through 9 region of Mdm2 is important for efficient interaction between p53 protein and Mdm2 RNA and protein. Our data suggests that there is a preferential choice to inhibit p53 translation in the presence of excess Mdm2-FL and this helps in enhanced Mdm2-FL translation compared to Mdm2-C. This raises the question: could it be that in the absence of stress, p53 might regulate its protein levels by enhancing the translation of the *mdm2* transcript? These data adds a level of complexity to the p53-Mdm2 interaction and the putative role Mdm2 isoform proteins play in p53 regulation.

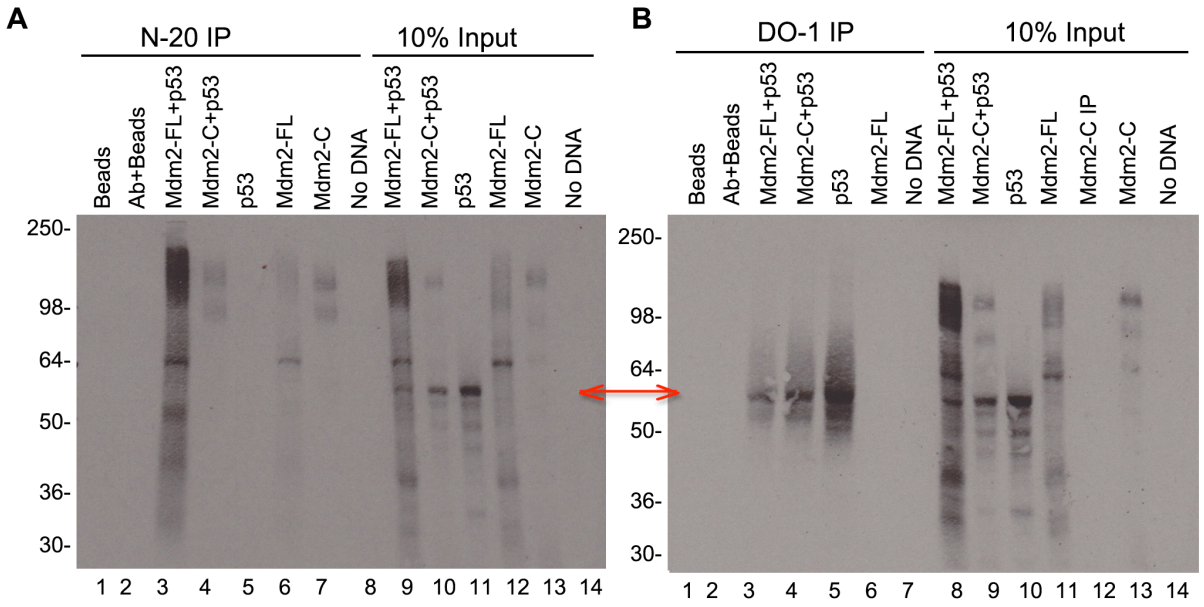

Figure 40: **A possible role for p53 in the translation enhancement of *mdm2* mRNA**. *Immunoprecipitation of ^{35}S methionine radioactive-labeled in vitro translated Mdm2-FL or Mdm2-C proteins.* pcDNA3-Mdm2-FL *or* pcDNA3-mdm2-C *plasmids were translated singly or co-translated with* PRK53 *(p53) plasmid. Immunoprecipitation was achieved by using* **A.** *N-20 monoclonal antibody or* **B.** *DO-1 monoclonal antibody. Protein ratios used in the pull down assay were 5:1 (Mdm2-C:Mdm2-FL/No DNA). Samples were electrophoresed on a 10% SDS-PAGE gel transferred to a nitrocellulose membrane and exposed to film for protein detection. The red arrow indicates the position of the p53 protein.*

5.2:
Future Directions

5.2.1 **Introduction**

Mdm2-C increases cell growth as shown by increased proliferation and increased colony formation in *p53*-null human cancer cells. This implies that Mdm2-C protein has p53-independent growth promoting functions. In addition, we see that the partial knockdown of *mdm2-C* in ER+ *mdm2* SNP309 T47D cells showed a modest increase in cell death (Fig. 29D). This was interesting because *mdm2* knockdown that was shRNA–mediated or via a siRNA smart pool did not result in increased death (data not shown) even though *mdm2-C* transcript was also decreased (Compare Fig. 28A and Fig. 29A). This highly suggests that Mdm2-C is important in the survival of ER+ *mdm2* SNP309 tumor cells with mutant p53. Therefore, although some Mdm2-C functions have been characterized so far, more questions remain unanswered such as: the mechanism through which Mdm2-C promotes growth and survival as well as the role the protein plays in tumor propagation.

We have identified several putative Mdm2-C binding proteins via specific pull-down of Mdm2-C and subsequent LC/MS/MS (Table 2). The identified are involved in several cellular pathways. Some of them are involved in transcription - transcription intermediary factor-1 (TIF1B/TRIM28) and Leucine-rich repeat flightless-interacting protein 1 (LRRF1). TIF1B/TRIM28 results in transcription repression through binding to Mdm2 (and possibly Mdm2-C) to contribute to p53 inactivation by promoting p53 ubiquitylation and degradation (Wang et al., 2005). In addition, LRRF1 represses transcription through binding to GC-rich sequences, of SP1-inducible genes such as PDGFA (platelet derived growth factor A), TNF (tumor necrosis factor) and EGFR (epidermal growth factor receptor) all of which are involved in cell proliferation. Some

are involved in splicing and translation- SYK-Lysyl-tRNA synthetase and SYMC-Methionyl-tRNA synthetase. Another group of proteins identified included those involved in metabolism- cAMP-specific 3", 5"-cyclic phosphodiesterase 4A (PDE4) and the energy production and consumption metabolic pathways – Aldehyde dehydrogenase family 16 member A1 (A16A1) and alkylhydroxyacetonephosphate synthase, peroxisomal (ADAS).

The LC/MS/MS experiment was performed only once and needs to be repeated to ascertain the presence and interaction of identified proteins with Mdm2-C. However, based on our preliminary results, we hypothesize that the p53-independent functions of Mdm2-C may reside possibly on its inhibitory or activating activity on proteins that function: on the chromatin, splicing, translation or metabolism, which could promote cellular transformation. In addition, examining the effect of Mdm2-C in these processes could help determine the influence the protein has on cellular transformation.

5.2.2 **Conditional Knockout of *mdm2***

Gene silencing is a technique used widely in many laboratories including the Bargonetti lab for the study of the function and importance of their favorite genes. In the study of Mdm2, gene silencing has been practiced to understand the role Mdm2 plays in p53 regulation, as well as in other processes such as cellular transformation (Brekman et al., 2011). These studies have shown that the knockdown of *mdm2* sensitizes cancer cells to DNA damage-induced arrest, apoptosis or decreased proliferation all of which is dependent on p53 activity. However, often times, *mdm2* knockdown is inefficient and does not result in the complete ablation of the total protein product of the knockdown

target. In the Bargonetti laboratory, we are interested in studying the function of Mdm2 isoforms without the context of endogenous Mdm2. Two laboratories have shown that the *mdm2* knockout mouse is lethal because of the hyper-activation of the transcription factor, p53, which results in arrest and apoptosis (Jones et al., 1995; Montes de Oca Luna et al., 1995); however, removing p53 rescues this lethality. Consequently, it is important to create a system in which *mdm2* can be conditionally knocked out when needed to eliminate the death of the cell by p53.

Several studies have addressed the function of the full-length form of Mdm2 (see review- (Ganguli and Wasylyk, 2003). However, studies examining the function of splice variant forms of *mdm2* in the context of endogenous Mdm2 have proved to be difficult. This is because there are numerous *mdm2* transcripts (over 40 (Bartel et al., 2002)) and single expression of *mdm2* splice variant transcript protein have been futile due to the mortality of these mice (Steinman et al., 2004). To date, there are no known published accounts of viable human cultured cells with the double knockout of *mdm2*. Therefore, we reasoned that the creation of a conditional knockout cell line for *mdm2* will provide a better tool to study *mdm2* splice variant transcripts and their possible functions in the cell (Okoro et al., 2012). Several results have placed Mdm2 in functions that range from DNA repair to translation (Iwakuma and Lozano, 2003) (Fig. 5). Creating a level of complexity is the presence of *mdm2* splice transcripts, which potentially increase the cellular proteome diversity. These isoforms may cooperate with full-length Mdm2 or work independently to promote cancer. Therefore, the focused study of individual Mdm2 isoforms is essential for the dissection of their functions as it pertains to cancer. Hence

it is important to create a mammalian cell line with the conditional knockout of *mdm2* to enable the study of each isoform independently.

5.2.2.1 **Approach to Knockout *mdm2* By Gene Deletion**

In order to knockout *mdm2*, we have worked on creating a conditional knockout construct that would integrate within the *mdm2* gene and eliminate endogenous *mdm2* production when induced. To do this, we designed primers that amplified *mdm2* from genomic DNA derived out of A875 cells (*mdm2 G/G*SNP309). The primers were specific to portions for the left arm, right arm and deleted region for the construct. The different regions consisted of: Left arm- portions of exon 1 and intron 1; deleted region- exon 2, intron 2 and exon 3; and the right arm- portions of intron 3 (Fig. 41A). The left and right arm sequences will be the means via which the transgene will be integrated within the genome. The deleted region sequence contains portions of the *mdm2* sequence, which upon deletion should disrupt transcription from the *mdm2* gene and the ability to produce a functional *mdm2* transcript. The process of cloning involved the individual amplification of each region and ligation into separate pNY carrier vectors (Fig. 41B). Following this, the regions were then systematically transferred one-by-one into the transfer pAAV vector (Fig. 42A), which harbors sequences for virus production. The final assembled vector (see Fig. 43A) was sequenced to verify correct cloning and sequence orientation.

A Partial *mdm2* genomic sequence (Exons and Introns)

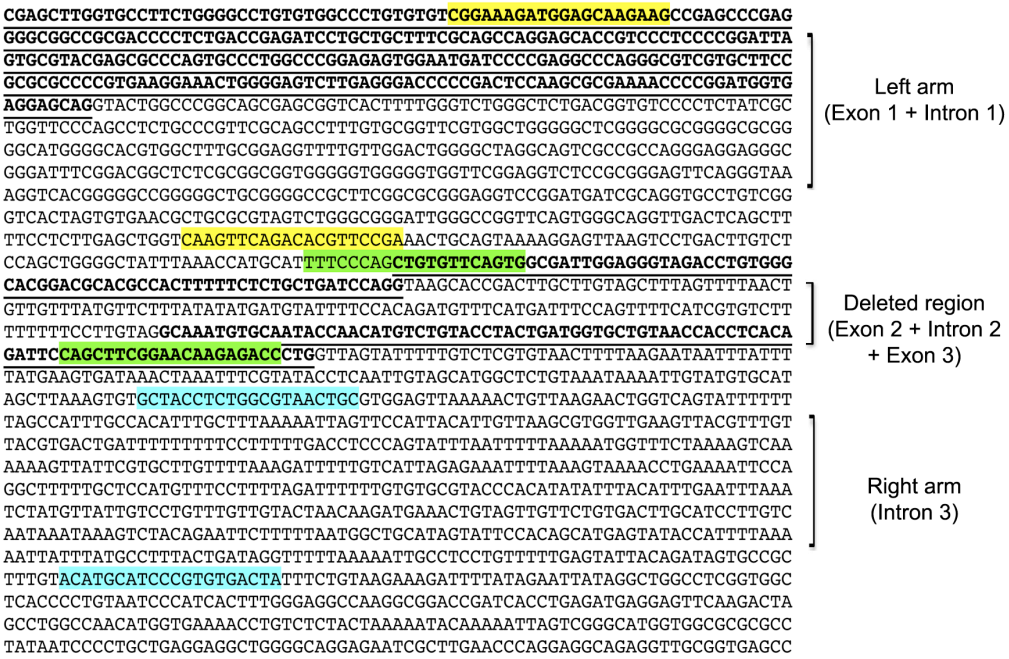

Left arm (Exon 1 + Intron 1)

Deleted region (Exon 2 + Intron 2 + Exon 3)

Right arm (Intron 3)

B pNY polylinker plasmid sequence

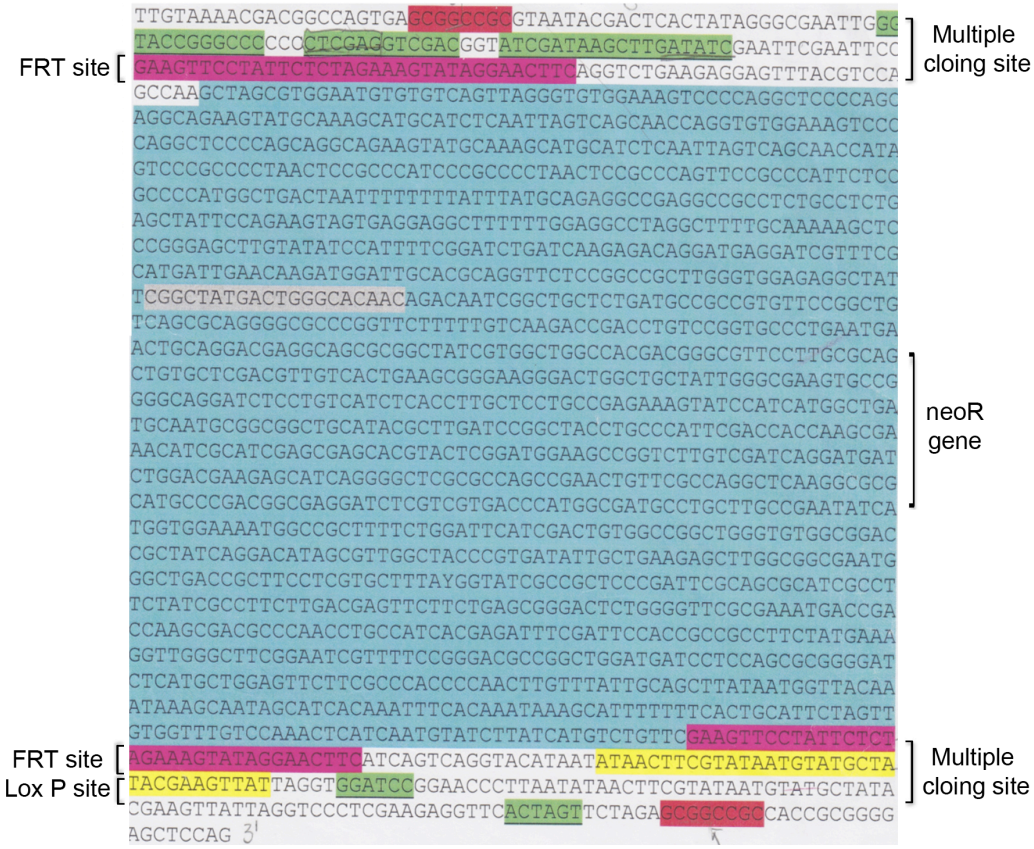

FRT site

Multiple cloing site

neoR gene

FRT site

Lox P site

Multiple cloing site

Figure 41**: Nucleotide sequences of carrier vector, pNY and the *mdm2* genomic sequence from A875. A.** *The partial genomic sequence for* mdm2*. The underlined sequences represent the exon regions of mdm2. The first is exon one, then exon 2 and lastly exon three. The sequences in between are intron sequences. The highlighted portions of the sequences represent the primers used to amplify the* mdm2 *sequences for each region for the creation of the* mdm2 *knockout construct. The first highlighted region (yellow) depicts the left arm, the second region (Goldstrohm et al.) depicts the deleted region and the third region (light blue) depicts the right arm sequences.* **B.** *The sequence represents portions of the pNY poly-linker vector. The highlighted regions depict the regions of multiple cloning sites, FRT gene for insertion of sequence into genome and the selection marker gene, Neomycin (neoR) for antibiotic resistant picking of positive clones in the cell. The red highlighted regions are the NotI sites for cloning of the sequence with all the arms into the pAAV vector. The yellow highlighted region represents the Lox P sites, which will aim in homologous recombination in the genome.*

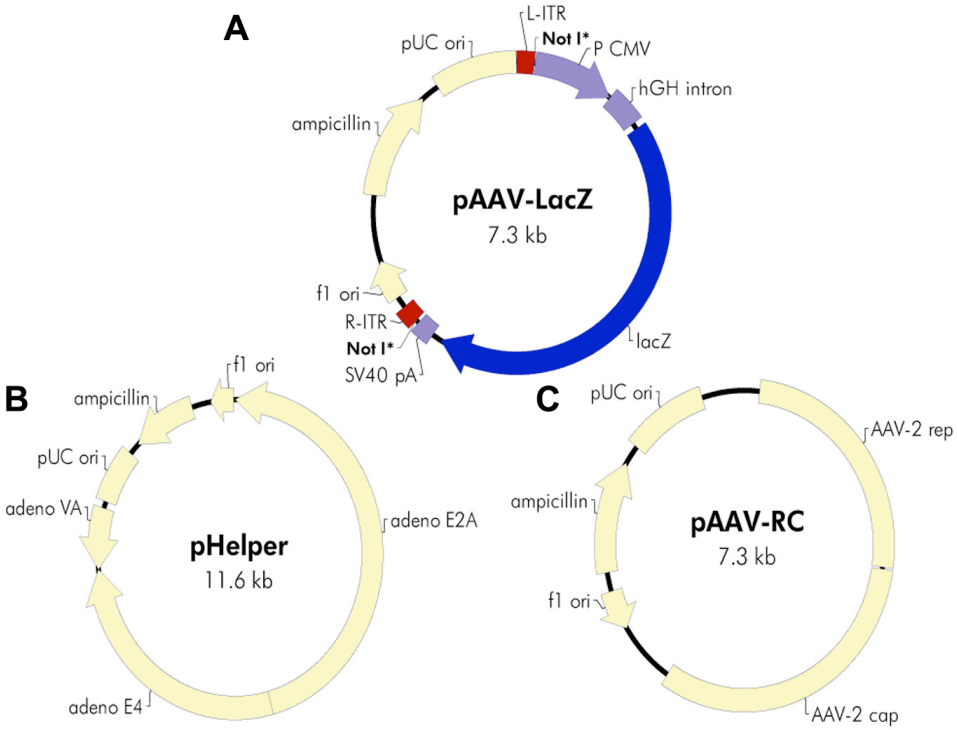

Figure 42**: Plasmid vectors to be used in the creation of *mdm2* knockout virus**
A. *The pAAV vector is the assembly vector that contains the left arm, deleted region and right arm sequences.* **B.** *The pHelper and* ***C.*** *pAAV-RC vectors to be co-transfected with the pAAV-*mdm2 *vector for the production of virus containing the sequences for the conditional knockout of* mdm2*.*

The *mdm2* knockout plasmid can be transfected into HEK 293 phoenix cells and packaged into viral particles with the help of co-plasmids-pAAV-RC and pHelper (Fig. 42B and C). Both of these plasmids help facilitate the packaging of viral particles by providing the replication and cap proteins as well as adenoviral genes necessary for high titer during virus production. Viral titers can be collected at 48, 72 and 96 hours post transfection. These titers can be used to infect the cell lines of choice to facilitate the integration of the *mdm2* knockout construct into the genome of a cell line of choice. Several rounds of viral infections must follow this initial infection and cells positive for integration can be screened via PCR and Southern blot analysis. Double infections ensure for the selection of clones that have the transgene integrated in both alleles of the genome. After this, the knockout of *mdm2* can be carried out by the expression of Cre recombinase enzyme in the transformed cells. Cre recombinase (Causes recombination) is an enzyme that was initially discovered in bacteriophage P1 (Sauer and Henderson, 1988). It excises sequences flanked by Lox-P sites. Lox-P sites are palindrome sequences acted upon by the Cre recombinase enzyme. Expression of Cre recombinase enables the excision of the arm bearing the deleted region thus rendering the expression of functional *mdm2* unlikely.

We know from previous work by our lab that cells that over-express Mdm2 due to the SNP309 in the *mdm2* gene have compromised p53 activity (Arva et al., 2005), and we also see that these cells have high *mdm2* transcript levels (Fig. 14B). An example of such cells is MANCAs (Burkitt's lymphoma), which have compromised p53 activity. We can infect these cells with the *mdm2* knockout construct to eliminate the production of Mdm2 conditionally. By creating MANCA cell lines with conditional knockout of *mdm2*,

the function of Mdm2 isoforms such as Mdm2-C, can be examined in these cells. Plasmids bearing *mdm2-C* can be transfected into cells with the conditional knockout construct embedded within their genome (Fig. 43B). This therefore creates the avenue to study the effect of individual Mdm2 isoforms in cells with or without endogenous p53.

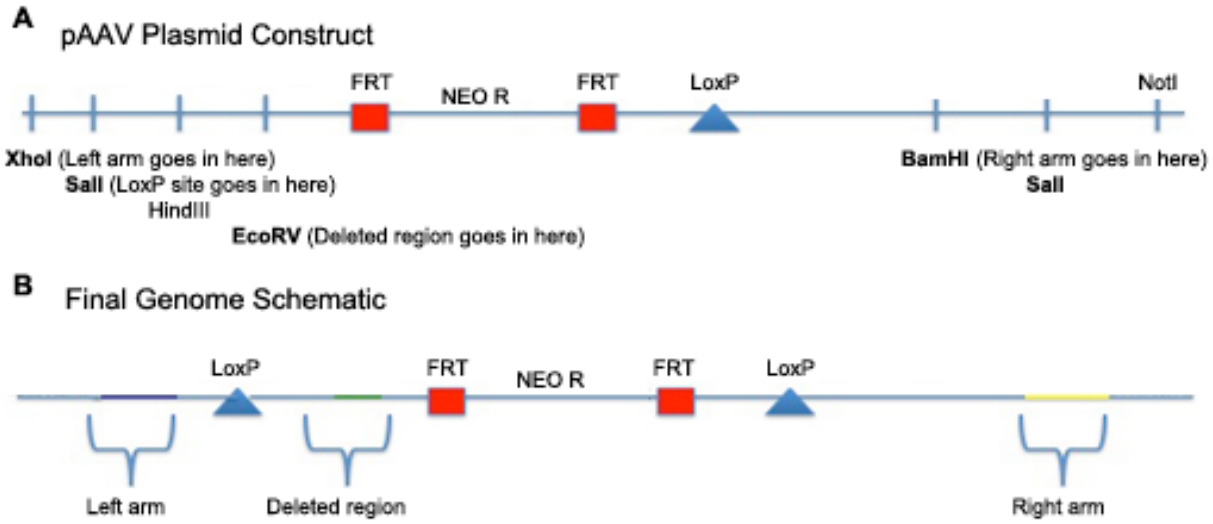

Figure 43: **Schematic of the pAAV carrier vector and the final *mdm2* genome schematic after insertion. A.** *Represents the pAAV construct, the multiple cloning sites into which individual* mdm2 *sequences were cloned and the LOXP and FRT sites*. **B.** *Represents the schematic of what the* mdm2 *genome would look like following viral infection and insertion of the pAAV plasmid into the genome. The Blue region- represents the left arm region consisting of exon 1 and intron 1 sequences; the Green region- represents the deleted region, which consists of sequences to exon2, intron 2 and exon 3; and the yellow region- represents the right arm, which consists of sequences to intron 3.*

5.2.3 **Mdm2-C, RNA Binding and Translation**

Liquid Chromatography /Mass Spectroscopy (LC/MS/MS) analysis after the specific immunoprecipitation of Mdm2-C, identified co-associated proteins involved in splicing and RNA binding (See Table 2). Despite the fact that Nucleolin was a predominant protein found in the LC/MS/MS screen of Mdm2-C interacting proteins

(See Table 2), we did not observe a strong co-localization of Nucleolin to Mdm2-C (Fig. 25 and 26). Full-length Mdm2 interacts with Nucleolin (Bhatt et al., 2012; Saxena et al., 2006) therefore it is possible that Nucleolin was detected because of an interaction between Mdm2-C and Mdm2-FL. In addition, we did not observe a strong co-localization of Mdm2-C with hnRNPA1 or EIF-4E (Fig. 26 and 27). However, correlating with the proteins that were identified in the LC/MS/MS screen, Mdm2-C might have a RNA-based role and might function in RNA processing and or ribosome biogenesis. It is possible that Mdm2-C pulled down the RNA binding proteins solely because the Mdm2-C protein was bound to an RNA transcript to which these RNA binding proteins were attached. An alternative is that the *mdm2-C* transcript also provides gene expression regulatory properties (Clancy, 2008; Serganov and Patel, 2007). We believe Mdm2-C is performing a function that is distinct from other Mdm2 isoforms and this relates to its binding partners and cellular localization.

Based on the number of splicing and translation related proteins identified tentatively (see Table 2), it is possible that Mdm2-C influences the splicing and translation of factors involved in growth promotion. To check the RNA binding ability of Mdm2-C, RNA immunoprecipitation (RIP) experiments could be performed followed by reverse transcription of the recovered RNAs and sequencing to determine what transcripts are preferentially associated with Mdm2-C. Also, confirmation studies like Co-immunoprecipitations (Co-IPs) need to be performed to confirm an Mdm2-C interaction with the detected proteins. Nevertheless, the LC/MS/MS needs to be repeated to confirm that the proteins identified after Mdm2-C IP can be duplicated.

5.2.4 **Mdm2-C Chromatin-based Functions**

Our data showed that the over-expression of Mdm2-C increased colony formation (Fig. 21). We also observed high levels of Mdm2-C protein in cellular extracts from the chromatin fraction (Fig. 19B) and the nuclear fraction (Fig. 39). In addition, specific protein species were observed in the nuclear fraction compared to the cytosolic fraction (Fig. 39). Analysis via LC/MS/MS after Mdm2-C IP identified a number of proteins involved in transcription and DNA repair (see Table 2). Therefore, it is probable that the Mdm2-C protein functions in the nucleus to increase the transcription of genes that promote cell proliferation. It is also possible that Mdm2-C could be preventing DNA damage sensing or allowing for chromosome translocation by disrupting proper segregation during cell division. Alterations in DNA unwinding could induce polyploidy and chromosome instability (Bouska and Eischen, 2009a; Bouska et al., 2008; Lushnikova et al., 2011). However, the interaction of Mdm2-C with the identified proteins needs to be determined.

In order to elucidate to the involvement of Mdm2-C in chromatin-based functions, analysis can be done via Co-IP and transient transfection experiments to assess a physical interaction with Mdm2-C and the effect of Mdm2-C over-expression on the functional activity of the candidate proteins. Chromatin fractionations can be performed to observe the global presence of chromatin-related proteins in the presence of DNA damage, with and without Mdm2-C over-expression. Mdm2 over-expression can be achieved via transient transfection experiments or by using cells that have endogenous Mdm2-C over-expression like MANCA and T47D cells. In addition, performing comet assays can assess chromosome instability due to Mdm2-C over expression. In order to

examine the effect of removing excess Mdm2-C, cells in which endogenous Mdm2 is conditionally knocked out could be used in examining the role Mdm2-C might play in chromatin functions.

5.2.5 **Mdm2-C, Cell Transformation & Tumor Formation**

The ability of Mdm2-C to transform mouse NIH3T3 cells has been documented (Sigalas et al., 1996). However, whether this Mdm2 isoform can transform human cells has not been addressed. We also know that Mdm2 plays a role in the anchorage-independent growth of MCF-7 cells when the cells are grown in soft agar. The knockdown of *mdm2* increased the presence of small colonies and decreased the number of larger colonies (Bargonetti lab observation-Angelika Brekman). We have observed that in *p53*-null H1299 cells, Mdm2-C increases cell proliferation of (Fig. 21). In light of this, we can ask how *mdm2-C* knockdown or over-expression would influence anchorage-independent growth. To do this, Mdm2-C can be transiently over-expressed exogenously in cells that would not normally grow in soft agar such as MCF10A. We can also over-express Mdm2-C in the MCF-10A cells via virus-mediated infection of the cells. MCF10A cells are a non-tumorigenic epithelial breast line that has been engineered to grow in culture. They do not grow in soft agar without the addition of a growth hormone (Zhu et al., 2005). The over-expression of Mdm2-C in these cells would determine whether it has oncogenic properties in human cells and possibly contributes to the tumorigenesis of cells over-expressing Mdm2-C. Also, *mdm2-C* can be knocked

down via an *mdm2-C* specific siRNA in cells with Mdm2-C over-expression e.g. T47D, to determine whether colony formation in soft agar would be inhibited.

In addition to checking for anchorage-independent growth, we can assess the influence of Mdm2-C on tumor formation in immune-compromised mice. Cells with stable expression of Mdm2-C can be injected into nude mice to check for tumor formation. The Mdm2-C stably expressing cells can be created via virus infection with *mdm2-C* bearing plasmids. So far, we have been unable to select for stably expressing Mdm2-C clones, however, this could be because the exogenously introduced Mdm2-C protein is degraded rapidly by endogenous Mdm2 protein. Mdm2 has been classified as a protein with substantial disordered regions that influences its interaction with a number of proteins (Dunker et al., 2005; Uversky et al., 2005). The Mdm2 protein was documented to possess about 26% of disordered regions, relative to its total number of amino acids. The disordered regions include portions in the p53 binding domain and the acidic and ZINC finger domains (Dunker et al., 2005). Regions of disorder in proteins have been suggested to increase the possible partners a protein can bind with (Patil et al., 2010). It is thought that the presence of disordered regions in a protein increases the flexibility of the protein and thus allows it to assume several conformations depending on its binding partner. The presence of disordered regions in proteins has also been implicated in cancers (Iakoucheva et al., 2002). Mdm2-C contains about 33% of disordered protein regions. Using the online program, Raptor (http://raptorx.uchicago.edu/), it was observed that the Mdm2-C polypeptide exists in an intrinsically disordered state (mainly loops and long strings of Beta sheets). Proteins that exist in mainly disordered states are highly unstable and have high turnover rates.

Therefore, this might explain why we have been unable to select stably expressing Mdm2-C clones.

Furthermore, an Mdm2-C mouse could be generated to examine how Mdm2-C influences the tumor spectrum and life span of the mouse. Experiments with Mdm2-A and Mdm2-B isoforms have shown that expression of either isoform in mice show a different tumor spectrum as compared to the non over-expressing mice. In addition, these mice have a shorter lifespan due to tumor formation (Steinman et al., 2004; Volk et al., 2009a). Therefore, creating an Mdm2-C mouse would be of great interest to resolve whether the protein has oncogenic functions in the context of a whole animal. Furthermore, the effect of Mdm2-C in the presence or absence of p53 would be analyzed. This is important because our experiments in culture have shown that Mdm2-C still possesses growth-promoting functions in the presence of p53 however, at a lower penetrance (Fig. 22A and B).

5.2.6 **Mdm2-C and Metabolism**

Proteins involved in cellular metabolism were identified after Mdm2-C IP and LC/MS/MS analysis (see Table 2). If these interactions prove to be true after Mdm2-C specific pull-down and subsequent LC/MS/MS, we could examine the influence of Mdm2-C on the function of the identified proteins. First, we will confirm whether Mdm2-C binds directly or indirectly to these proteins via Co-IPs in cell lines such as MANCA or T47D cells, with endogenous Mdm2-C over-expression. To examine the effect of Mdm2-C on the function of these proteins, transient transfections and expression of the

metabolism pathway-related proteins in the presence and absence of Mdm2-C could be assessed. This will help elucidate whether Mdm2-C influences the function of these proteins in cellular metabolism. A slight indication of the involvement of Mdm2-C in cell metabolism might lie in our observation that the specific knockdown of *mdm2-C* in ER+ mutant p53 *mdm2 G/G* SNP309 T47D cells resulted in a modest increase in death. This increase in death was not observed in cells with a heterogeneous mix of *mdm2* knockdown via shRNA or siRNA smart pool (data not shown and Fig. 29D). To check whether Mdm2-C is involved in cell metabolism, first we would have to enhance the knockdown of *mdm2-C* observed. Also, we would check for the effect of *mdm2-C* knockdown in other cell lines such as MANCA with Mdm2-C over-expression. Furthermore, we could perform experiments in which, in the presence and absence of Mdm2-C over-expression and knockdown, the amount of glucose uptake is measured (Robey et al., 2005; Yamamoto et al., 2011). Conversely, we could examine the levels of Mdm2-C protein in the presence of glucose restriction.

CHAPTER 6:

Perspective

The ability of Mdm2 to act as an oncogene has been thought to lie solely in its capacity to inhibit p53 tumor suppressive functions. However, several investigators have documented that Mdm2 possesses p53-independent functions that greatly contribute to tumorigenesis in the cell. Mdm2 over-expression is often times a negative prognostic marker in cancer. In addition, *mdm2* splice variant transcripts have been found over-expressed and implicated in the aggressiveness and overall survival of patients in which they are found. Although there are over seventy alternatively spliced transcripts of *mdm2*, their functions have not been well characterized except for two variants- *mdm2-A* and *mdm2-B*. The over-expression of full-length Mdm2 in culture cells showed that the protein has growth suppressive functions. Thus suggesting that the tumor promoting functions of Mdm2 might lie in the expression of its splice variant isoforms. Nonetheless, the study of these variants have produced conflicting results that show that both variants are tumor suppressive in a p53-dependent manner, however, they are also tumor promoting in the absence of functional p53. As a result, we embarked on the study of Mdm2-C, one of the most common splice variant transcripts found over-expressed in cancer.

We have observed that unlike Mdm2-A and Mdm2-B, Mdm2-C promotes growth in the presence and absence of p53 and does not activate p53 transcriptional activity. We have also detected endogenous Mdm2-C protein, something that has not been observed with the other Mdm2 isoforms. In addition, we saw an estrogen-dependent increase in Mdm2-C in two ER+ *mdm2*SNP309 breast cancer cells and this increase was independent of p53. The partial knockdown of *mdm2-C* in G/G *mdm2*SNP309 T47D breast cancer cells with mutant p53 resulted in an increase in death. This

suggests that Mdm2-C could be a survival factor in cells that over express the protein. These data point to the possible identification of a growth promoting protein that helps in the propagation of cancer whether p53 is present or not. Thus examining the levels of Mdm2-C in cancer tissues could help in the identification of cancers with treatment options that are possibly p53-independent. Further experiments to determine the pathway in which Mdm2-C works is important in order for targeted treatment options to be developed and tested.

CHAPTER 7:

Bibliography

Adachi, T., Oda, Y., Sakamoto, A., Saito, T., Tamiya, S., Masuda, K., and Tsuneyoshi, M. (2001). Immunoreactivity of p53, mdm2, and p21WAF1 in dedifferentiated liposarcoma: special emphasis on the distinct immunophenotype of the well-differentiated component. Int J Surg Pathol *9*, 99-109.

Albertson, T.M., Ogawa, M., Bugni, J.M., Hays, L.E., Chen, Y., Wang, Y., Treuting, P.M., Heddle, J.A., Goldsby, R.E., and Preston, B.D. (2009). DNA polymerase epsilon and delta proofreading suppress discrete mutator and cancer phenotypes in mice. Proc Natl Acad Sci U S A *106*, 17101-17104.

Allende-Vega, N., Dias, S., Milne, D., and Meek, D. (2005). Phosphorylation of the acidic domain of Mdm2 by protein kinase CK2. Mol Cell Biochem *274*, 85-90.

Alt, J.R., Bouska, A., Fernandez, M.R., Cerny, R.L., Xiao, H., and Eischen, C.M. (2005). Mdm2 binds to Nbs1 at sites of DNA damage and regulates double strand break repair. The Journal of biological chemistry *280*, 18771-18781.

Anderson, J.J., Challen, C., Atkins, H., Suaeyun, R., Crosier, S., and Lunec, J. (2007). MDM2 RNA binding is blocked by novel monoclonal antibody h-MDM2-F4-14. Int J Oncol *31*, 545-555.

Argentini, M., Barboule, N., and Wasylyk, B. (2001). The contribution of the acidic domain of MDM2 to p53 and MDM2 stability. Oncogene *20*, 1267-1275.

Armstrong, J.F., Kaufman, M.H., Harrison, D.J., and Clarke, A.R. (1995). High-frequency developmental abnormalities in p53-deficient mice. Curr Biol *5*, 931-936.

Arriola, E.L., Lopez, A.R., and Chresta, C.M. (1999). Differential regulation of p21waf-1/cip-1 and Mdm2 by etoposide: etoposide inhibits the p53-Mdm2 autoregulatory feedback loop. Oncogene *18*, 1081-1091.

Arva, N.C., Gopen, T.R., Talbott, K.E., Campbell, L.E., Chicas, A., White, D.E., Bond, G.L., Levine, A.J., and Bargonetti, J. (2005). A chromatin-associated and transcriptionally inactive p53-Mdm2 complex occurs in mdm2 SNP309 homozygous cells. The Journal of biological chemistry *280*, 26776-26787.

Arva, N.C., Talbott, K.E., Okoro, D.R., Brekman, A., Qiu, W.G., and Bargonetti, J. (2008). Disruption of the p53-Mdm2 complex by Nutlin-3 reveals different cancer cell phenotypes. Ethn Dis *18*, S2-1-8.

Asahara, H., Li, Y., Fuss, J., Haines, D.S., Vlatkovic, N., Boyd, M.T., and Linn, S. (2003). Stimulation of human DNA polymerase epsilon by MDM2. Nucleic acids research *31*, 2451-2459.

Avantaggiati, M.L., Ogryzko, V., Gardner, K., Giordano, A., Levine, A.S., and Kelly, K. (1997). Recruitment of p300/CBP in p53-dependent signal pathways. Cell *89*, 1175-1184.

Baker, S.J., Fearon, E.R., Nigro, J.M., Hamilton, S.R., Preisinger, A.C., Jessup, J.M., vanTuinen, P., Ledbetter, D.H., Barker, D.F., Nakamura, Y*., et al.* (1989). Chromosome 17 deletions and p53 gene mutations in colorectal carcinomas. Science *244*, 217-221.

Baker, S.J., Preisinger, A.C., Jessup, J.M., Paraskeva, C., Markowitz, S., Willson, J.K., Hamilton, S., and Vogelstein, B. (1990). p53 gene mutations occur in combination with 17p allelic deletions as late events in colorectal tumorigenesis. Cancer research *50*, 7717-7722.

Barak, Y., Juven, T., Haffner, R., and Oren, M. (1993). mdm2 expression is induced by wild type p53 activity. Embo J *12*, 461-468.

Bargonetti, J., Manfredi, J.J., Chen, X., Marshak, D.R., and Prives, C. (1993). A proteolytic fragment from the central region of p53 has marked sequence-specific DNA-binding activity when generated from wild-type but not from oncogenic mutant p53 protein. Genes Dev *7*, 2565-2574.

Bartel, F., Harris, L.C., Wurl, P., and Taubert, H. (2004). MDM2 and its splice variant messenger RNAs: expression in tumors and down-regulation using antisense oligonucleotides. Molecular cancer research : MCR *2*, 29-35.

Bartel, F., Meye, A., Wurl, P., Kappler, M., Bache, M., Lautenschlager, C., Grunbaum, U., Schmidt, H., and Taubert, H. (2001a). Amplification of the MDM2 gene, but not expression of splice variants of MDM2 MRNA, is associated with prognosis in soft tissue sarcoma. Int J Cancer *95*, 168-175.

Bartel, F., Taubert, H., and Harris, L.C. (2002). Alternative and aberrant splicing of MDM2 mRNA in human cancer. Cancer Cell *2*, 9-15.

Bartel, F., Taylor, A.C., Taubert, H., and Harris, L.C. (2001b). Novel mdm2 splice variants identified in pediatric rhabdomyosarcoma tumors and cell lines. Oncol Res *12*, 451-457.

Bennett-Lovsey, R., Hart, S.E., Shirai, H., and Mizuguchi, K. (2002). The SWIB and the MDM2 domains are homologous and share a common fold. Bioinformatics *18*, 626-630.

Bhatt, P., d'Avout, C., Kane, N.S., Borowiec, J.A., and Saxena, A. (2012). Specific domains of nucleolin interact with Hdm2 and antagonize Hdm2-mediated p53 ubiquitination. Febs J *279*, 370-383.

Black, D.L. (2003). Mechanisms of alternative pre-messenger RNA splicing. Annu Rev Biochem *72*, 291-336.

Blattner, C., Hay, T., Meek, D.W., and Lane, D.P. (2002). Hypophosphorylation of Mdm2 augments p53 stability. Mol Cell Biol *22*, 6170-6182.

Boersma, B.J., Howe, T.M., Goodman, J.E., Yfantis, H.G., Lee, D.H., Chanock, S.J., and Ambs, S. (2006). Association of breast cancer outcome with status of p53 and MDM2 SNP309. Journal of the National Cancer Institute *98*, 911-919.

Bond, G.L., Hirshfield, K.M., Kirchhoff, T., Alexe, G., Bond, E.E., Robins, H., Bartel, F., Taubert, H., Wuerl, P., Hait, W*., et al.* (2006a). MDM2 SNP309 accelerates tumor formation in a gender-specific and hormone-dependent manner. Cancer research *66*, 5104-5110.

Bond, G.L., Hu, W., Bond, E.E., Robins, H., Lutzker, S.G., Arva, N.C., Bargonetti, J., Bartel, F., Taubert, H., Wuerl, P*., et al.* (2004). A single nucleotide polymorphism in the MDM2 promoter attenuates the p53 tumor suppressor pathway and accelerates tumor formation in humans. Cell *119*, 591-602.

Bond, G.L., Hu, W., and Levine, A. (2005). A single nucleotide polymorphism in the MDM2 gene: from a molecular and cellular explanation to clinical effect. Cancer research *65*, 5481-5484.

Bond, G.L., Menin, C., Bertorelle, R., Alhopuro, P., Aaltonen, L.A., and Levine, A.J. (2006b). MDM2 SNP309 accelerates colorectal tumour formation in women. J Med Genet *43*, 950-952.

Bouska, A., and Eischen, C.M. (2009a). Mdm2 affects genome stability independent of p53. Cancer research *69*, 1697-1701.

Bouska, A., and Eischen, C.M. (2009b). Murine double minute 2: p53-independent roads lead to genome instability or death. Trends Biochem Sci *34*, 279-286.

Bouska, A., Lushnikova, T., Plaza, S., and Eischen, C.M. (2008). Mdm2 promotes genetic instability and transformation independent of p53. Mol Cell Biol *28*, 4862-4874.

Brekman, A., Singh, K.E., Polotskaia, A., Kundu, N., and Bargonetti, J. (2011). A p53-independent role of Mdm2 in estrogen-mediated activation of breast cancer cell proliferation. Breast Cancer Res *13*, R3.

Brown, C.J., Lain, S., Verma, C.S., Fersht, A.R., and Lane, D.P. (2009). Awakening guardian angels: drugging the p53 pathway. Nat Rev Cancer *9*, 862-873.

Brown, C.Y., Mize, G.J., Pineda, M., George, D.L., and Morris, D.R. (1999). Role of two upstream open reading frames in the translational control of oncogene mdm2. Oncogene *18*, 5631-5637.

Bueso-Ramos, C.E., Yang, Y., deLeon, E., McCown, P., Stass, S.A., and Albitar, M. (1993). The human MDM-2 oncogene is overexpressed in leukemias. Blood *82*, 2617-2623.

Burch, L.R., Midgley, C.A., Currie, R.A., Lane, D.P., and Hupp, T.R. (2000). Mdm2 binding to a conformationally sensitive domain on p53 can be modulated by RNA. FEBS Lett *472*, 93-98.

Buschmann, T., Lerner, D., Lee, C.G., and Ronai, Z. (2001). The Mdm-2 amino terminus is required for Mdm2 binding and SUMO-1 conjugation by the E2 SUMO-1 conjugating enzyme Ubc9. The Journal of biological chemistry *276*, 40389-40395.

Cahilly-Snyder, L., Yang-Feng, T., Francke, U., and George, D.L. (1987). Molecular analysis and chromosomal mapping of amplified genes isolated from a transformed mouse 3T3 cell line. Somat Cell Mol Genet *13*, 235-244.

Candeias, M.M., Malbert-Colas, L., Powell, D.J., Daskalogianni, C., Maslon, M.M., Naski, N., Bourougaa, K., Calvo, F., and Fahraeus, R. (2008). P53 mRNA controls p53 activity by managing Mdm2 functions. Nature cell biology *10*, 1098-1105.

Canman, C.E., Lim, D.S., Cimprich, K.A., Taya, Y., Tamai, K., Sakaguchi, K., Appella, E., Kastan, M.B., and Siliciano, J.D. (1998). Activation of the ATM kinase by ionizing radiation and phosphorylation of p53. Science *281*, 1677-1679.

Challen, C., Anderson, J.J., Chrzanowska-Lightowlers, Z.M., Lightowlers, R.N., and Lunec, J. (2011). Recombinant human MDM2 oncoprotein shows sequence composition selectivity. Int J Oncol.

Chandler, D.S., Singh, R.K., Caldwell, L.C., Bitler, J.L., and Lozano, G. (2006). Genotoxic stress induces coordinately regulated alternative splicing of the p53 modulators MDM2 and MDM4. Cancer Res *66*, 9502-9508.

Chen, C.Y., Oliner, J.D., Zhan, Q., Fornace, A.J., Jr., Vogelstein, B., and Kastan, M.B. (1994). Interactions between p53 and MDM2 in a mammalian cell cycle checkpoint pathway. Proc Natl Acad Sci U S A *91*, 2684-2688.

Chen, J., Lin, J., and Levine, A.J. (1995). Regulation of transcription functions of the p53 tumor suppressor by the mdm-2 oncogene. Mol Med *1*, 142-152.

Chen, J., Marechal, V., and Levine, A.J. (1993). Mapping of the p53 and mdm-2 interaction domains. Mol Cell Biol *13*, 4107-4114.

Cheng, Q., Cross, B., Li, B., Chen, L., Li, Z., and Chen, J. (2011). Regulation of MDM2 E3 ligase activity by phosphorylation after DNA damage. Mol Cell Biol *31*, 4951-4963.

Ciliberto, A., Novak, B., and Tyson, J.J. (2005). Steady states and oscillations in the p53/Mdm2 network. Cell Cycle *4*, 488-493.

Clancy, S. (2008). RNA functions. . Nature Education *1*.

Cordon-Cardo, C., Latres, E., Drobnjak, M., Oliva, M.R., Pollack, D., Woodruff, J.M., Marechal, V., Chen, J., Brennan, M.F., and Levine, A.J. (1994). Molecular abnormalities of mdm2 and p53 genes in adult soft tissue sarcomas. Cancer research *54*, 794-799.

Coupland, S.E., Anastassiou, G., Stang, A., Schilling, H., Anagnostopoulos, I., Bornfeld, N., and Stein, H. (2000). The prognostic value of cyclin D1, p53, and MDM2 protein expression in uveal melanoma. J Pathol *191*, 120-126.

Dai, M.S., and Lu, H. (2004). Inhibition of MDM2-mediated p53 ubiquitination and degradation by ribosomal protein L5. The Journal of biological chemistry *279*, 44475-44482.

Dai, M.S., Shi, D., Jin, Y., Sun, X.X., Zhang, Y., Grossman, S.R., and Lu, H. (2006). Regulation of the MDM2-p53 pathway by ribosomal protein L11 involves a post-ubiquitination mechanism. The Journal of biological chemistry *281*, 24304-24313.

Dai, M.S., Zeng, S.X., Jin, Y., Sun, X.X., David, L., and Lu, H. (2004). Ribosomal protein L23 activates p53 by inhibiting MDM2 function in response to ribosomal perturbation but not to translation inhibition. Mol Cell Biol *24*, 7654-7668.

Dang, J., Kuo, M.L., Eischen, C.M., Stepanova, L., Sherr, C.J., and Roussel, M.F. (2002). The RING domain of Mdm2 can inhibit cell proliferation. Cancer Res *62*, 1222-1230.

Datto, M.B., Yu, Y., and Wang, X.F. (1995). Functional analysis of the transforming growth factor beta responsive elements in the WAF1/Cip1/p21 promoter. The Journal of biological chemistry *270*, 28623-28628.

de Toledo, S.M., Azzam, E.I., Dahlberg, W.K., Gooding, T.B., and Little, J.B. (2000). ATM complexes with HDM2 and promotes its rapid phosphorylation in a p53-independent manner in normal and tumor human cells exposed to ionizing radiation. Oncogene *19*, 6185-6193.

Deb, S.P. (2003). Cell cycle regulatory functions of the human oncoprotein MDM2. Molecular cancer research : MCR *1*, 1009-1016.

Dias, C.S., Liu, Y., Yau, A., Westrick, L., and Evans, S.C. (2006). Regulation of hdm2 by stress-induced hdm2alt1 in tumor and nontumorigenic cell lines correlating with p53 stability. Cancer research *66*, 9467-9473.

Donehower, L.A., Harvey, M., Slagle, B.L., McArthur, M.J., Montgomery, C.A., Jr., Butel, J.S., and Bradley, A. (1992). Mice deficient for p53 are developmentally normal but susceptible to spontaneous tumours. Nature *356*, 215-221.

Dunker, A.K., Cortese, M.S., Romero, P., Iakoucheva, L.M., and Uversky, V.N. (2005). Flexible nets. The roles of intrinsic disorder in protein interaction networks. Febs J *272*, 5129-5148.

Elenbaas, B., Dobbelstein, M., Roth, J., Shenk, T., and Levine, A.J. (1996). The MDM2 oncoprotein binds specifically to RNA through its RING finger domain. Mol Med *2*, 439-451.

Enge, M., Bao, W., Hedstrom, E., Jackson, S.P., Moumen, A., and Selivanova, G. (2009). MDM2-dependent downregulation of p21 and hnRNP K provides a switch between apoptosis and growth arrest induced by pharmacologically activated p53. Cancer Cell *15*, 171-183.

Evans, S.C., Viswanathan, M., Grier, J.D., Narayana, M., El-Naggar, A.K., and Lozano, G. (2001). An alternatively spliced HDM2 product increases p53 activity by inhibiting HDM2. Oncogene *20*, 4041-4049.

Fackenthal, J.D., and Godley, L.A. (2008). Aberrant RNA splicing and its functional consequences in cancer cells. Dis Model Mech *1*, 37-42.

Fakharzadeh, S.S., Trusko, S.P., and George, D.L. (1991). Tumorigenic potential associated with enhanced expression of a gene that is amplified in a mouse tumor cell line. Embo J *10*, 1565-1569.

Fang, S., Jensen, J.P., Ludwig, R.L., Vousden, K.H., and Weissman, A.M. (2000). Mdm2 is a RING finger-dependent ubiquitin protein ligase for itself and p53. J Biol Chem *275*, 8945-8951.

Fontoura, B.M., Sorokina, E.A., David, E., and Carroll, R.B. (1992). p53 is covalently linked to 5.8S rRNA. Mol Cell Biol *12*, 5145-5151.

Freedman, D.A., and Levine, A.J. (1998). Nuclear export is required for degradation of endogenous p53 by MDM2 and human papillomavirus E6. Mol Cell Biol *18*, 7288-7293.

Freedman, D.A., Wu, L., and Levine, A.J. (1999). Functions of the MDM2 oncoprotein. Cell Mol Life Sci *55*, 96-107.

Fridman, J.S., Hernando, E., Hemann, M.T., de Stanchina, E., Cordon-Cardo, C., and Lowe, S.W. (2003). Tumor promotion by Mdm2 splice variants unable to bind p53. Cancer research *63*, 5703-5706.

Galy, B., Creancier, L., Prado-Lourenco, L., Prats, A.C., and Prats, H. (2001). p53 directs conformational change and translation initiation blockade of human fibroblast growth factor 2 mRNA. Oncogene *20*, 4613-4620.

Ganguli, G., and Wasylyk, B. (2003). p53-independent functions of MDM2. Molecular cancer research : MCR *1*, 1027-1035.

Giaccia, A.J., and Kastan, M.B. (1998). The complexity of p53 modulation: emerging patterns from divergent signals. Genes Dev *12*, 2973-2983.

Gilkes, D.M., Pan, Y., Coppola, D., Yeatman, T., Reuther, G.W., and Chen, J. (2008). Regulation of MDMX expression by mitogenic signaling. Mol Cell Biol *28*, 1999-2010.

Goldberg, Z., Vogt Sionov, R., Berger, M., Zwang, Y., Perets, R., Van Etten, R.A., Oren, M., Taya, Y., and Haupt, Y. (2002). Tyrosine phosphorylation of Mdm2 by c-Abl: implications for p53 regulation. Embo J *21*, 3715-3727.

Goldstrohm, A.C., Greenleaf, A.L., and Garcia-Blanco, M.A. (2001). Co-transcriptional splicing of pre-messenger RNAs: considerations for the mechanism of alternative splicing. Gene *277*, 31-47.

Gotz, C., Kartarius, S., Scholtes, P., Nastainczyk, W., and Montenarh, M. (1999). Identification of a CK2 phosphorylation site in mdm2. Eur J Biochem *266*, 493-501.

Graveley, B.R. (2001). Alternative splicing: increasing diversity in the proteomic world. Trends Genet *17*, 100-107.

Grossman, S.R., Deato, M.E., Brignone, C., Chan, H.M., Kung, A.L., Tagami, H., Nakatani, Y., and Livingston, D.M. (2003). Polyubiquitination of p53 by a ubiquitin ligase activity of p300. Science *300*, 342-344.

Grossman, S.R., Perez, M., Kung, A.L., Joseph, M., Mansur, C., Xiao, Z.X., Kumar, S., Howley, P.M., and Livingston, D.M. (1998). p300/MDM2 complexes participate in MDM2-mediated p53 degradation. Mol Cell *2*, 405-415.

Gryshchenko, I., Hofbauer, S., Stoecher, M., Daniel, P.T., Steurer, M., Gaiger, A., Eigenberger, K., Greil, R., and Tinhofer, I. (2008). MDM2 SNP309 is associated with poor outcome in B-cell chronic lymphocytic leukemia. J Clin Oncol *26*, 2252-2257.

Gu, L., Zhang, H., He, J., Li, J., Huang, M., and Zhou, M. (2012). MDM2 regulates MYCN mRNA stabilization and translation in human neuroblastoma cells. Oncogene *31*, 1342-1353.

Gu, L., Zhu, N., Zhang, H., Durden, D.L., Feng, Y., and Zhou, M. (2009). Regulation of XIAP translation and induction by MDM2 following irradiation. Cancer Cell *15*, 363-375.

Gu, W., Shi, X.L., and Roeder, R.G. (1997). Synergistic activation of transcription by CBP and p53. Nature *387*, 819-823.

Haines, D.S., Landers, J.E., Engle, L.J., and George, D.L. (1994). Physical and functional interaction between wild-type p53 and mdm2 proteins. Mol Cell Biol *14*, 1171-1178.

Harris, L.C. (2005). MDM2 splice variants and their therapeutic implications. Curr Cancer Drug Targets *5*, 21-26.

Haupt, Y., Maya, R., Kazaz, A., and Oren, M. (1997). Mdm2 promotes the rapid degradation of p53. Nature *387*, 296-299.

Hay, T.J., and Meek, D.W. (2000). Multiple sites of in vivo phosphorylation in the MDM2 oncoprotein cluster within two important functional domains. FEBS Lett *478*, 183-186.

He, J., Reifenberger, G., Liu, L., Collins, V.P., and James, C.D. (1994). Analysis of glioma cell lines for amplification and overexpression of MDM2. Genes, chromosomes & cancer *11*, 91-96.

Hjerrild, M., Milne, D., Dumaz, N., Hay, T., Issinger, O.G., and Meek, D. (2001). Phosphorylation of murine double minute clone 2 (MDM2) protein at serine-267 by protein kinase CK2 in vitro and in cultured cells. Biochem J *355*, 347-356.

Honda, R., Tanaka, H., and Yasuda, H. (1997). Oncoprotein MDM2 is a ubiquitin ligase E3 for tumor suppressor p53. FEBS Lett *420*, 25-27.

Honda, R., and Yasuda, H. (1999). Association of p19(ARF) with Mdm2 inhibits ubiquitin ligase activity of Mdm2 for tumor suppressor p53. Embo J *18*, 22-27.

Honda, R., and Yasuda, H. (2000). Activity of MDM2, a ubiquitin ligase, toward p53 or itself is dependent on the RING finger domain of the ligase. Oncogene *19*, 1473-1476.

Hu, W., Feng, Z., Ma, L., Wagner, J., Rice, J.J., Stolovitzky, G., and Levine, A.J. (2007). A single nucleotide polymorphism in the MDM2 gene disrupts the oscillation of p53 and MDM2 levels in cells. Cancer research *67*, 2757-2765.

Iakoucheva, L.M., Brown, C.J., Lawson, J.D., Obradovic, Z., and Dunker, A.K. (2002). Intrinsic disorder in cell-signaling and cancer-associated proteins. J Mol Biol *323*, 573-584.

Iwakuma, T., and Lozano, G. (2003). MDM2, an introduction. Mol Cancer Res *1*, 993-1000.

Jacks, T., Remington, L., Williams, B.O., Schmitt, E.M., Halachmi, S., Bronson, R.T., and Weinberg, R.A. (1994). Tumor spectrum analysis in p53-mutant mice. Curr Biol *4*, 1-7.

Jeyaraj, S., O'Brien, D.M., and Chandler, D.S. (2009). MDM2 and MDM4 splicing: an integral part of the cancer spliceome. Front Biosci *14*, 2647-2656.

Jin, A., Itahana, K., O'Keefe, K., and Zhang, Y. (2004). Inhibition of HDM2 and activation of p53 by ribosomal protein L23. Mol Cell Biol *24*, 7669-7680.

Jin, Y., Lee, H., Zeng, S.X., Dai, M.S., and Lu, H. (2003). MDM2 promotes p21waf1/cip1 proteasomal turnover independently of ubiquitylation. Embo J *22*, 6365-6377.

Jin, Y., Zeng, S.X., Dai, M.S., Yang, X.J., and Lu, H. (2002). MDM2 inhibits PCAF (p300/CREB-binding protein-associated factor)-mediated p53 acetylation. The Journal of biological chemistry *277*, 30838-30843.

Johnson-Pais, T., Degnin, C., and Thayer, M.J. (2001). pRB induces Sp1 activity by relieving inhibition mediated by MDM2. Proc Natl Acad Sci U S A *98*, 2211-2216.

Jones, S.N., Roe, A.E., Donehower, L.A., and Bradley, A. (1995). Rescue of embryonic lethality in Mdm2-deficient mice by absence of p53. Nature *378*, 206-208.

Jones, S.N., Sands, A.T., Hancock, A.R., Vogel, H., Donehower, L.A., Linke, S.P., Wahl, G.M., and Bradley, A. (1996). The tumorigenic potential and cell growth characteristics of p53-deficient cells are equivalent in the presence or absence of Mdm2. Proc Natl Acad Sci U S A *93*, 14106-14111.

Jung, Y.S., Qian, Y., and Chen, X. (2011). DNA polymerase eta is targeted by Mdm2 for polyubiquitination and proteasomal degradation in response to ultraviolet irradiation. DNA Repair (Amst).

Juven, T., Barak, Y., Zauberman, A., George, D.L., and Oren, M. (1993). Wild type p53 can mediate sequence-specific transactivation of an internal promoter within the mdm2 gene. Oncogene *8*, 3411-3416.

Kalnina, Z., Zayakin, P., Silina, K., and Line, A. (2005). Alterations of pre-mRNA splicing in cancer. Genes Chromosomes Cancer *42*, 342-357.

Kamrul, H.M., Wadhwa, R., and Kaul, S.C. (2007). CARF binds to three members (ARF, p53, and HDM2) of the p53 tumor-suppressor pathway. Ann N Y Acad Sci *1100*, 312-315.

Karve, T.M., and Cheema, A.K. (2011). Small changes huge impact: the role of protein posttranslational modifications in cellular homeostasis and disease. J Amino Acids *2011*, 207691.

Kawai, H., Wiederschain, D., and Yuan, Z.M. (2003). Critical contribution of the MDM2 acidic domain to p53 ubiquitination. Mol Cell Biol *23*, 4939-4947.

Khosravi, R., Maya, R., Gottlieb, T., Oren, M., Shiloh, Y., and Shkedy, D. (1999). Rapid ATM-dependent phosphorylation of MDM2 precedes p53 accumulation in response to DNA damage. Proc Natl Acad Sci U S A *96*, 14973-14977.

Kubbutat, M.H., Jones, S.N., and Vousden, K.H. (1997). Regulation of p53 stability by Mdm2. Nature *387*, 299-303.

Lai, R., Medeiros, L.J., Wilson, C.S., Sun, N.C., Koo, C., McCourty, A., and Brynes, R.K. (1998). Expression of the cell-cycle-related proteins E2F-1, p53, mdm-2, p21waf-1, and Ki-67 in multiple myeloma: correlation with cyclin-D1 immunoreactivity. Mod Pathol *11*, 642-647.

Landers, J.E., Cassel, S.L., and George, D.L. (1997). Translational enhancement of mdm2 oncogene expression in human tumor cells containing a stabilized wild-type p53 protein. Cancer Res *57*, 3562-3568.

Landers, J.E., Haines, D.S., Strauss, J.F., 3rd, and George, D.L. (1994). Enhanced translation: a novel mechanism of mdm2 oncogene overexpression identified in human tumor cells. Oncogene *9*, 2745-2750.

Lane, D.P., Cheok, C.F., Brown, C., Madhumalar, A., Ghadessy, F.J., and Verma, C. (2010a). Mdm2 and p53 are highly conserved from placozoans to man. Cell Cycle *9*, 540-547.

Lane, D.P., Cheok, C.F., Brown, C.J., Madhumalar, A., Ghadessy, F.J., and Verma, C. (2010b). The Mdm2 and p53 genes are conserved in the Arachnids. Cell Cycle *9*, 748-754.

Li, D., Marchenko, N.D., Schulz, R., Fischer, V., Velasco-Hernandez, T., Talos, F., and Moll, U.M. (2011). Functional inactivation of endogenous MDM2 and CHIP by HSP90 causes aberrant stabilization of mutant p53 in human cancer cells. Molecular cancer research : MCR *9*, 577-588.

Li, M., Brooks, C.L., Wu-Baer, F., Chen, D., Baer, R., and Gu, W. (2003). Mono- versus polyubiquitination: differential control of p53 fate by Mdm2. Science *302*, 1972-1975.

Liang, H., Atkins, H., Abdel-Fattah, R., Jones, S.N., and Lunec, J. (2004). Genomic organisation of the human MDM2 oncogene and relationship to its alternatively spliced mRNAs. Gene *338*, 217-223.

Lill, N.L., Grossman, S.R., Ginsberg, D., DeCaprio, J., and Livingston, D.M. (1997). Binding and modulation of p53 by p300/CBP coactivators. Nature *387*, 823-827.

Linke, K., Mace, P.D., Smith, C.A., Vaux, D.L., Silke, J., and Day, C.L. (2008). Structure of the MDM2/MDMX RING domain heterodimer reveals dimerization is required for their ubiquitylation in trans. Cell Death Differ *15*, 841-848.

Linzer, D.I., and Levine, A.J. (1979). Characterization of a 54K dalton cellular SV40 tumor antigen present in SV40-transformed cells and uninfected embryonal carcinoma cells. Cell *17*, 43-52.

Ljungman, M., and Zhang, F. (1996). Blockage of RNA polymerase as a possible trigger for u.v. light-induced apoptosis. Oncogene *13*, 823-831.

Lohrum, M.A., Ludwig, R.L., Kubbutat, M.H., Hanlon, M., and Vousden, K.H. (2003). Regulation of HDM2 activity by the ribosomal protein L11. Cancer Cell *3*, 577-587.

Loughran, O., and La Thangue, N.B. (2000). Apoptotic and growth-promoting activity of E2F modulated by MDM2. Mol Cell Biol *20*, 2186-2197.

Lukas, J., Gao, D.Q., Keshmeshian, M., Wen, W.H., Tsao-Wei, D., Rosenberg, S., and Press, M.F. (2001). Alternative and aberrant messenger RNA splicing of the mdm2 oncogene in invasive breast cancer. Cancer Res *61*, 3212-3219.

Lundgren, K., Montes de Oca Luna, R., McNeill, Y.B., Emerick, E.P., Spencer, B., Barfield, C.R., Lozano, G., Rosenberg, M.P., and Finlay, C.A. (1997). Targeted expression of MDM2 uncouples S phase from mitosis and inhibits mammary gland development independent of p53. Genes Dev *11*, 714-725.

Lushnikova, T., Bouska, A., Odvody, J., Dupont, W.D., and Eischen, C.M. (2011). Aging mice have increased chromosome instability that is exacerbated by elevated Mdm2 expression. Oncogene *30*, 4622-4631.

Ma, J., Martin, J.D., Zhang, H., Auger, K.R., Ho, T.F., Kirkpatrick, R.B., Grooms, M.H., Johanson, K.O., Tummino, P.J., Copeland, R.A.*, et al.* (2006). A second p53 binding site in the central domain of Mdm2 is essential for p53 ubiquitination. Biochemistry *45*, 9238-9245.

Marechal, V., Elenbaas, B., Piette, J., Nicolas, J.C., and Levine, A.J. (1994). The ribosomal L5 protein is associated with mdm-2 and mdm-2-p53 complexes. Mol Cell Biol *14*, 7414-7420.

Martin, K., Trouche, D., Hagemeier, C., Sorensen, T.S., La Thangue, N.B., and Kouzarides, T. (1995). Stimulation of E2F1/DP1 transcriptional activity by MDM2 oncoprotein. Nature *375*, 691-694.

Matsumoto, R., Tada, M., Nozaki, M., Zhang, C.L., Sawamura, Y., and Abe, H. (1998). Short alternative splice transcripts of the mdm2 oncogene correlate to malignancy in human astrocytic neoplasms. Cancer research *58*, 609-613.

Maya, R., Balass, M., Kim, S.T., Shkedy, D., Leal, J.F., Shifman, O., Moas, M., Buschmann, T., Ronai, Z., Shiloh, Y.*, et al.* (2001). ATM-dependent phosphorylation of Mdm2 on serine 395: role in p53 activation by DNA damage. Genes Dev *15*, 1067-1077.

Mayo, L.D., and Donner, D.B. (2001). A phosphatidylinositol 3-kinase/Akt pathway promotes translocation of Mdm2 from the cytoplasm to the nucleus. Proc Natl Acad Sci U S A *98*, 11598-11603.

McDonnell, T.J., Montes de Oca Luna, R., Cho, S., Amelse, L.L., Chavez-Reyes, A., and Lozano, G. (1999). Loss of one but not two mdm2 null alleles alters the tumour spectrum in p53 null mice. J Pathol *188*, 322-328.

Meddeb, M., Valent, A., Danglot, G., Nguyen, V.C., Duverger, A., Fouquet, F., Terrier-Lacombe, M.J., Oberlin, O., and Bernheim, A. (1996). MDM2 amplification in a primary alveolar rhabdomyosarcoma displaying a t(2;13)(q35;q14). Cytogenet Cell Genet *73*, 325-330.

Meek, D.W., and Knippschild, U. (2003). Posttranslational modification of MDM2. Molecular cancer research : MCR *1*, 1017-1026.

Meulmeester, E., Frenk, R., Stad, R., de Graaf, P., Marine, J.C., Vousden, K.H., and Jochemsen, A.G. (2003). Critical role for a central part of Mdm2 in the ubiquitylation of p53. Mol Cell Biol *23*, 4929-4938.

Miller, S.J., Suthiphongchai, T., Zambetti, G.P., and Ewen, M.E. (2000). p53 binds selectively to the 5' untranslated region of cdk4, an RNA element necessary and sufficient for transforming growth factor beta- and p53-mediated translational inhibition of cdk4. Mol Cell Biol *20*, 8420-8431.

Milne, D., Kampanis, P., Nicol, S., Dias, S., Campbell, D.G., Fuller-Pace, F., and Meek, D. (2004). A novel site of AKT-mediated phosphorylation in the human MDM2 onco-protein. FEBS Lett *577*, 270-276.

Minsky, N., and Oren, M. (2004). The RING domain of Mdm2 mediates histone ubiquitylation and transcriptional repression. Mol Cell *16*, 631-639.

Momand, J., Jung, D., Wilczynski, S., and Niland, J. (1998). The MDM2 gene amplification database. Nucleic acids research *26*, 3453-3459.

Momand, J., Zambetti, G.P., Olson, D.C., George, D., and Levine, A.J. (1992). The mdm-2 oncogene product forms a complex with the p53 protein and inhibits p53-mediated transactivation. Cell *69*, 1237-1245.

Montes de Oca Luna, R., Amelse, L.L., Chavez-Reyes, A., Evans, S.C., Brugarolas, J., Jacks, T., and Lozano, G. (1997). Deletion of p21 cannot substitute for p53 loss in rescue of mdm2 null lethality. Nat Genet *16*, 336-337.

Montes de Oca Luna, R., Wagner, D.S., and Lozano, G. (1995). Rescue of early embryonic lethality in mdm2-deficient mice by deletion of p53. Nature *378*, 203-206.

Morgan, R.J., Newcomb, P.V., Hardwick, R.H., and Alderson, D. (1999). Amplification of cyclin D1 and MDM-2 in oesophageal carcinoma. Eur J Surg Oncol *25*, 364-367.

Morgenstern, J.P., and Land, H. (1990). Advanced mammalian gene transfer: high titre retroviral vectors with multiple drug selection markers and a complementary helper-free packaging cell line. Nucleic acids research *18*, 3587-3596.

Mosner, J., Mummenbrauer, T., Bauer, C., Sczakiel, G., Grosse, F., and Deppert, W. (1995). Negative feedback regulation of wild-type p53 biosynthesis. Embo J *14*, 4442-4449.

Mozzherin, D.J., and Fisher, P.A. (1996). Human DNA polymerase epsilon: enzymologic mechanism and gap-filling synthesis. Biochemistry *35*, 3572-3577.

Nakayama, T., Toguchida, J., Wadayama, B., Kanoe, H., Kotoura, Y., and Sasaki, M.S. (1995). MDM2 gene amplification in bone and soft-tissue tumors: association with tumor progression in differentiated adipose-tissue tumors. Int J Cancer *64*, 342-346.

Naski, N., Gajjar, M., Bourougaa, K., Malbert-Colas, L., Fahraeus, R., and Candeias, M.M. (2009). The p53 mRNA-Mdm2 interaction. Cell Cycle *8*, 31-34.

Nevins, J.R. (2001). The Rb/E2F pathway and cancer. Human molecular genetics *10*, 699-703.

Oberosler, P., Hloch, P., Ramsperger, U., and Stahl, H. (1993). p53-catalyzed annealing of complementary single-stranded nucleic acids. Embo J *12*, 2389-2396.

Ofir-Rosenfeld, Y., Boggs, K., Michael, D., Kastan, M.B., and Oren, M. (2008). Mdm2 regulates p53 mRNA translation through inhibitory interactions with ribosomal protein L26. Mol Cell *32*, 180-189.

Ogawara, Y., Kishishita, S., Obata, T., Isazawa, Y., Suzuki, T., Tanaka, K., Masuyama, N., and Gotoh, Y. (2002). Akt enhances Mdm2-mediated ubiquitination and degradation of p53. The Journal of biological chemistry *277*, 21843-21850.

Okoro, D.R., Rosso, M., and Bargonetti, J. (2012). Splicing Up Mdm2 for Cancer Proteome Diversity. Genes & Cancer.

Oliner, J.D., Kinzler, K.W., Meltzer, P.S., George, D.L., and Vogelstein, B. (1992). Amplification of a gene encoding a p53-associated protein in human sarcomas. Nature *358*, 80-83.

Oliner, J.D., Pietenpol, J.A., Thiagalingam, S., Gyuris, J., Kinzler, K.W., and Vogelstein, B. (1993). Oncoprotein MDM2 conceals the activation domain of tumour suppressor p53. Nature *362*, 857-860.

Olson, D.C., Marechal, V., Momand, J., Chen, J., Romocki, C., and Levine, A.J. (1993). Identification and characterization of multiple mdm-2 proteins and mdm-2-p53 protein complexes. Oncogene *8*, 2353-2360.

Ostler, K.R., Davis, E.M., Payne, S.L., Gosalia, B.B., Exposito-Cespedes, J., Le Beau, M.M., and Godley, L.A. (2007). Cancer cells express aberrant DNMT3B transcripts encoding truncated proteins. Oncogene *26*, 5553-5563.

Pan, Y., and Chen, J. (2003). MDM2 promotes ubiquitination and degradation of MDMX. Mol Cell Biol *23*, 5113-5121.

Parada, L.F., Land, H., Weinberg, R.A., Wolf, D., and Rotter, V. (1984). Cooperation between gene encoding p53 tumour antigen and ras in cellular transformation. Nature *312*, 649-651.

Patil, A., Kinoshita, K., and Nakamura, H. (2010). Hub promiscuity in protein-protein interaction networks. Int J Mol Sci *11*, 1930-1943.

Paull, T.T., and Lee, J.H. (2005). The Mre11/Rad50/Nbs1 complex and its role as a DNA double-strand break sensor for ATM. Cell Cycle *4*, 737-740.

Perry, M.E., Piette, J., Zawadzki, J.A., Harvey, D., and Levine, A.J. (1993). The mdm-2 gene is induced in response to UV light in a p53-dependent manner. Proc Natl Acad Sci U S A *90*, 11623-11627.

Phelps, M., Darley, M., Primrose, J.N., and Blaydes, J.P. (2003). p53-independent activation of the hdm2-P2 promoter through multiple transcription factor response elements results in elevated hdm2 expression in estrogen receptor alpha-positive breast cancer cells. Cancer Res *63*, 2616-2623.

Pignataro, L., Capaccio, P., Pruneri, G., Carboni, N., Buffa, R., Neri, A., and Ottaviani, A. (1998). The predictive value of p53, MDM-2, cyclin D1 and Ki67 in the progression from low-grade dysplasia towards carcinoma of the larynx. J Laryngol Otol *112*, 455-459.

Post, S.M., Quintas-Cardama, A., Pant, V., Iwakuma, T., Hamir, A., Jackson, J.G., Maccio, D.R., Bond, G.L., Johnson, D.G., Levine, A.J.*, et al.* (2010). A high-frequency regulatory polymorphism in the p53 pathway accelerates tumor development. Cancer Cell *18*, 220-230.

Poyurovsky, M.V., Katz, C., Laptenko, O., Beckerman, R., Lokshin, M., Ahn, J., Byeon, I.J., Gabizon, R., Mattia, M., Zupnick, A.*, et al.* (2010). The C terminus of p53 binds the N-terminal domain of MDM2. Nat Struct Mol Biol *17*, 982-989.

Poyurovsky, M.V., Priest, C., Kentsis, A., Borden, K.L., Pan, Z.Q., Pavletich, N., and Prives, C. (2007). The Mdm2 RING domain C-terminus is required for supramolecular assembly and ubiquitin ligase activity. Embo J *26*, 90-101.

Reifenberger, G., Liu, L., Ichimura, K., Schmidt, E.E., and Collins, V.P. (1993). Amplification and overexpression of the MDM2 gene in a subset of human malignant gliomas without p53 mutations. Cancer research *53*, 2736-2739.

Riou, J.F., Gabillot, M., and Riou, G. (1993). Analysis of topoisomerase II-mediated DNA cleavage of the c-myc gene during HL60 differentiation. FEBS Lett *334*, 369-372.

Robey, I.F., Lien, A.D., Welsh, S.J., Baggett, B.K., and Gillies, R.J. (2005). Hypoxia-inducible factor-1alpha and the glycolytic phenotype in tumors. Neoplasia *7*, 324-330.

Roth, J., Dobbelstein, M., Freedman, D.A., Shenk, T., and Levine, A.J. (1998). Nucleo-cytoplasmic shuttling of the hdm2 oncoprotein regulates the levels of the p53 protein via a pathway used by the human immunodeficiency virus rev protein. Embo J *17*, 554-564.

Saito, Y., Kanai, Y., Sakamoto, M., Saito, H., Ishii, H., and Hirohashi, S. (2002). Overexpression of a splice variant of DNA methyltransferase 3b, DNMT3b4, associated with DNA hypomethylation on pericentromeric satellite regions during human hepatocarcinogenesis. Proc Natl Acad Sci U S A *99*, 10060-10065.

Sakaguchi, K., Herrera, J.E., Saito, S., Miki, T., Bustin, M., Vassilev, A., Anderson, C.W., and Appella, E. (1998). DNA damage activates p53 through a phosphorylation-acetylation cascade. Genes Dev *12*, 2831-2841.

Sam, K.K., Gan, C.P., Yee, P.S., Chong, C.E., Lim, K.P., Karen-Ng, L.P., Chang, W.S., Nathan, S., Rahman, Z.A., Ismail, S.M.*, et al.* (2012). Novel MDM2 splice variants identified from oral squamous cell carcinoma. Oral Oncol *48*, 1128-1135.

Samad, A., and Carroll, R.B. (1991). The tumor suppressor p53 is bound to RNA by a stable covalent linkage. Mol Cell Biol *11*, 1598-1606.

Sanchez-Aguilera, A., Garcia, J.F., Sanchez-Beato, M., and Piris, M.A. (2006). Hodgkin's lymphoma cells express alternatively spliced forms of HDM2 with multiple effects on cell cycle control. Oncogene *25*, 2565-2574.

Sandberg, A.A. (2004). Updates on the cytogenetics and molecular genetics of bone and soft tissue tumors: liposarcoma. Cancer Genet Cytogenet *155*, 1-24.

Saucedo, L.J., Myers, C.D., and Perry, M.E. (1999). Multiple murine double minute gene 2 (MDM2) proteins are induced by ultraviolet light. J Biol Chem *274*, 8161-8168.

Sauer, B., and Henderson, N. (1988). Site-specific DNA recombination in mammalian cells by the Cre recombinase of bacteriophage P1. Proc Natl Acad Sci U S A *85*, 5166-5170.

Saxena, A., Rorie, C.J., Dimitrova, D., Daniely, Y., and Borowiec, J.A. (2006). Nucleolin inhibits Hdm2 by multiple pathways leading to p53 stabilization. Oncogene *25*, 7274-7288.

Schneider-Stock, R., Walter, H., Radig, K., Rys, J., Bosse, A., Kuhnen, C., Hoang-Vu, C., and Roessner, A. (1998). MDM2 amplification and loss of heterozygosity at Rb and p53 genes: no simultaneous alterations in the oncogenesis of liposarcomas. J Cancer Res Clin Oncol *124*, 532-540.

Schuster, K., Fan, L., and Harris, L.C. (2007). MDM2 splice variants predominantly localize to the nucleoplasm mediated by a COOH-terminal nuclear localization signal. Molecular cancer research : MCR *5*, 403-412.

Sdek, P., Ying, H., Chang, D.L., Qiu, W., Zheng, H., Touitou, R., Allday, M.J., and Xiao, Z.X. (2005). MDM2 promotes proteasome-dependent ubiquitin-independent degradation of retinoblastoma protein. Mol Cell *20*, 699-708.

Sdek, P., Ying, H., Zheng, H., Margulis, A., Tang, X., Tian, K., and Xiao, Z.X. (2004). The central acidic domain of MDM2 is critical in inhibition of retinoblastoma-mediated suppression of E2F and cell growth. The Journal of biological chemistry *279*, 53317-53322.

Serganov, A., and Patel, D.J. (2007). Ribozymes, riboswitches and beyond: regulation of gene expression without proteins. Nat Rev Genet *8*, 776-790.

Sharp, D.A., Kratowicz, S.A., Sank, M.J., and George, D.L. (1999). Stabilization of the MDM2 oncoprotein by interaction with the structurally related MDMX protein. J Biol Chem *274*, 38189-38196.

Sheikh, M.S., Shao, Z.M., Hussain, A., and Fontana, J.A. (1993). The p53-binding protein MDM2 gene is differentially expressed in human breast carcinoma. Cancer research *53*, 3226-3228.

Sigalas, I., Calvert, A.H., Anderson, J.J., Neal, D.E., and Lunec, J. (1996). Alternatively spliced mdm2 transcripts with loss of p53 binding domain sequences: transforming ability and frequent detection in human cancer. Nature medicine *2*, 912-917.

Singh, R.K., Tapia-Santos, A., Bebee, T.W., and Chandler, D.S. (2009). Conserved sequences in the final intron of MDM2 are essential for the regulation of alternative splicing of MDM2 in response to stress. Exp Cell Res *315*, 3419-3432.

Sionov, R.V., Moallem, E., Berger, M., Kazaz, A., Gerlitz, O., Ben-Neriah, Y., Oren, M., and Haupt, Y. (1999). c-Abl neutralizes the inhibitory effect of Mdm2 on p53. The Journal of biological chemistry *274*, 8371-8374.

Stamm, S. (2002). Signals and their transduction pathways regulating alternative splicing: a new dimension of the human genome. Hum Mol Genet *11*, 2409-2416.

Steinman, H.A., Burstein, E., Lengner, C., Gosselin, J., Pihan, G., Duckett, C.S., and Jones, S.N. (2004). An Alternative Splice Form of Mdm2 Induces p53-independent Cell Growth and Tumorigenesis. The Journal of biological chemistry *279*, 4877-4886.

Takagi, M., Absalon, M.J., McLure, K.G., and Kastan, M.B. (2005). Regulation of p53 translation and induction after DNA damage by ribosomal protein L26 and nucleolin. Cell *123*, 49-63.

Tamborini, E., Della Torre, G., Lavarino, C., Azzarelli, A., Carpinelli, P., Pierotti, M.A., and Pilotti, S. (2001). Analysis of the molecular species generated by MDM2 gene amplification in liposarcomas. Int J Cancer *92*, 790-796.

Tanimura, S., Ohtsuka, S., Mitsui, K., Shirouzu, K., Yoshimura, A., and Ohtsubo, M. (1999). MDM2 interacts with MDMX through their RING finger domains. FEBS Lett *447*, 5-9.

Thut, C.J., Goodrich, J.A., and Tjian, R. (1997). Repression of p53-mediated transcription by MDM2: a dual mechanism. Genes and Development *11*, 1974-1986.

Tovar, C., Rosinski, J., Filipovic, Z., Higgins, B., Kolinsky, K., Hilton, H., Zhao, X., Vu, B.T., Qing, W., Packman, K.*, et al.* (2006). Small-molecule MDM2 antagonists reveal aberrant p53 signaling in cancer: implications for therapy. Proc Natl Acad Sci U S A *103*, 1888-1893.

Trinh, E., Boutillier, A.L., and Loeffler, J.P. (2001). Regulation of the retinoblastoma-dependent Mdm2 and E2F-1 signaling pathways during neuronal apoptosis. Mol Cell Neurosci *17*, 342-353.

Uchida, C., Miwa, S., Isobe, T., Kitagawa, K., Hattori, T., Oda, T., Yasuda, H., and Kitagawa, M. (2006). Effects of MdmX on Mdm2-mediated downregulation of pRB. FEBS Lett *580*, 1753-1758.

Udayakumar, T., Shareef, M.M., Diaz, D.A., Ahmed, M.M., and Pollack, A. (2010). The E2F1/Rb and p53/MDM2 pathways in DNA repair and apoptosis: understanding the crosstalk to develop novel strategies for prostate cancer radiotherapy. Semin Radiat Oncol *20*, 258-266.

Udayakumar, T.S., Hachem, P., Ahmed, M.M., Agrawal, S., and Pollack, A. (2008). Antisense MDM2 enhances E2F1-induced apoptosis and the combination sensitizes androgen-sensitive [corrected] and androgen-insensitive [corrected] prostate cancer cells to radiation. Molecular cancer research : MCR *6*, 1742-1754.

Uversky, V.N., Oldfield, C.J., and Dunker, A.K. (2005). Showing your ID: intrinsic disorder as an ID for recognition, regulation and cell signaling. J Mol Recognit *18*, 343-384.

Varki, A., Kannagi, R., and Toole, B.P. (2009). Glycosylation Changes in Cancer. In Essentials of Glycobiology, A. Varki, R.D. Cummings, J.D. Esko, H.H. Freeze, P. Stanley, C.R. Bertozzi, G.W. Hart, and M.E. Etzler, eds. (Cold Spring Harbor (NY)).

Verhaegen, M., Checinska, A., Riblett, M.B., Wang, S., and Soengas, M.S. (2012). E2F1-dependent oncogenic addiction of melanoma cells to MDM2. Oncogene *31*, 828-841.

Vlatkovic, N., Guerrera, S., Li, Y., Linn, S., Haines, D.S., and Boyd, M.T. (2000). MDM2 interacts with the C-terminus of the catalytic subunit of DNA polymerase epsilon. Nucleic acids research *28*, 3581-3586.

Vogelstein, B., Lane, D., and Levine, A.J. (2000). Surfing the p53 network. Nature *408*, 307-310.

Volk, E.L., Fan, L., Schuster, K., Rehg, J.E., and Harris, L.C. (2009a). The MDM2-a splice variant of MDM2 alters transformation in vitro and the tumor spectrum in both Arf- and p53-null models of tumorigenesis. Molecular cancer research : MCR *7*, 863-869.

Volk, E.L., Schuster, K., Nemeth, K.M., Fan, L., and Harris, L.C. (2009b). MDM2-A, a common Mdm2 splice variant, causes perinatal lethality, reduced longevity and enhanced senescence. Dis Model Mech *2*, 47-55.

Vousden, K.H., and Lu, X. (2002). Live or let die: the cell's response to p53. Nat Rev Cancer *2*, 594-604.

Wallace, M., Worrall, E., Pettersson, S., Hupp, T.R., and Ball, K.L. (2006). Dual-site regulation of MDM2 E3-ubiquitin ligase activity. Mol Cell *23*, 251-263.

Walsh, C.S., Miller, C.W., Karlan, B.Y., and Koeffler, H.P. (2007). Association between a functional single nucleotide polymorphism in the MDM2 gene and sporadic endometrial cancer risk. Gynecol Oncol *104*, 660-664.

Wang, C., Ivanov, A., Chen, L., Fredericks, W.J., Seto, E., Rauscher, F.J., 3rd, and Chen, J. (2005). MDM2 interaction with nuclear corepressor KAP1 contributes to p53 inactivation. Embo J *24*, 3279-3290.

Wang, P., Lushnikova, T., Odvody, J., Greiner, T.C., Jones, S.N., and Eischen, C.M. (2008). Elevated Mdm2 expression induces chromosomal instability and confers a survival and growth advantage to B cells. Oncogene *27*, 1590-1598.

Watanabe, T., Hotta, T., Ichikawa, A., Kinoshita, T., Nagai, H., Uchida, T., Murate, T., and Saito, H. (1994). The MDM2 oncogene overexpression in chronic lymphocytic leukemia and low-grade lymphoma of B-cell origin. Blood *84*, 3158-3165.

Weber, J.D., Taylor, L.J., Roussel, M.F., Sherr, C.J., and Bar-Sagi, D. (1999). Nucleolar Arf sequesters Mdm2 and activates p53. Nature cell biology *1*, 20-26.

White, D.E., Talbott, K.E., Arva, N.C., and Bargonetti, J. (2006). Mouse double minute 2 associates with chromatin in the presence of p53 and is released to facilitate activation of transcription. Cancer research *66*, 3463-3470.

Winter, M., Milne, D., Dias, S., Kulikov, R., Knippschild, U., Blattner, C., and Meek, D. (2004). Protein kinase CK1delta phosphorylates key sites in the acidic domain of murine double-minute clone 2 protein (MDM2) that regulate p53 turnover. Biochemistry *43*, 16356-16364.

Wu, L., and Levine, A.J. (1997). Differential regulation of the p21/WAF-1 and mdm2 genes after high-dose UV irradiation: p53-dependent and p53-independent regulation of the mdm2 gene. Mol Med *3*, 441-451.

Wu, X., Bayle, J.H., Olson, D., and Levine, A.J. (1993). The p53-mdm-2 autoregulatory feedback loop. Genes and Development *7*, 1126-1132.

Xiao, G., White, D., and Bargonetti, J. (1998). p53 binds to a constitutively nucleosome free region of the mdm2 gene. Oncogene *16*, 1171-1181.

Xiao, Z.X., Chen, J., Levine, A.J., Modjtahedi, N., Xing, J., Sellers, W.R., and Livingston, D.M. (1995). Interaction between the retinoblastoma protein and the oncoprotein MDM2. Nature *375*, 694-698.

Xu, H., Zhang, Z., Li, M., and Zhang, R. (2010). MDM2 promotes proteasomal degradation of p21Waf1 via a conformation change. The Journal of biological chemistry *285*, 18407-18414.

Yamamoto, N., Ueda, M., Sato, T., Kawasaki, K., Sawada, K., Kawabata, K., and Ashida, H. (2011). Measurement of glucose uptake in cultured cells. Curr Protoc Pharmacol *Chapter 12*, Unit 12 14 11-22.

Yu, G.W., Allen, M.D., Andreeva, A., Fersht, A.R., and Bycroft, M. (2006). Solution structure of the C4 zinc finger domain of HDM2. Protein Sci *15*, 384-389.

Zauberman, A., Flusberg, D., Haupt, Y., Barak, Y., and Oren, M. (1995). A functional p53-responsive intronic promoter is contained within the human mdm2 gene. Nucleic Acids Res *23*, 2584-2592.

Zeng, S.X., Jin, Y., Kuninger, D.T., Rotwein, P., and Lu, H. (2003). The acetylase activity of p300 is dispensable for MDM2 stabilization. The Journal of biological chemistry *278*, 7453-7458.

Zha, J., Weiler, S., Oh, K.J., Wei, M.C., and Korsmeyer, S.J. (2000). Posttranslational N-myristoylation of BID as a molecular switch for targeting mitochondria and apoptosis. Science *290*, 1761-1765.

Zhang, Q., Xiao, H., Chai, S.C., Hoang, Q.Q., and Lu, H. (2011). Hydrophilic residues are crucial for ribosomal protein L11 (RPL11) interaction with zinc finger domain of MDM2 and p53 protein activation. The Journal of biological chemistry *286*, 38264-38274.

Zhang, Y., Shi, Y., Li, X., Du, W., Luo, G., Gou, Y., Wang, X., Guo, X., Liu, J., Ding, J.*, et al.* (2010). Inhibition of the p53-MDM2 interaction by adenovirus delivery of ribosomal protein L23 stabilizes p53 and induces cell cycle arrest and apoptosis in gastric cancer. J Gene Med *12*, 147-156.

Zhang, Y., Wolf, G.W., Bhat, K., Jin, A., Allio, T., Burkhart, W.A., and Xiong, Y. (2003). Ribosomal protein L11 negatively regulates oncoprotein MDM2 and mediates a p53-dependent ribosomal-stress checkpoint pathway. Mol Cell Biol *23*, 8902-8912.

Zhang, Y., Xiong, Y., and Yarbrough, W.G. (1998). ARF promotes MDM2 degradation and stabilizes p53: ARF-INK4a locus deletion impairs both the Rb and p53 tumor suppression pathways. Cell *92*, 725-734.

Zhang, Z., Wang, H., Li, M., Agrawal, S., Chen, X., and Zhang, R. (2004). MDM2 is a negative regulator of p21WAF1/CIP1, independent of p53. The Journal of biological chemistry *279*, 16000-16006.

Zhang, Z., Wang, H., Li, M., Rayburn, E.R., Agrawal, S., and Zhang, R. (2005). Stabilization of E2F1 protein by MDM2 through the E2F1 ubiquitination pathway. Oncogene *24*, 7238-7247.

Zhao, L., Samuels, T., Winckler, S., Korgaonkar, C., Tompkins, V., Horne, M.C., and Quelle, D.E. (2003). Cyclin G1 has growth inhibitory activity linked to the ARF-Mdm2-p53 and pRb tumor suppressor pathways. Molecular cancer research : MCR *1*, 195-206.

Zhou, S., Gu, L., He, J., Zhang, H., and Zhou, M. (2011). MDM2 regulates vascular endothelial growth factor mRNA stabilization in hypoxia. Mol Cell Biol *31*, 4928-4937.

Zhu, Q., Yao, J., Wani, G., Wani, M.A., and Wani, A.A. (2001). Mdm2 mutant defective in binding p300 promotes ubiquitination but not degradation of p53: evidence for the role of p300 in integrating ubiquitination and proteolysis. The Journal of biological chemistry *276*, 29695-29701.

Zhu, T., Starling-Emerald, B., Zhang, X., Lee, K.O., Gluckman, P.D., Mertani, H.C., and Lobie, P.E. (2005). Oncogenic transformation of human mammary epithelial cells by autocrine human growth hormone. Cancer research *65*, 317-324.